Doctoral School of Earth Sciences

Complex characterisation of Mecsekalja Zone using single quartz grains of drill cuttings from Sztl-1 well

A Mecsekalja-zóna komplex jellemzése a Sztl-1 fúrás furadékanyagának kvarcszemcséi alapján

Ph.D. Thesis

Author:

Ágnes Skultéti

Supervisor:

Dr. Tivadar M. Tóth

University of Szeged
Faculty of Science and Informatics
Department of Mineralogy, Petrology and Geochemistry

Szeged
2017

Table of Contents

List of Figures

mylonitization and recrystallization (~450 °C, Szederkényi 1977, 1983; Lelkes-Felvári et al. 2000; Király and Török 2003; M. Tóth et al. 2005). Based on the current results, the early regional metamorphism (II.) occurred between 500 and 575 °C, while recrystallization (III.) occurred between 400 and 475 °C.

Figure V.1: Flow chart of the methods, used during the complex analysis of drill cuttings from the Sztl-1 well, and results.

List of Tables

Chapter I.: Introduction

I.1 Shear zones

The distribution of the strain inside the Earth's crust is not homogeneous in most cases; instead, it tends to be localised into planar horizons. The *shear zones* are deformation localisation structures, tabular zones in which strain is notably higher than in the surrounding rock body (Ramsay, 1980; Ramsay and Huber, 1987; van der Plujim and Marshak, 2004; Passchier and Trouw, 2005; Fossen, 2010). The width of these structures can vary from grain scale to km-scale, while their length is significantly bigger than their width (~5:1) (Ramsay and Huber, 1987). The shear zones are bounded by two shear zone walls that separate the shear zone from its wall rock (van der Plujim and Marshak, 2004; Fossen, 2010). These structures involve displacement parallel to the walls (Passchier and Trouw, 2005; Fossen, 2010), which can be of significantly different scale (mm to km). The distribution of strain in shear zones is generally heterogenic. In the degree of deformation there is a special spatial distribution (deformation gradient). In the shear zones the degree of deformation grows from the margins to the centre (strain localization) (Passchier and Trouw, 2005; Fossen, 2010).

The shear zones appear in a wide range of depth intervals and can form in any tectonic regime *(Fig. I.1)* (Ramsay and Huber, 1987; van der Plujim and Marshak, 2004; Passchier and Trouw, 2005; Fossen, 2010). Shear zones can be classified according to ductility (continuity of markers) and plasticity (degree of plastic versus brittle deformation mechanisms) (Fossen, 2010). The activity of deformation mechanisms depends on temperature, pressure, metamorphic reactions, strain rate and amount of fluid (Passchier and Trouw, 2005; Fossen, 2010). In the lithosphere these characteristics vary with depth. In the overall brittle regime of the upper crust (~0–10 km) brittle deformation mechanisms dominate. Shear zones form predominantly by brittle deformation mechanisms are called *brittle shear zones (faults)* (Ramsay, 1980; Ramsay and Huber, 1987; Scholz, 2002; van der Plujim and Marshak, 2004; Passchier and Trouw, 2005; Twiss and Moores, 2006; Fossen, 2010). Deeper in the crust in the plastic regime (>15 km) the plastic deformation mechanisms dominate. Where plastic deformation mechanisms dominate we get *plastic shear zones* (Ramsay, 1980; Ramsay and Huber, 1987; van der Plujim and Marshak, 2004; Passchier and Trouw, 2005; Twiss and Moores, 2006; Fossen, 2010; Vitale and Mazzoli, 2016). In the brittle–plastic

transitional zones (~10–15 km in granitic rocks) *brittle–plastic shear zones (semi-brittle or semi-ductile)* (Ramsay, 1980; Ramsay and Huber, 1987; Fossen, 2010) form in which both brittle and plastic deformation mechanisms are important. Based on ductility (continuity of markers) shear zones can be *brittle- (faults), semi-ductile- and ductile shear zones* (Fossen, 2010).

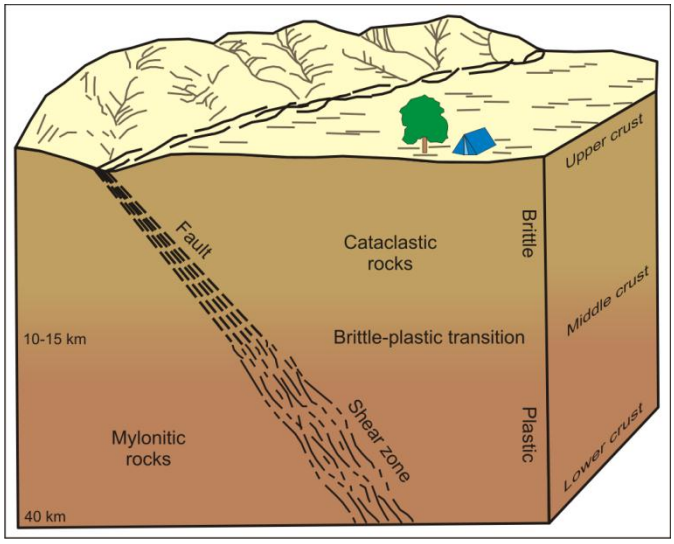

Figure I.1: The simplified model of the connection between ductile and brittle shear zones (faults) (based on Fossen, 2010).

The *brittle shear zones*, faults are such special types of shear zones in the shallow Earth's crust, which are dominated by brittle deformation. The faults are complex structures, which accumulate large amount of deformation in the upper crust. The deformation is concentrated in narrow discontinuities (van der Plujim and Marshak, 2004; Passchier and Trouw, 2005; Twiss and Moores, 2006; Fossen, 2010). Along these narrow zones, proportioning by numerous discontinuities, measurable displacement occurs. In a brittle shear zone generally develop a central fault core or slip surface surrounded by a volume of brittle deformed wall rock known as fault damage zone (Passchier and Trouw, 2005; Fossen, 2010). In the brittle regime of the upper crust the deformation occurs by cataclastic flow which results in cataclastic cohesive and non-cohesive fault rocks (Passchier and Trouw, 2005; Fossen, 2010).

The *ductile shear zones* form as a result of ductile shearing in the middle-lower crust. In the ductile shear zones both the deformation and displacement are driven by ductile processes (Passchier and Trouw, 2005; Fossen, 2010; Vitale and Mazzoli, 2016). The ductile shear zones are common in deformed rocks of crystalline basement, which deformed among metamorphic conditions, at greenschist, blueschist, amphibolite and granulite facies (Ramsay, 1980). In ductile shear zones deformation covers wider zone

and its distribution in the zone is gradual; there is not any discontinuity (van der Plujim and Marshak, 2004; Twiss and Moores, 2006). The ductile shear zones are dominated by plastic deformation mechanisms, which result rocks formed with plastic deformation, recrystallization and chemical variation of previous minerals. These rocks, suffered intensive ductile deformation are mylonites (White et al., 1980; Passchier and Trouw, 2005; Fossen, 2010).

The transitional *brittle-plastic shear zones (semi-ductile, semi-brittle)* can be characterised with the combination of the previous brittle-, and ductile shear zone properties (Ramsay, 1980; Ramsay and Huber, 1987; Fossen, 2010). These shear zones include the stamps of both brittle and plastic deformation mechanisms.

The heterogenic shear zones are common in the lithosphere (well documented examples are South Armorican Shear Zone and North Armorican Shear Zone in Brittany, North Anatolian Fault Zone in Turkey, Dead Sea Fault in Israel, San Andreas Fault in California, Alpine Fault in New Zealand, Tonale Fault Zone in Italy among numerous others). The shear zones reveal the crystalline basement, thus provide excellent opportunity to analyse structures with increasing deformation (Ramsay and Huber, 1987; Fossen, 2010; Vitale and Mazzoli, 2016). These special structures give insight into the deformation processes and mechanisms operate in the shear zone (White et al., 1980), and refer to the *P-T* conditions, type of deformation and deformation history, which are very important parameters in concern the tectonic evolution of the area in question (Passchier and Trouw, 2005; Fossen, 2010). Faults and shear zones have crucial effect on physical, mechanical and hydrodynamic behaviour of the rock bodies. They can behave as softening zones, determine the spatial arrangement of rock units and influence the permeability and fluid migration of rock bodies (van der Plujim and Marshak, 2004). Faults play an important role in petroleum industry, geothermal energy exploitation and cause challenges during build of geotechnical facilities (for example tunnels) (Fossen, 2010).

I.2 Mecsekalja Zone

The studied tectonic belt, the Mecsekalja Zone is situated in the *Pannonian Basin*, surrounded by the Alpine-Carpathian-Dinaric orogenic belt. The Pannonian Basin was formed as a result of a complicated extension process during the Miocene (Tari et al., 1992). Due to the widespread subsidence during the late Tertiary ages, it was filled up

by one to eight km-thick series of sediments (Szederkényi, 1977, 1983; Árkai and Nagy, 1994; Lelkes-Felvári et al., 2000; Király and Török, 2003; M. Tóth et al., 2005), so the crystalline basement outcrops only in relatively small, isolated areas (Bergerat, 1989; Horváth and Cloetingh, 1996; Csontos and Nagymarosy, 1998). The Alcapa and Tisza Mega-unit are the main structural units in the basement of the Pannonian Basin, which were juxtaposed only in the Neogene. The crystalline basement of the *Tisza Mega-unit* consists of three units (Slavonia-Drava-, Kunság- and Békés Unit) have been separated from each other by major fracture zones (Szederkényi et al., 2012; Kovács et al., 2000). The Slavonia-Drava Unit is located in south-eastern Transdanubia and can be subdivided into two subunits, Babócsa and Baksa Complex. The northwestern border of the Baksa Complex is the *Mecsekalja Zone* running between the Kunság and Slavonia-Drava Units (Kassai, 1977). The Mecsekalja Zone is a ~1.5 km wide tectonic belt, an active strike-slip fault zone since the Permian and so determines the structural evolution of the adjacent areas significantly (Szederkényi, 1977, 1979). In the dislocation zone formations with various lithologies and in most parts intensively mylonitised metamorphic rocks outcrop.

The recognition of the crystalline basement of Mecsekalja Zone is very important in several aspects. In several places, because of their intensive deformation, shear zones behave as excellent fractured fluid (hydrocarbon or geothermal) reservoirs. Among several others, the drilling in the focus of the present dissertation (Szentlőrinc-1) is a geothermal well, which penetrated fractured basement rocks. Petrographic and structural characterisation of shear zone formations inside these hard rock reservoirs are of basic importance. Recently, the low and intermediate level radioactive waste repository of Hungary has been set up in the South-Transdanubian region in the rocks of Mórágy Granite Formation (Balla et al., 2009).

In the Mecsekalja Zone significant strike-slip movements along the basement rock have caused high secondary porosity and along some tectonic lines, high pressure geothermal conditions were generated (Árpási et al., 2000; Tóth and Almási, 2001). The first well, Sztl-1 has been drilled in the vicinity of town Szentlőrinc that had primarily evaluated in respect to geothermal energy (Thorbergsóttir et al., 2010). The well site was a conclusion of a large project with the aim of locating possible well sites for geothermal utilization in Hungary. The Sztl-1 deep drilling (Thorbergsdottir et al., 2010) reached the base of depth at 1820 m. Below Cenozoic and Mesozoic sedimentary formations (clay, silt, sand, conglomerate and limestone) the well penetrated

metamorphic rocks of the Mecsekalja Zone (gneiss and mica-schist). From the well borecores are not available, only drilling chips were taken in the 1600–1820 m interval. The drill cuttings take the form of μm-mm-size debris, constituted by mineral and rock pieces dominated by quartz fragments.

I.3 Quartz

Quartz is one of the most frequent rock-forming minerals in the Earth's crust. It is stable within a wide range of temperature and pressure conditions. Nevertheless, the mineral is very sensitive to stress and, under different *P-T* conditions, it deforms in different ways following diverse deformation mechanisms, resulting in grains of varying microstructures. As a consequence quartz may allow valuable information concerning the structural evolution of several distinct rock types (Hirth and Tullis, 1992; Stipp et al., 2002; Passchier and Trouw, 2005). In the quartz lattice various trace elements (Al, Ti, Ge, Na, K, Li, B) (Götze et al., 2004) may change Si in the SiO_4 tetrahedrons at different physical conditions and so metamorphic evolution determines the chemical composition of quartz. Quartz is a "nominally anhydrous mineral" (NAM), but in its crystal lattice hydrogen ('water') may occur both in the form of hydroxyl defects (OH^-) and molecular water (H_2O) (Stenina, 2004). The hydroxyl defects in the crystal lattice of quartz mostly are enclosed in crystal defects (point defects) and along grain boundaries, while the molecular water occurs freely in form of fluid (nano-) inclusions (Stadler and Konzett, 2012). The amount of 'water' in the quartz lattice significantly influences its brittle and ductile behaviour through reducing its mechanical strength (Jones, 1975).

I.4 Aims and structure of the dissertation

The aim of the project is to work out a reproducible method for metamorphic- and deformation history reconstruction using single quartz grains of drill cuttings. Based on the developed method (among numerous others) and using the drill cuttings of the Sztl-1 well, the project aims the metamorphic and structural reconstruction of the Mecsekalja Zone along the sampled interval of the well. Afterwards the manuscript presents the spatial correlation of the borehole data with previous results from the whole study area.

Following this brief introduction *(Chapter I.)* each part of the dissertation represents a different stage of the research. *Chapter II.* presents the detailed

microstructural analysis of the drill cuttings from Sztl-1 drill and the separated groups with microstructurally different quartz grain types. In addition, in this chapter the description of the Raman spectroscopy method was introduced to separate the microstructurally different quartz grain types. Moreover in this chapter different deformation mechanisms, which produce various microstructures are introduced and a descriptive way for temperature estimation of these processes is outlined.

Chapter III. presents the analysis of the volume ratio of microstructurally different quartz grain types along the Sztl-1 well. Based on these data the position of the ductile shear zones are localized and compared with the depths of the brittle shear zones realized using well-log information. In addition I present possible explanations for the geodynamic evolution of the coinciding ductile and brittle shear zones.

Chapter IV. presents the temperature estimation from quartz grains, where quartz could grow and the quartz 'water' content variation along the localized shear zones and the possible interpretations and explanations of these data. Moreover the chapter introduces a model, in which the metamorphic and structural evolution of the Mecsekalja Zone is reconstructed, based on the novel data and the previous surface models.

Finally, *Chapter V.* includes the summary and conclusion of the whole dissertation, with the possible direction of the further researches and application opportunities. An aggregated reference list can be found at the end of the dissertation.

Chapter II.: Deformation history reconstruction using single quartz grain Raman microspectroscopy data

Ágnes Skultéti

Department of Mineralogy Geochemistry and Petrology,
University of Szeged, Szeged, Hungary
skulteti.agi@gmail.com

Tivadar M. Tóth

Department of Mineralogy Geochemistry and Petrology,
University of Szeged, Szeged, Hungary
mtoth@geo.u-szeged.hu

Krisztián Fintor

Department of Mineralogy Geochemistry and Petrology,
University of Szeged, Szeged, Hungary
efkrisz@gmail.com

Félix Schubert

Department of Mineralogy Geochemistry and Petrology,
University of Szeged, Szeged, Hungary
schubert@geo.u-szeged.hu

Journal of Raman Spectroscopy
45/4, 314-321 (2014)
DOI 10.1002/jrs.4456

Deformation history reconstruction using single quartz grain Raman microspectroscopy data

Abstract

One of the most common minerals in the Earth's crust, quartz is stable across a wide range of temperature and pressure conditions. As its microstructure is sensitive to diverse deformation mechanisms, quartz may provide valuable information regarding the structural evolution of many different rock types. Using Raman microspectroscopy, single quartz grains and monomineralic domains characterized by different deformation conditions can be identified and separated. In this study three microstructurally extreme quartz grain types were discriminated from a subsurface shear zone: grains with undulose extinction (U), grains with subgrains (S), and grains with recrystallized grains (R). Moreover, several microstructurally transitional grains were measured which represent combinations of the above extremes. Statistical analysis revealed that the microscopically identified extreme grains possess significantly different spectral attributes, and as such can be divided on the basis of certain variables of their respective Raman spectra. The three extreme quartz grain types were formed by different deformation mechanisms and thus represent distinct deformation conditions. The U-S-R spectral space can therefore also be considered a virtual deformational space. Although each complex quartz grain measured also appears elsewhere in the deformation process defined by U-S-R extreme conditions, they together represent a successive deformation path. This combined pathway is assumed to be characteristic for the whole rock volume under study. Finally, the computed Raman spectroscopy-based virtual deformational space enabled the determination of the structural evolution of the analysed shear zone.

Keywords: quartz, microstructure, deformation, Raman spectroscopy

II.1 Introduction

Quartz is present in the Earth's crust as a common and resistant mineral, and is stable across a rather wide range of temperature and pressure conditions. However, the mineral is nevertheless very sensitive to stress, and under different *P-T* conditions deforms in different ways following diverse deformation mechanisms, resulting in grains of varying microstructure (Hirth and Tullis, 1992; Vernon, 2004; Passchier and

Trouw, 2005). As a consequence, each grain in a quartz-bearing rock may provide valuable information regarding the deformation history of the rock body itself. As ductile deformation processes are usually very slow in reaching equilibrium, each quartz grain theoretically also appears elsewhere in the evolution process. Nevertheless, their combined analysis may help to outline the deformation history of the host rock body.

The selected study area is an active shear zone situated in the South Transdanubian region of Hungary, Central Europe. As almost the entire Mecsekalja-zone is buried, petrographic characterization of the shear zone rocks has thus far been carried out exclusively using only a few surface outcrop specimens. However, obtaining a deep understanding of the present and past behavior of this 1.5 km wide and several hundred km long tectonic zone is crucial for several reasons. For example, not only does the zone pass a few km north of a radioactive waste deposition site in Hungary, in several places, due to the intense deformation, shear zone rocks behave as an excellent fractured fluid reservoir. Our samples were obtained from a newly bored geothermal well located inside the dislocation zone, with the drilling chips brought to the surface from around 2 km depth providing an exclusive chance to investigate the shear zone beneath. This drilling chip collection includes only a few small rock grains unsuitable for traditional petrographic evaluation; more than 80% of the material consists of tiny (<1 mm) randomly oriented single quartz grains.

The aim of the present work is to discriminate and characterize the microstructurally different quartz grains using a combination of traditional optical methods and Raman spectroscopy. A secondary objective is to develop a method enabling the reconstruction of the shear zone's deformation history using only the tiny quartz chips.

II.2 Theoretical background

II.2.1 Deformation mechanism of natural quartz

The crystal structure of a sheared quartz grain develops as a result of a range of deformation mechanisms taking place under different temperature and lithostatic pressure conditions. At low temperatures and shallow crustal depths, quartz deformation is dominated by fracturing, whereas at greater depths and at around 200 °C ductile deformation becomes typical (Wintsch and Yi, 2002). During brittle deformation,

cleavages and microcracks develop inside the grain. In contrast, ductile deformation is characterized by the appearance of kink bands (Nishikawa and Takeshita, 1999), deformation lamellae, and Dauphiné deformation twinning (Barber and Wenk, 1991; Lloyd et al., 1992; Heidelbach et al., 2000; Lloyd, 2000). During ductile deformation, dislocations in different slip planes may interfere with each other, inhibiting their movement and hence further deformation of the mineral (Vernon, 2004; Passchier and Trouw, 2005). Recovery and recrystallization processes tend to reduce the concentration of dislocations, and so produce volumes of material capable of continued deformation. Recovery includes all processes that attempt to return a crystal to its undeformed state, with dislocations migrating to form subgrain boundaries which are walls of organized dislocations (Chalmers, 1959; Hobbs et al., 1976). Recrystallization involves the formation of strain-free volumes via the creation and/or movement of grain boundaries, in response to deformation (Vernon, 2004; Passchier and Trouw, 2005).

Recrystallization may occur either during deformation (dynamic recrystallization) or after deformation (static recrystallization) (Vernon, 2004; Passchier and Trouw, 2005). Dynamically recrystallized grains can be recognized by the presence of subgrains, deformation bands and deformation lamellae, in contrast to the optically strain-free state associated with static recrystallization (White, 1977). Dislocation creep is an important deformation mechanism in the case of quartz aggregates, and is defined by various different mechanisms of dynamic recrystallization (Hirth and Tullis, 1992). Dynamic recrystallization can take place in the following three ways depending on temperature and strain rate: bulging (Regime 1), subgrain rotation (Regime 2) and grain-boundary migration (Regime 3), with increasing temperature and decreasing strain rate *(Fig. II.1)* (Hirth and Tullis, 1992). Bulging recrystallization (BLG) (Hirth and Tullis, 1992) occurs at low temperatures (<300–400 °C for quartz) (Passchier and Trouw, 2005) and is characterized by deformed parent grains with a high dislocation concentration and undulose extinction (Halfpenny et al., 2012). Bulging takes place mainly at the grain boundaries of parent grains and at the triple junctions separating small, new, independent grains. Subgrain rotation recrystallization (SGR) develops at higher temperatures (Hirth and Tullis, 1992) (400–500 °C for quartz) (Passchier and Trouw, 2005) and is characterized by ductily deformed, elongated and ribbon-shaped parent grains with many subgrains. As a result of this process the remains of old grains are commonly surrounded by groups of recrystallized grains (a feature known as a core-and-mantel structure) (Gifkins, 1976; Shigematsu, 1999) or may be completely replaced

by recrystallized material (Hirth and Tullis, 1992; Stipp et al., 2002). High temperature grain-boundary migration recrystallization (GBM) (Hirth and Tullis, 1992) (500– < 700 °C for quartz) is characterized by grains with new, lobate grain boundaries (Vernon, 2004; Passchier and Trouw, 2005); the size of these recrystallized grains increases with rising temperature. The grain boundary area reduction (GBAR) mechanism takes place during static recrystallization (Passchier and Trouw, 2005). As a result, the irregular grain boundaries which developed during previous deformation and dynamic recrystallizations become straightened, forming a polygonal shape. Simultaneously, some small grains may be eliminated. The resulting grains are characterized by a lack of undulose extinction and subgrains (Passchier and Trouw, 2005).

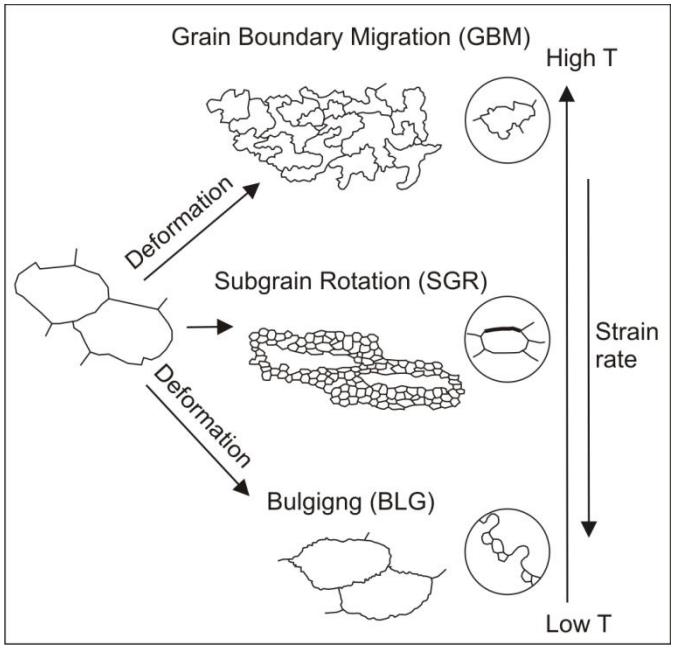

Figure II.1: The three main types of dynamic recrystallization (based on Passchier and Trouw, 2005)

II.2.2 Raman characteristics of natural quartz

Low quartz or α-quartz belongs to the $P3_121$ space group of the enantiomorphous hemihedral class of the trigonal system. The unit cell of the α-quartz structure consists of three SiO_2 groups, with the prime characteristic of the silicons and oxygens being that each silicon atom is tetrahedrally surrounded by four oxygen atoms, and each oxygen atom connected to two silicon atoms.

Fifteen principal and thirty-three subsidiary frequency bands constitute the main features of the Raman spectrum of α-quartz (Krishnamurti, 1958; Ostroumov et al., 2002), which also features stretching vibrational bands localized in two specific regions:

symmetrical stretching bands at 700–800 cm^{-1} and asymmetrical bands at 1050–1100 cm^{-1} (Etchepare et al., 1974; Ostroumov et al., 2002). The bands in these regions belong to the Si-O bonds inside the SiO_4 tetrahedron (Etchepare et al., 1974). The bending vibrations of the O-Si-O angles are localized in the 350-500 cm^{-1} region, while the bending vibrations of the Si-O-Si angles and twistings are situated below 300 cm^{-1} (Etchepare et al., 1974).

Low quartz can correspondingly be identified on the basis of its three principal (i.e. most intense) bands, which are situated at 128, 206 and 464 cm^{-1} in the Raman spectrum. The band at 464 cm^{-1} is the most intense and dominant, and belongs to the change in O-Si-O bond angle inside the SiO_4 tetrahedron. As a result it is indicative of deformational vibration modes, namely symmetric bending along the O-Si-O bond angle (Etchepare et al., 1974). The band at 206 cm^{-1} is a broad band belonging to the Si-O-Si bond angle inside the SiO_4 tetrahedron, and indicates a deformational bending vibrational mode (Etchepare et al., 1974). Changes in this angle are responsible for the anomalously high compressibility of quartz (Levien et al., 1980). The band at 128 cm^{-1} corresponds with the rotation of the tetrahedron around its twofold axis perpendicular to the crystallographic c axis, associated with OO repulsion (de Boer et al., 1996).

Broadening and shifting of the ideal Raman bands can be caused by the distortion of the crystal lattice due to changes in temperature and pressure (Asell and Nicol, 1968; Lin, 1997; Ostroumov et al., 2002). In α-quartz, the Si-O-Si bond angle increases and the average Si-O bond length decreases with increasing temperature. These changes can lead to a major decrease in the frequency of the 206 cm^{-1} band and a minor decrease in the frequency of the 128 and 464 cm^{-1} bands, resulting in a shift toward lower wavenumbers (Asell and Nicol, 1968). In contrast, the Si-O-Si bond angle and Si-O bond length both decrease with rising pressure (Levien et al., 1980), which can cause a significant increase in the frequency of all three bands and a shift toward higher wavenumbers (Asell and Nicol, 1968). The tetrahedral O-Si-O bond angle does not display any significant change with varying temperature and pressure, because these tetrahedral angles are much less flexible than the Si-O-Si angles (de Boer et al., 1996). Distortion causes a decrease in the degree of structural ordering inside the crystal lattice, which greatly influences the Raman spectra; with an increase in crystal lattice disorder, the characteristic bands become less intense, less sharp, and the vibrational frequencies of all bands decreases, with the latter shifting toward lower wavenumbers (Ostroumov et al., 2002). This shift in the main Raman bands toward lower

wavenumbers is indicative of a slight increase in the average distance between atoms, and thus also a minor expansion of the crystal lattice. During disorder, the distribution of bond lengths and angles within and between SiO_4 tetrahedrons becomes increasingly irregular. As a result, the increase in band half-widths and the accompanying decrease in intensity can be interpreted wavenumbers (Ostroumov et al., 2002).

In the Raman spectra of disordered quartz grains, the position, full width at half-max (FWHM) and intensity of the characteristic bands are a reflection of the combination of temperature change, pressure change and the degree of crystal lattice ordering.

II.3 Samples

Located in the South Transdanubian region of Hungary, Central Europe, the study area forms part of the Mecsekalja Shear Zone, which is situated in the foreground of the Mecsek Mountains. The dislocation zone is predominantly buried; the few surface outcrops consist mainly of mylonitic rocks (Szederkényi, 1974).

The investigated samples were obtained from the Szenlőrinc-1 deep drilling project, the base of which reached a depth of 1820 m. Drilling chips were taken every 5 m in the 1600–1820 m interval, although in the present study only one section of the well was evaluated (1600–1605 m). The drilling chips take the form of small detrital grains a few mm in diameter, constituted by single mineral and rock pieces in an 80:20 ratio. The mineral grains consist predominantly of randomly oriented pure quartz.

II.4 Methods

II.4.1 Analytical methods

II.4.1.1 Microscopy

Microscopic analysis of normal thin sections was carried out on an Olympus BX-41 polarization microscope using a magnification of 10x and 40x objectives. Around 500 single quartz grains were studied. The aim of microscopic analysis was the identification and microstructural characterization of these quartz grains, including a calculation of the size distribution of recrystallized grains in specific samples.

II.4.1.2 Raman spectroscopy

Analyses were performed on a Thermo Scientific DXR Raman microscope equipped with a diode-pumped frequency-doubled Nd-YAG laser at 10 mW maximum laser power. Samples were irradiated by laser light at a wavelength of 532.2 nm, with the laser beam focused using a 100x objective lens, resulting in a spot size of ca. 0.7 μm. The backscattered light collected by the microscope objective was filtered via an edge filter, dispersed by a single grating (1800 grooves mm^{-1}) and gathered in a CCD detector cooled to -20 °C by the Peltier effect. The instrument had a spectral resolution better than 2 cm^{-1} and a spatial resolution of a few μm^3; a 50 μm pinhole confocal aperture was used for each measurement. In every case, 10 mW laser power was used to record the spectra. Sample exposures were obtained by operating the DXR Raman microscope in auto-exposure operating mode, in which the instrument attempts to reach a specified signal-to-noise ratio (S/N) during the measurement (in this case, S/N=100). In this measuring mode, a maximum exposure time (i.e. if the specified S/N value cannot be achieved) also has to be set, with a value of 1 min for each spectrum selected in the present study. During analysis of the selected quartz grains, 50 points per 5 μm were measured along a line. The applied Raman microscope is equipped with a laser source operating with depolarized laser beam, where the degree of polarization (DOP) is below 0.08 (at the used wavelength of 532.2 nm). The beam of unpolarised radiation vibrations take place in randomly oriented directions and polarized in all possible directions perpendicular to the propagation of the wave, so it minimizes orientation dependence in measurements.

II.4.2 Methods of interpretation

II.4.2.1 Raman spectral analysis

The Seasolve PeakFit 4.12 software program was employed to evaluate Raman spectra. A Gaussian deconvolution approach based on the Voight-type curve fitting procedure was used to determine the peak position (center), amplitude, full width at half maximum (FWHM), full width at base (FW base), integrated area, and standard deviation (Std. Dev.) of the bands of interest.

The characteristic spectral variables can be divided into four groups based on the type of information provided regarding the spectral bands. Peak position (center) (1) is related to the position of the bands, while amplitude (2) determines band intensity. Full

width at half-max (FWHM), full width at base (FW base) and standard deviation (Std. Dev.) values (3) provide information regarding the deviation around an expected value (i.e. band width), and finally, area (%) (4) reflects the integrated area of the bands. Quartz Raman band assignment was based on the work of Krishnamurti (1958), Etchepare et al. (1974) and Ostroumov et al. (2002), with the characteristic spectral parameters being amplitude, peak position and FWHM of the 128 cm^{-1}, 206 cm^{-1} and 464 cm^{-1} bands.

II.4.2.2 Discriminant function analysis

Statistical analysis was performed using IBM SPSS Statistics Version 20.0. During discriminant function analysis the stepwise algorithm with Wilk's lambda method was applied. The aim of the calculations was to find those functions of the original spectral parameters which best separated individual quartz groups.

II.5 Results

The 500 randomly oriented single quartz grains examined under the microscope exhibit various microstructures, with three microstructurally extreme types identifiable: grains with undulose extinction (undulatory: U) *(Fig. II.2/a)*, grains with subgrains (subgrain: S) *(Fig. II.2/b)*, and grains consisting of small, undeformed recrystallized grains (recrystallized: R) *(Fig. II.2/c)*. U grains are petrographically entirely homogeneous without any subgrains and/or recrystallized grain boundaries. S grains are characterized by smaller domains with different orientations and extinction angles, which are bordered not along sharp, optically observable grain boundaries, but along border bands. R grains include small (a few tens of microns in diameter) newly recrystallized grains, which are characterized by concrete, optically observed boundaries and a lack of undulose extinction and subgrains. Based on 100 single measurements, the average size of these new grains is 45 ± 20 μm *(Fig. II.3)*. Besides those belonging to the above groups, numerous grains with heterogeneous microstructure were also observed *(Fig. II.2/d)*. These exhibit the simultaneous presence of a more extreme texture within a single grain (i.e. transitional grains).

In the first step of the Raman spectroscopic investigation, three representative extreme randomly oriented quartz grains were measured at 50 points along a 250 μm long line *(Fig. II.4/a, b, c)*. Afterwards, ten microstructurally transitional grains were

studied in a similar way. The resulting spectra were evaluated using the PeakFit software program in order to obtain the numerical spectral parameters. Discriminant function analysis for the three extreme groups produced the following *F1* and *F2* functions (1, 2):

$$F1 = -0.79 * center\_128 + 1.64 * area\_128 - 2.92 * area\_206 + 0.83 * center\_464 - 283.85 \quad (1)$$

$$F2 = 4.56 * center_{128} - 3.92 * center_{206} - 0.53 * area_{206} + 7.70 * center_{464} - 3354.57 \quad (2)$$

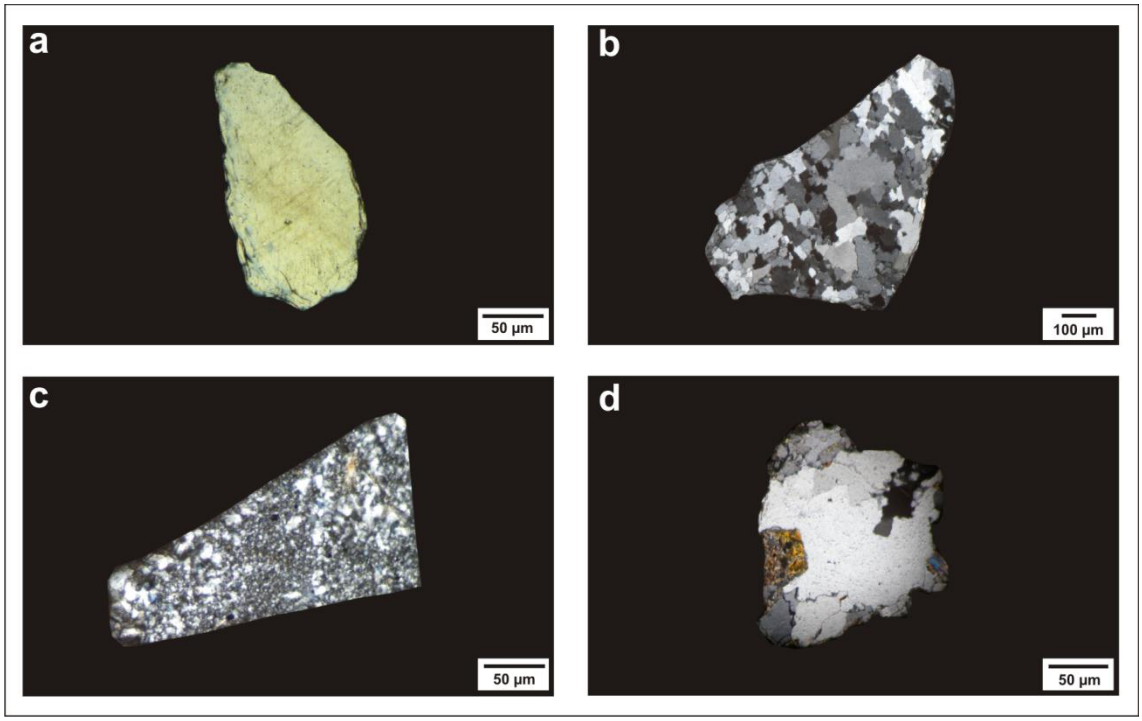

Figure II.2: Characteristic quartz grain types in the analyzed samples. (a) Quartz grain with undulose extinction (undulatory: U), (b) quartz grain with subgrains (subgrain: S), (c) quartz grain with small, undeformed recrystallized grains (recrystallized: R), and (d) transitional quartz grain with heterogeneous microstructure

This statistical analysis reveals that the microscopically defined extreme grains have significantly different spectral attributes, and thus can also be classified based on certain Raman spectral variables.

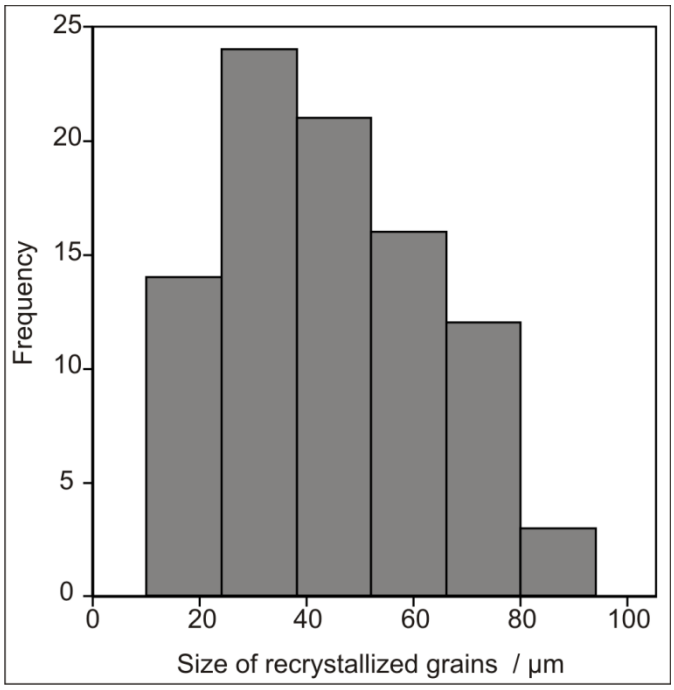

Figure II.3: Frequency distribution of recrystallized grain size in the R quartz grain type (n=100)

The extreme grains appear as rather tight clouds of points, with their centers defining a triangle in the *F1-F2* spectral space *(Fig. II.5/a)*. The most important (large weights in the discriminant function) spectral attribute best describing the difference between U and S grains is the integrated area of the 128 and 206 cm^{-1} bands, while the difference between S and R grains is mainly characterized by the positions of the 128, 206, and 464 cm^{-1} bands.

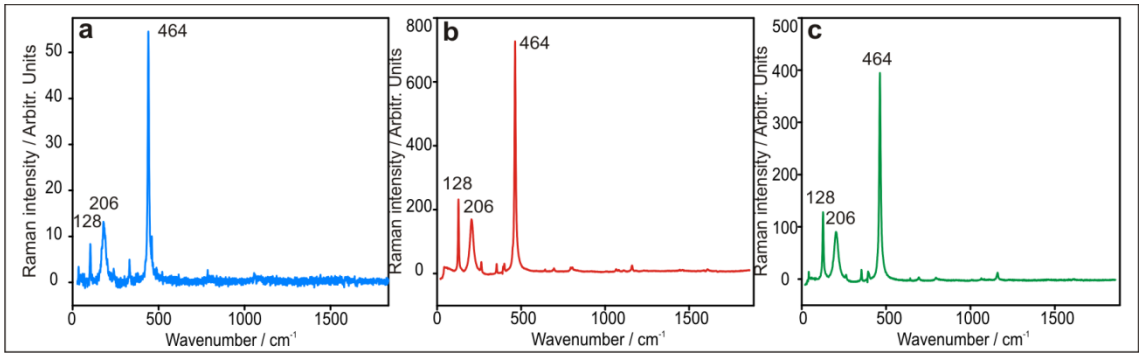

Figure II.4: Raman spectra of the three extreme quartz grain types. (a) Raman spectrum of the U grain type, (b) Raman spectrum of the S grain type, and (c) Raman spectrum of the R grain type

Based on histograms of the variables *(Fig. II.6)*, the integrated area of the 128 cm^{-1} band is increased *(Fig. II.6/a, b)* and that of the 206 cm^{-1} band is decreased *(Fig. II.6/c, d)* in S grains compared to U grains. The peak positions of the 128 and 464 cm^{-1} bands are shifted toward higher wavenumbers *(Fig. II.6/ e, f, i, j)* and that of the 206 cm^{-1} band shifted toward a lower wavenumber *(Fig. II.6/ g, h)* in R grains compared to S grains. The *F1* and *F2* discriminant functions were also then applied in order to calculate the spectral positions of the ten transitional grains, with the results revealing each transitional grain to be situated inside the triangle defined by the U, S and R extreme grains *(Fig. II.5/b)*. The spectra measured along a line inside the quartz grains also appear along a line, or at least in a cluster of points, in the spectral space.

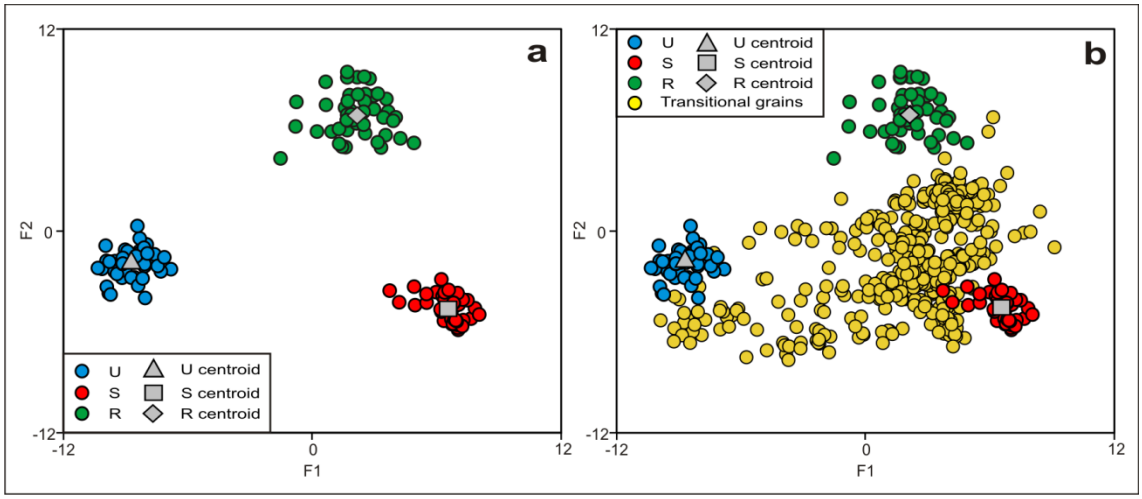

Figure II.5: Position of grains in the spectral space. (a) Position of U-S-R extreme quartz grain types in the spectral space (U-S-R triangle) and (b) U-S-R spectral space with transitional grains

In order to better follow tendencies, clusters of points for each transitional, randomly oriented quartz grain were substituted for characteristic trend-lines in the U-S-R field *(Fig. II.7)*. Analysis of *Fig. 7* reveals every line to extend between the U-S and S-R apexes, with all trend-lines going from U to S becoming discontinuous before reaching S *(Fig. II.7/b)*. Others consist of two segments: one part extends from U towards S and the other from S to R *(Fig. II.7/a)*. A number of additional trend-lines without any discontinuities are also apparent.

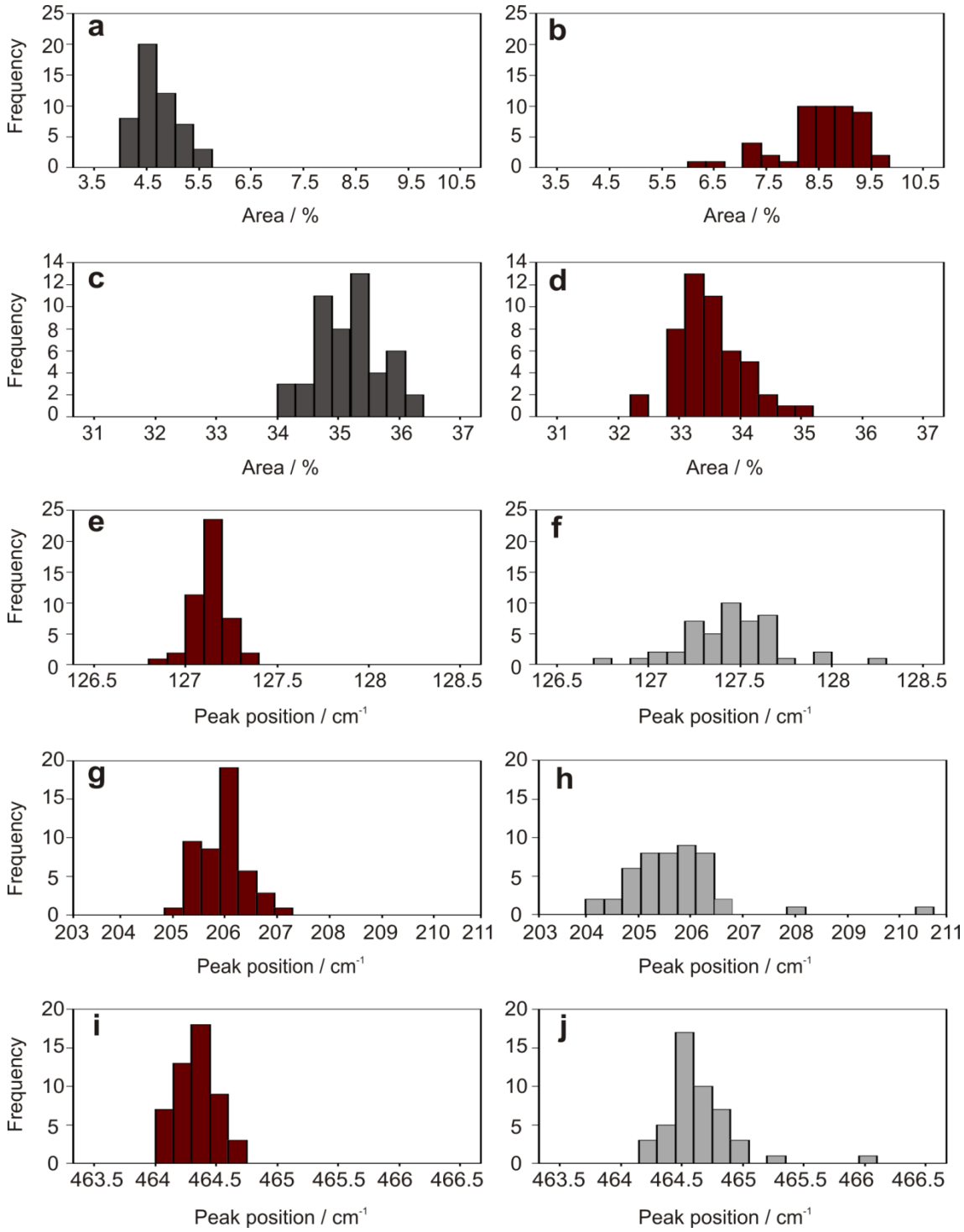

Figure II.6: Histograms of spectral variables. (a) Integrated area of the 128 cm^{-1} band for the U grain type, (b) integrated area of the 128 cm^{-1} band for the S grain type, (c) integrated area of the 206 cm^{-1} band for the U grain type, (d) integrated area of the 206 cm^{-1} band for the S grain type, (e) peak position of the 128 cm^{-1} band for the S grain type, (f) peak position of the 128 cm^{-1} band for the R grain type, (g) peak position of the 206 cm^{-1} band for the S grain type, (h) peak position of the 206 cm^{-1} band for the R grain type, (i) peak position of the 464 cm^{-1} band for the S grain type, and (j) peak position of the 464 cm^{-1} band for the R grain type

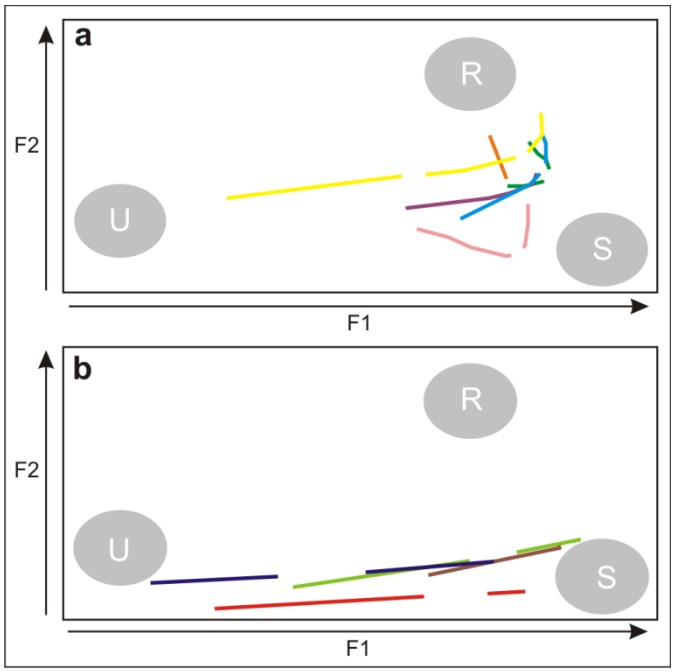

Figure II.7: Developmental path of ten transitional quartz grains in the U-S-R virtual deformational space. (a) Curved trend lines and (b) straight trend lines

II.6 Discussion

II.6.1 Extreme grains

The crystal structure of quartz develops due to various deformation mechanisms taking place under different pressure and temperature conditions (Hirth and Tullis 1992; Stipp et al., 2002; Vernon, 2004; Passchier and Trouw, 2005; Halfpenny et al., 2012). As a consequence, analysis of microstructure can reveal the deformation process responsible. In the present study, three microstructurally extreme quartz grain types were identified: grains with undulose extinction (U) *(Fig. II.2/a)*, grains with subgrains (S) *(Fig. II.2/b)*, and grains consisting of small, undeformed recrystallized grains (R) *(Fig. II.2/c)*.

Textural evidence indicates that the U quartz grains were formed via bulging recrystallization (BLG), a mechanism usually acting at low temperatures ($T \leq 300–400$ °C) and high strain rates. In contrast, the S and R quartz grains probably developed via subgrain rotation recrystallization at different temperature ranges (SGR I, SGR II) – although the latter process is generally characteristic at medium temperatures (T=400–500 °C) and strain rates. Given these results, the three extreme microstructural types were formed by different deformation mechanisms *(Fig. II.1)* and thus represent a range of conditions, with increasing temperature from U through to R (Hirth and Tullis 1992; Stipp et al., 2002; Vernon, 2004; Passchier and Trouw, 2005; Halfpenny et al., 2012).

As these grains are separated in the spectral space on the basis of the selected Raman spectral parameters, the U-S-R triangle *(Fig. II.5/a)* also represents a virtual deformational space.

II.6.2 Connection between extreme grains

The BLG mechanism is characterized by quartz grains with many curved dislocations, because the rate of dislocation production is greater than the rate of dislocation climb. In contrast, during SGR, with an increase in temperature or decrease in flow stress, microstructural observations indicate that the rate of dislocation climb becomes sufficiently rapid to accommodate recovery (Hirth and Tullis 1992). Thus in this regime the ordering of dislocations may start in subgrain boundaries (SGR I) and grain boundaries (SGR II).

The most important spectral attributes describing the difference between the U and S grain types are the integrated areas of the 128 and 206 cm^{-1} bands. The intensity of any band changes proportionally with its integrated area, and also decreases with an increase in the microstructural disordering of quartz grains (Ostroumov et al., 2002). The internal structure of S with respect to that of U grains displays a higher degree of ordering, because the recovery process had already started in the former. According to the histograms of spectral variables, the integrated area of the 128 cm^{-1} band is increased in S grains relative to U grains *(Fig. II.6/a, b)*, whereas the integrated area of the 206 cm^{-1} band is decreased *(Fig. II.6/c, d)*. The difference between S and R grains is largely characterized by the peak positions of the 128, 206 and 464 cm^{-1} bands. Band position is shifted toward lower wavenumbers due to an increase in microstructural disordering (Ostroumov et al., 2002). The internal structure of R grains exhibits a higher degree of ordering than that of S grains, affirming that the recovery mechanism has already reached a more advanced state in the former. Histogram analysis reveals the position of the 128 and 464 cm^{-1} bands to be shifted toward higher wavenumbers in R grains *(Fig. II.6/e, f, i, j)*. In contrast, the position of the 206 cm^{-1} band is shifted toward lower wavenumbers *(Fig. II.6/g, h)*.

The behavior of the 206 cm^{-1} band is specific for both U-S and S-R pairs, likely reflecting the fact that the 206 cm^{-1} band is associated with the temperature-dependent Si-O-Si bond angle inside the SiO_4 tetrahedron, which is controlled by thermal expansion (Levien et al., 1980). With rising temperature, an enormous broadening of the

206 cm^{-1} band is observed, which is clearly attributable to progressive α-β alteration in the structure before transformation (Krishnamurti, 1958). As line broadening results in a decrease in band intensity (Ostroumov et al., 2002), the combination of different processes taking place with increasing temperature leads to both a reduction in the band intensity of the 206 cm^{-1} band and a shift toward lower wavenumbers of the band position (Lin, 1997).

During our investigation randomly oriented quartz grains were analysed. Difference in orientations can cause considerable change in the relative intensity of bands in Raman spectra if polarized laser beam is used (Dionot and Brändlein 2011). However, because in our study, the effectiveness of the utilised depolarized laser beam is very good (DOP< 8%), the orientation dependence in measurements must be minimal.

II.6.3 Transitional grains

The microstructure of the transitional grains formed as a result of various deformation mechanisms. Placing these microstructurally transitional quartz grains in the U-S-R virtual deformational space *(Fig. II.7)* enables information to be obtained regarding the type of deformational transitions represented. A number of quartz grains appear transitional between extreme deformational conditions (denoted by continuous trend-lines) *(Fig. II.7)*, while others are composites of domains characterized by different deformational conditions (denoted by intermittent trend-lines) *(Fig. II.7)*. Although each quartz grain also appears elsewhere in the structural evolution and U-S-R fields, these data can together be used to determine the pathway characteristic of the deformation history of the rock volume they represent. In *Fig. II.7* the ten lines of the transitional grains are situated between U-S and S-R, with no lines extending between U-R. This pattern clearly confirms the fact that deformation proceeded from U towards R and across S in the investigated rock volume, a result in good agreement with the process of dislocation climbing defined by dynamic recrystallization (Hirth and Tullis 1992; Stipp et al., 2002; Vernon, 2004; Passchier and Trouw, 2005; Halfpenny et al., 2012). However, as more trend-lines break between the U and S states *(Fig. II.7/b)*, one cannot exclude the presence of a late deformation event under U conditions.

On the basis of the reconstructed deformation history, two deformational events, D1 and D2, can be supposed. During the first deformational event (D1), U quartz grains with undulose extinction and high dislocation density were transformed into S quartz

grains with subgrains. Later on during the D1 event, the recovery process began and thus the effect of microstructural ordering increased inside the grains, leading to the development of subgrains. During the second deformational event (D2), when R grains developed within small undeformed recrystallized grains, the recovery process was already more advanced, and as a result microstructural ordering became observable and the dislocations were ordered into grain boundaries.

On the basis of the microstructure of the quartz grains, the temperature of the deformational events can be roughly estimated (Hirth and Tullis 1992; Passchier and Trouw, 2005). Thus, U microstructure likely formed at ca. T=250–350 °C, while the temperature of the D1 event was potentially significantly higher at ca. T=400–450 °C. The maximum temperature reached during the deformation process can be predicted from the recrystallized grain size of R quartz grains (Stipp et al., 2002). Because the average grain size of the latter is only a few tens of microns, the temperature probably did not exceed T=500 °C, and thus the D2 event probably took place at ca. T=450–500 °C. In summary, the deformation history represented by the D1 and D2 events likely defines a pathway between ca. 250 and 500 °C conditions.

II.7 Summary and conclusions

Examination of the microstructure of the newly-available detrital quartz grains has provided valuable information regarding the evolution of a subsurface shear zone. Raman microspectroscopic analysis enabled single quartz grains and monomineralic domains, which are characterized by different deformation conditions, to be identified and classified. Three microstructurally-extreme quartz grain types were discriminated in the subsurface shear zone: U grains with undulose extinction, S grains with subgrains, and R grains consisting of small, undeformed recrystallized grains. The above extremes exhibit significantly different spectral attributes, and thus the quartz grains can accordingly be divided on the basis of certain Raman spectral variables. The spectra of all extreme grains (U, S, R) define closed groups of points in the spectral space, with each transitional grain situated inside this triangle. The three extreme quartz grain types were formed by different deformation mechanisms (BLG, SGR I, SGR II), and thus represent a range of deformation conditions associated with increasing temperature from U to R (ΔT≈250–500 °C). The U-S-R spectral space can therefore also be considered a virtual deformational space. Although each complex quartz grain analyzed

appears elsewhere in the deformation process defined by the U-S-R extreme conditions, they together represent a deformation development pathway. This combined pathway can be assumed characteristic for the whole rock volume under study.

Determination of the virtual deformational space enabled the reconstruction of the deformation history of the examined shear zone based on the available detrital quartz grains. Further study should involve establishing a generalization of the created local system.

Chapter III.: Localisation of ductile and brittle shear zones along Szentlőrinc-1 well in the Mecsekalja Zone using quartz microstructural and well-log data

Ágnes Skultéti

Department of Mineralogy Geochemistry and Petrology,
University of Szeged, Szeged, Hungary
skulteti.agi@gmail.com

Tivadar M. Tóth

Department of Mineralogy Geochemistry and Petrology,
University of Szeged, Szeged, Hungary
mtoth@geo.u-szeged.hu

Acta Geodaetica et Geophysica
51/2, 295-314 (2016)
DOI 10.1007/s40328-015-0127-3

Localisation of ductile and brittle shear zones along Szentlőrinc-1 well in the Mecsekalja Zone using quartz microstructural and well-log data

Abstract

Quartz is among the most common minerals in the Earth's crust and is stable within a wide range of temperature and pressure conditions. As its microstructure is sensitive to different deformation mechanisms, quartz may present information about the structural evolution of many different rock types. The Szentlőrinc-1 well with its drill cuttings brought to the surface from approximately 2 km depth provides an exclusive chance to investigate the shear zone beneath. The drill cutting collection includes only a few small rock grains, and more than 80% of the material consists of tiny (< 1 mm) single quartz grains. In this study, three microstructurally extreme quartz grain types were separated during microscopic analysis: grains with undulose extinction (U), grains with subgrains (S), and grains with recrystallized grains (R). Moreover, numerous microstructurally transitional grains were measured, which represent combinations of the above extremes. The characterisation of single quartz grain microstructures along the whole well enables identification and localisation of the ductile shear zones inside the crystalline complex. This information was combined with well-log data, which could provide information about the brittle deformation. Using these logs, brittle shear zones can be localised along the well. When comparing depths and extensions of the deformed horizons, a coincidence of the brittle and ductile zones becomes clear. This behaviour may suggest two different evolution schemes: it could be caused by primarily evolved softened regions, or it could be described by a detachment fault model.

Keywords drill cuttings, quartz, microstructure, well-log data, shear zone localisation, brittle and ductile shear zones

III.1 Introduction

In several places, because of their intensive deformation, shear zones behave as excellent fractured fluid (hydrocarbon or geothermal) reservoirs. Therefore, the petrographic and structural characterisation of shear zone formations is of basic importance. The investigation of shear zone rocks is usually possible only in surface

outcrops and, in cases of covered hard rock bodies, using drill core specimens, which provide only rather diffuse information. Our samples represent a newly bored geothermal well located inside the Mecsekalja Shear Zone, in the South Transdanubian region of Hungary *(Fig. III.1/a)*. There was no borecore recovery in the Szentlőrinc-1 well, and drill cuttings were brought to the surface from approximately 2 km depth, providing an exclusive chance to investigate the material of the shear zones beneath. The drill cutting collection includes only a few small rock fragments unsuitable for traditional petrographic and structural evaluation; more than 80% of the material consists of tiny (< 1 mm) pieces of single quartz.

Quartz is present in the Earth's crust as a common and resistant mineral, and is stable across a rather wide range of temperature and pressure conditions. Its microstructure is nevertheless very sensitive to stress and, at various *P-T* conditions quartz deforms by different deformation mechanisms resulting in grains with various microstructures. As a consequence quartz may provide valuable information regarding the structural evolution of numerous distinct rock types (Hirth and Tullis, 1992; Stipp et al., 2002; Vernon, 2004; Passchier and Trouw, 2005; Halfpenny et al., 2012). During the deformation of quartz aggregates dislocation creep is an important mechanism defined by different dynamic recrystallization mechanisms (Hirth and Tullis, 1992; Tullis et al., 2000). Dynamic recrystallization can occur in various forms depending on temperature and strain rate. These are bulging (Regime 1), subgrain rotation (Regime 2) and grain-boundary migration (Regime 3), with increasing temperature and decreasing strain rate (Hirth and Tullis, 1992). The bulging recrystallization (BLG) (Hirth and Tullis, 1992) takes place at low temperatures (<300–400 °C for quartz) (Passchier and Trouw, 2005) and is characterized by deformed parent grains with a high dislocation concentration and undulose extinction (Halfpenny et al., 2012). Subgrain rotation recrystallization (SGR) occurs at higher temperatures (Hirth and Tullis, 1992) (400–500 °C for quartz) (Passchier and Trouw, 2005) and is characterized by ductily deformed, elongated and ribbon-shaped parent grains with many subgrains. As a result of this process the remains of old grains are commonly surrounded by groups of recrystallized grains (a feature known as a core-and-mantle structure in Gifkins, 1976; White, 1976; Shigematsu, 1999) or may be completely replaced by recrystallized material (Hirth and Tullis, 1992; Stipp et al., 2002). High temperature grain-boundary migration recrystallization (GBM) (Hirth and Tullis, 1992) (500– < 700 °C for quartz) is

characterized by grains with new, lobate grain boundaries (Vernon, 2004; Passchier and Trouw, 2005).

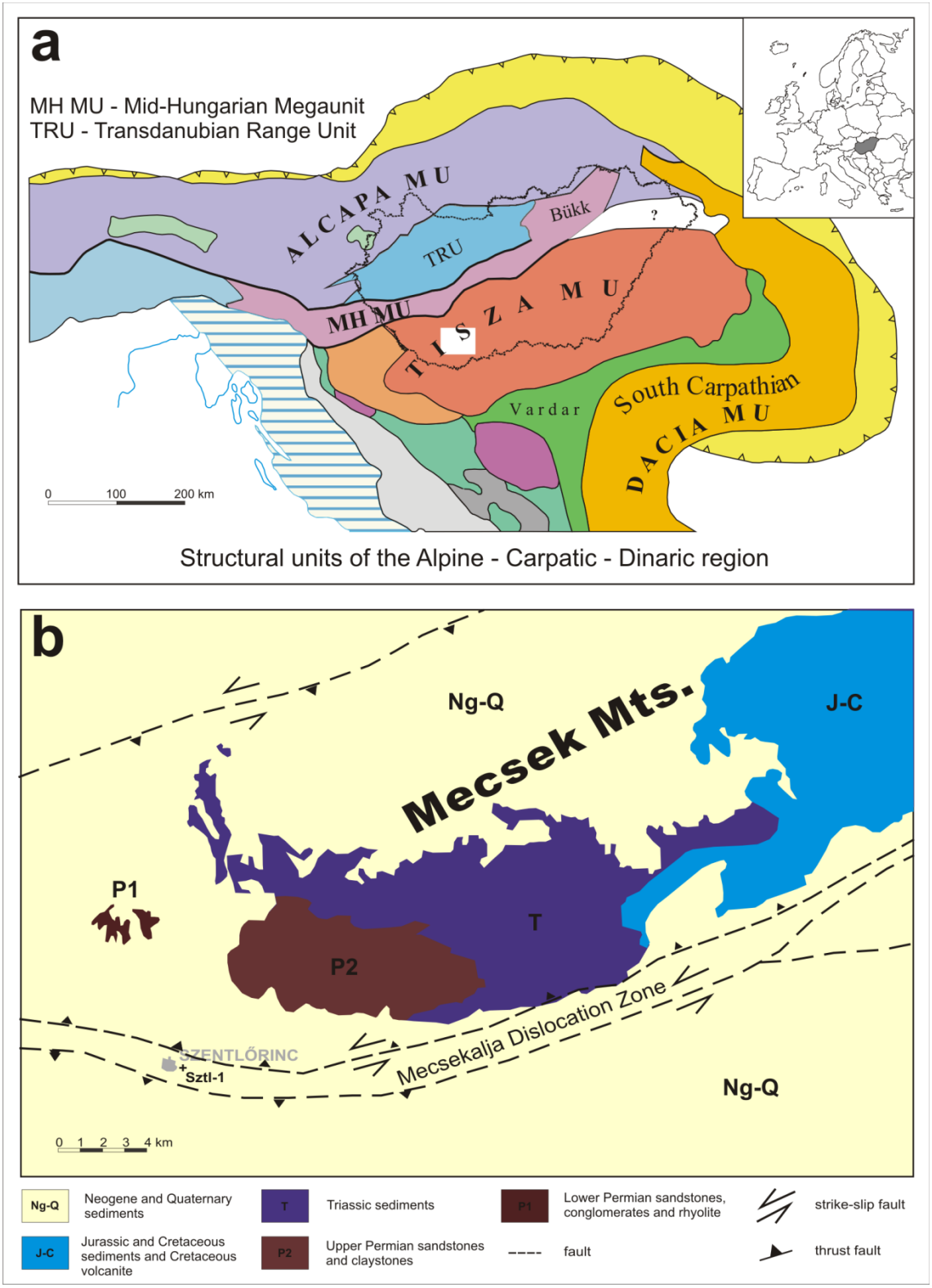

Figure III.1: (a) Location of the study area (white square) inside of the Pannonian Basin (based on Haas et al. 2010). (b) The Mecsekalja Zone with the studied Szentlőrinc-1 (Sztl-1) well (based on Konrád et al. 2010)

In the previous phase of the recent research during the microscopic analysis of quartz grains, three microstructurally different end-member quartz grain types were distinguished from the subsurface shear zone in study: grains with undulose extinction (undulatory: U), grains with subgrains (subgrain: S), and grains with recrystallized grains (recrystallized: R). Moreover, several microstructurally transitional grains were identified, which represent combinations of the above end-members (Skultéti et al., 2014). The U type quartz grains were formed by the bulging recrystallization mechanism (BLG) (Hirth and Tullis, 1992), while the S and R type quartz grains most likely developed by subgrain rotation recrystallization (SGR) (Hirth and Tullis, 1992) under different physical conditions (SGR I, SGR II) (Skultéti et al., 2014). In accordance with this phenomenon, the three end-member microstructural types formed by different deformation mechanisms represent diverse conditions with increasing temperature and/or decreasing strain rates from U toward R type (Skultéti et al., 2014).

The primary aim of our study is to identify and locate the ductile shear zones inside the Mecsekalja Shear Zone along the Szentlőrinc-1 well by characterising deformation mechanisms in a large set of single quartz chips at various depths. Afterwards, the brittle shear zones are determined using a wide set of well-logs and are compared to the depths of the ductile zones. Thus, the final aim is the reconstruction of the structure and deformation history of the fractured geothermal reservoir.

III.2 Geological settings

The Pannonian Basin was formed as a result of a complicated extension process during the Miocene (Tari et al., 1992). Its pre-Neogene, basically crystalline basement consists of crustal blocks of diverse origins and complex structural evolutions. The Alcapa and Tisza-Dacia Blocks are the main structural units in the basement of the Pannonian Basin, which were juxtaposed only in the Neogene *(Fig. III.1/a)*.

In the Tisza-Dacia block, the structural evolution of the crystalline basement started during the Variscan orogeny (Szederkényi, 1984, 1996; Árkai et al., 1985; Lelkes-Felvári and Frank, 2006). The Variscan tectonic events were followed by a pervasive extension in the Jurassic (Csontos et al., 1992; Haas and Péró, 2004) and then the nappe formation in the Cretaceous (Tari et al., 1999; Haas and Péró, 2004). As a result of the complex basin subsidence in the Neogene (Bergerat, 1989; Tari et al., 1992; Horváth and Cloetingh, 1996; Csontos and Nagymarosy, 1998), more kilometre

deep sub-basins (Békés Basin, Makó Trough) and metamorphic basement highs (Tari et al., 1992; Tari et al., 1999; Zachar and M. Tóth, 2004, Schubert and M. Tóth, 2001; M. Tóth et al., 2000; M. Tóth and Zachar, 2006) covered with several km thick sediment were formed. The basement formations deformed intensively during the Neogene subsidence. As a result of the complex tectonic evolution, the crystalline basement is made up from blocks with various metamorphic and structural evolutions (M. Tóth et al., 2000; Schubert and M. Tóth, 2001).

The Mecsekalja Zone is a 1.5 km wide tectonic zone inside of the Tisza-Dacia block; an active transcurrent zone since the Permian (Szederkényi, 1977, 1979). In this dislocation belt *(Fig. III.1/b)*, formations with various lithologies and in most parts intensively mylonitised metamorphic rocks were outcropped. The gneiss, quartzphyllite, crystalline limestone, serpentinite and amphibolite that fill out the Mecsekalja Zone belong to the Ófalu Group lithostratigraphically.

The oldest pre-Variscan and Variscan (Balla et al., 2009) events of the research area were the magmatic formation of the protolith (granite) and early regional metamorphism of the Studervölgy Gneiss. The rocks of the Ófalu Group were assembled by intensive tectonic movements into a new, larger coherent geological unit during the Early Carboniferous orogenic phase of the Variscian tectogenesis. Thus the following late Variscan tectonometamorphic events uniformly affected the newly formed geological and tectonic unit. During the principal postintrusive metamorphic event of the tectonometamorphic evolution of the Mecsekalja Zone, the rocks of the Ófalu Group uniformly suffered high-temperature greenschist facies (>350–400 °C) regional metamorphism (Balla et al., 2009).

Based on geophysical data (Thorbergsdottir et al., 2010), it can be assumed that the studied Szentlőrinc-1 well penetrated the deep sections of the Mecsekalja Zone. The lithologies revealed by the well are Cenozoic, Mesozoic and Paleozoic aged. The Cenozoic, Miocene and Eocene formations are predominantly clastic sediments and sedimentary rocks. The Mesozoic includes limestone with clay intercalations, while the Paleozoic section consists of metamorphic rocks, mainly gneiss and mica-schist (Thorbergsdottir et al., 2010); the crystalline basement was penetrated by the well at 1330 m depth. Analyses of the samples from the basement enable the recognition of the subsurface formations of the Mecsekalja Zone.

III.3 Samples

The investigated samples represent the Szentlőrinc-1 (Sztl-1) deep drilling, the base of which reached a depth of 1820 m. The well penetrated rocks of the Mecsekalja Shear Zone. Drill cuttings were taken every 5 m in the 1600-1820 m interval. The drill cuttings take the form of mm-size debris, constituted by single mineral and rock pieces in an 80:20 ratio, for the most part dominated by single quartz grains. The analysed samples were mainly individual quartz grains and quartz grain fragments. In this part of the research, the available quartz grains were examined every 25 m, and analysis was performed every 5 m in the possible fractured zones defined by well-log interpretation.

III.4 Methods

III.4.1 Microstructural analysis

The microscopic analysis of the 17 normal thin sections, made from samples representing different depth intervals along the well (1600–1820 m), was performed using an Olympus BX-41 polarisation microscope using magnification of 10x and 40x objectives. Within the confines of microstructural analyses, the quartz grains of the available drill cutting samples were analysed every 25 m (1600, 1625, 1650, 1675, 1700, 1725, 1750, 1775, 1800, 1820 m), and in the possible fractured zones, the 1605, 1610, 1615, 1620 m and 1755, 1760, 1765 m samples were also studied. During the microscopic analysis, 100 pieces of randomly selected (JMicroVision: point counting method) quartz grains were microstructurally examined in every sample. The ratio of the microstructurally different quartz grains was analysed in the case of every depth interval.

The microstructural types identified during the examination were as follows *(Fig. III.2)*. End-member quartz grain types: grains with undulatory extinction (U), grains with subgrains (S) and grains with recrystallized grains (R); microstructurally transitional quartz grain types: heterogeneous grains in which U and S type domains were observed in an approximately equal ratio (U≈S), grains in which U type grains were dominant (U>S), grains in which S type grains were dominant (S>U), transitional grains in which S and R type domains were observed in an approximately equal ratio (S≈R), grains in which S type domains predominated (S>R), and grains in which R type grains predominated (R>S). Moreover, there are such grains in which all of the three microstructural types appear in grains (U-S-R). During the analysis of every measured

sample (100 quartz grains), the proportion of the microstructurally different quartz grains was determined as a percentage (%).

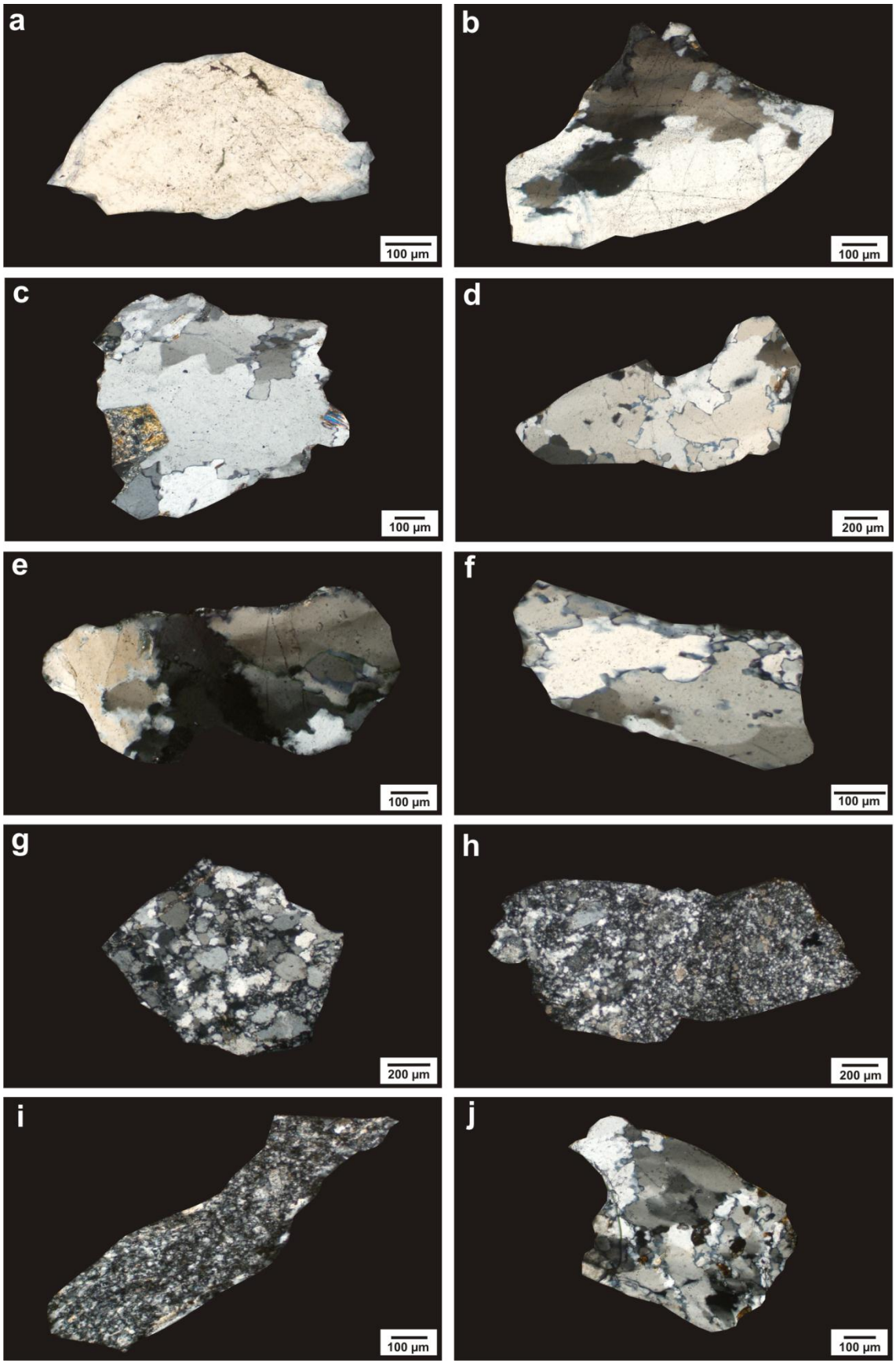

<<
Figure III.2: Microstructural types of quartz in the studied samples (a) U (microstructural class with undulatory extinction), (b) U>S, (c) U≈S, (d) S<U, (e) S (microstructural class with subgrains), (f) S>R, (g) S≈R, (h) R>S, (i) R (microstructural class with recrystallized grains), (j) U-S-R

The resulting data were plotted on special triangle diagrams *(Fig. III.3)* every 25 m in depth, along the studied well section (1600–1820 m). At certain peak points of the diagram, the three extreme quartz grain types were represented. The cells between these three (U, S, R) vertices and the central small triangle represented the microstructurally transitional quartz grains. On these special triangle diagrams, the percentile of the microstructurally different quartz grain types was marked by filling with various grey levels (0%=white, 60%=black).

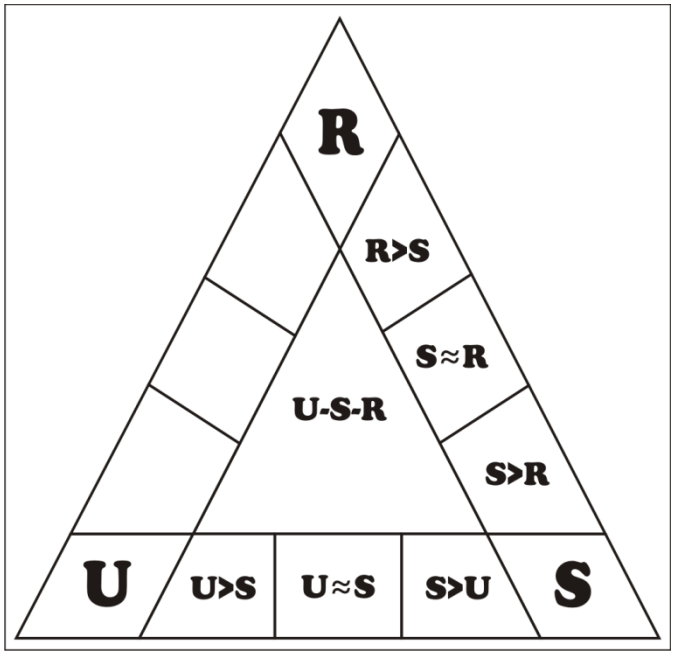

Figure III.3: Shape of the U–S–R triangle diagram. In certain peak points of the diagram, the three extreme quartz grain types are represented: grains with undulatory extinction (U), grains with subgrains (S) and grains with recrystallized grains (R), subgrains. The cells between these three peak points and the central small triangle represent microstructurally transitional quartz grains

III.4.2 Well-log data analysis

The aim of the well-log analysis was to determine the position of the intensively deformed brittle shear zones inside of the metamorphic section (1370–1820 m) of the studied well.

From the analysed Szentlőrinc-1 deep drilling (Thorbergsdottir et al., 2010), coarse geophysical data every 10 cm and analogous well-logs are available for the whole drilling (2–1822 m). During the assimilation of the coarse geophysical data, the

corresponding well-logs were first sorted. Within the confines of separation, the porosity logs (density log) were sorted to determine those that could be used to locate the fractured, permeable zones (gamma, resistivity, spontaneous potential and calliper log). Then, the data of the selected well-logs were restricted to those intervals from which drill cutting samples are available. Thus, in the following, the data were analysed from 1600 to 1820 m.

III.4.2.1 Analysed well-logs

The density log (long 35 cm detector distances) (DEL) is a porosity log that measures the formation's bulk density, including solid matrix and the fluid enclosed in the pores (Rider, 1996). The formation bulk density is a function of the matrix density, porosity and density of the fluid in the pores. During the density measurement, a radioactive source emits gamma rays into the formation (Schlumberger, 1989), where they collide with electrons. The collisions result in a loss of energy from the gamma ray particle. The amount of scattered gamma rays reaching the detector is proportional to the electron density of the formation (Asquith and Gibson, 1982; Schlumberger, 1989). In most rock types, the electron density is related to the formation's true bulk density (Tittman and Wahl, 1965), and the bulk density is a function of porosity (Asquith and Gibson, 1982; Schlumberger, 1989). Comparing the density log with gamma and calliper logs enables the determination of fractured zones (Rider, 1996).

The gamma ray log (GR) is a lithology log, which measures the natural radioactivity of the formation. The natural radioactivity of the formations derives from ^{40}K, ^{238}U, ^{232}Th and their daughter elements (Asquith and Gibson, 1982; Rider, 1996). In the case of non-radioactive formations, the potassium content mostly relates to clay minerals and K-feldspar (Schlumberger, 1989). The geological significance of radioactivity lies in knowing the distribution of these three elements in the rocks. Most rocks are radioactive to some degree, igneous and metamorphic rocks more so than sediments. The gamma ray log often is used to determine clayey rock zones (Rider, 1996).

The resistivity log (160 cm electrode distances) (R160) displays the formation's resistance to the passage of an electric current. Electricity can pass through a formation only because of the conductive fluid it contains. Dry rocks are good electrical insulators (Schlumberger, 1989), although perfectly dry rocks are very rarely encountered in

nature. Therefore, the subsurface formations have measurable resistivity because of the resistivity of the fluid in their pores or absorbed on their interstitial clay (Asquith and Gibson, 1982; Schlumberger, 1989). The resistivity of the formation depends on the resistivity and amount of formation water and the pore structure geometry (Schlumberger, 1989). The resistivity of the formation can be measured by either sending current into the formation and measuring the ease of the electrical flow through it or by inducing an electric current into the formation and measuring how large it is (Schlumberger, 1989). The resistivity log can be used to indicate permeable zones and determine resistivity porosity (Asquith and Gibson, 1982).

The spontaneous potential log (SP) measures the direct current voltage differences between an electrode in the borehole and a reference electrode at the surface (Asquith and Gibson, 1982; Schlumberger, 1989; Rider, 1996). They originate from the electrical disequilibrium created by connecting formations vertically (in the electrical sense) when in nature they are isolated (Rider, 1996). Three factors are necessary to provoke an SP current: (1) a conductive fluid in the borehole, (2) a porous and permeable bed surrounded with an impermeable formation and (3) a difference in salinity or in pressure between the borehole fluid and the formation fluid (Rider, 1996). If the bed is not permeable, the ions cannot move; accordingly, flow does not occur and there is no potential change, so there is no spontaneous potential (Schlumberger, 1989). SP currents are created when two solutions of different salinity concentrations are in contact by two principal electrochemical effects: diffusion potential and shale potential (Asquith and Gibson, 1982; Schlumberger, 1989; Rider, 1996). The SP log displays not absolute values but the deflection of the curve from zero into positive or negative directions. The zero point is defined on thick shale intervals where the SP does not move and is called the shale base line. All values are related to this line (Rider, 1996). The spontaneous potential log can be used to characterise the permeability of formations. Permeable zones are indicated where SP deflection appears from the shale baseline. However, the amount of deflection does not indicate the amount of permeability: a very slightly permeable bed will give the same value as a permeable bed (Asquith and Gibson, 1982; Schlumberger, 1989; Rider, 1996).

The calliper log (CL) displays the borehole diameter with the depth, where diameter is defined by the bit size. The simple calliper log records the vertical profile of the borehole diameter, while the more complex borehole geometry tools provide accurate information about the borehole shape, orientation and volume. The deflection

from the bit size can be caused by various factors but is often due to lithological reasons and indicates the instability of the borehole wall. The calliper log can be used to dissociate the fractured zones, in which the borehole is enlarged because the rocks are mechanically less stabile (Schlumberger, 1989).

III.4.2.2 Interpretation of well-logs: discriminant function analysis

Each well-log provides some information about the depth position of the fractured zones through increased porosity and permeability as well as enhanced clay mineral content in the formation along the studied well section. However, a simultaneous application of the analysed well-logs could provide a more reliable and general idea about the location of the fractured zones (Molnár et al., 2015a).

During the analysis of the combination of the various well-logs, the well-log was selected first in which the highly fractured and the fresh rock zones along the well were most markedly distinct. Based on this choice, inside of the well, ca. 10 m long fractured and fresh rock zones were selected, and the coarse geophysical data representing these sections were selected from all of the analysed well-logs.

Next, discriminant function analysis was performed for the geophysical data that represent the fractured and fresh rock zones along the well, respectively. In this way, the linear combination of the well-logs can be computed to best discriminate the fractured and fresh rock zones. The final aim of the statistical analysis was to use this separation function for the whole studied section. The discriminant function analysis was performed using IBM SPSS Statistics Version 20.0.

III.5 Results

III.5.1 Microstructural results

The proportion of quartz grains of different microstructural classes in drill cuttings that represent consecutive depth intervals (1600-1820 m) are summarised in *Fig. III.4* and *Table III.1*. In the studied drill cutting samples, beside the quartz grains, rock fragments are also present that consist of muscovite, biotite, K-feldspar and plagioclase. Inside the upper part of the analysed well section ca. 1600–1750 m, muscovite and K-feldspar are dominant phases of the rock fragments, while further downward (1775–1820 m), the amount of biotite and plagioclase increases.

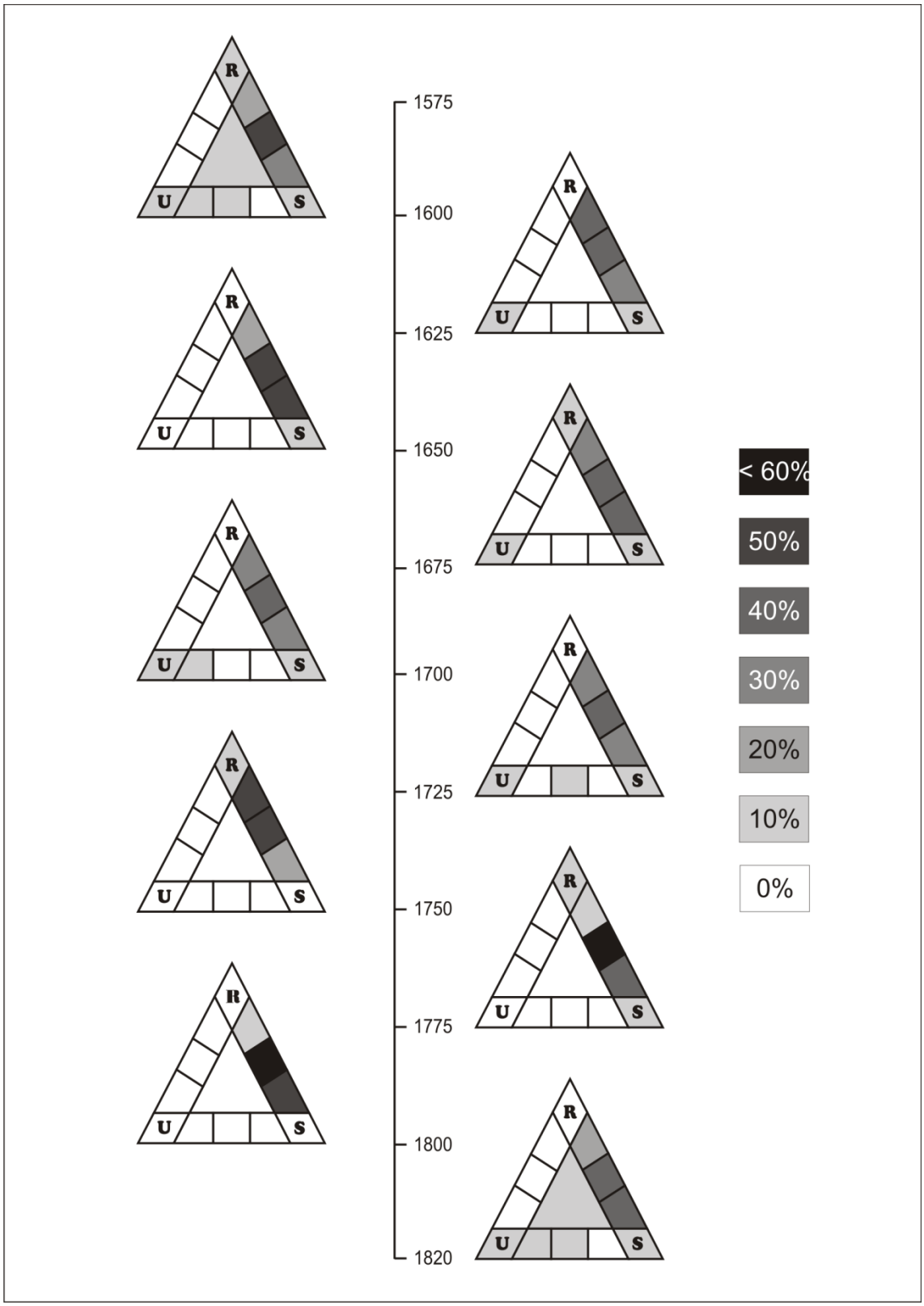

Figure III.4: Proportion (%) of the microstructurally different quartz grain types along the studied well with depth delineated on U-S-R triangle diagrams

Depth (m)	Quartz grain types (%)									
	U	S	R	S=R	S>R	R>S	U=S	U>S	S>U	U-S-R
1600	4	6	1	46	23	16	1	2	0	1
1605	2	11	5	22	38	21	0	0	1	0
1610	1	5	3	47	23	15	1	2	0	3
1615	0	1	2	30	12	54	0	0	0	0
1620	1	2	0	43	18	36	0	0	0	0
1625	1	3	0	35	21	40	0	0	0	0
1650	0	1	0	44	44	11	0	0	0	0
1675	1	6	1	38	31	23	0	0	0	0
1700	2	4	0	37	30	26	0	1	0	0
1725	3	3	0	35	28	30	1	0	0	0
1750	0	0	2	44	13	41	0	0	0	0
1755	0	2	0	68	20	7	0	0	0	3
1760	0	1	0	70	20	8	0	0	0	1
1765	0	3	0	65	24	7	0	0	0	1
1775	0	1	1	57	35	7	0	0	0	0
1800	0	0	0	51	45	4	0	0	0	0
1820	5	8	0	31	34	13	1	2	0	6

Table III.1 Amount of microstructurally diverse quartz grain types at different depth intervals along the Sztl-1 well

III.5.2 Geophysical results

In this study, the resistivity, density, gamma, spontaneous potential and calliper logs were interpreted *(Fig. III.5)*.

The resistivity log *(Fig. III.5/a)* displays a decrease in resistivity values ca. 1580–1605 m. After that, a significant resistivity increase could be observed from 1605 m down to ca. 1615 m, and the resistivity falls markedly between 1615–1635 m again. Between 1750–1765 m, the resistivity log similarly displays a significant decrease. Moreover, along the well-log, smaller, less significant resistivity drops can be observed (at 1650, 1680, 1705 and 1738 m).

The density log *(Fig. III.5/b)* displays a significant density increase between 1605–1615 m, which is followed by a density reduction between 1615–1635 m. Between 1750–1765 m, a density decrease could be observed. In addition, smaller density falls could be determined at 1650, 1680 and 1705 m.

On the gamma log *(Fig. III.5/c)*, one could observe that the gamma values are generally higher (>20 μR/h) between 1600–1710 m, while they tend to be smaller between 1710 and 1820 m (<20 μR/h). Thus, along the well-log, zones with higher and lower gamma values could be separated. Inside of the zone between 1600–1710 m, from 1605 to 1610 m, significantly higher gamma values are typical than in the sections between 1600–1605 m and 1610–1615 m.

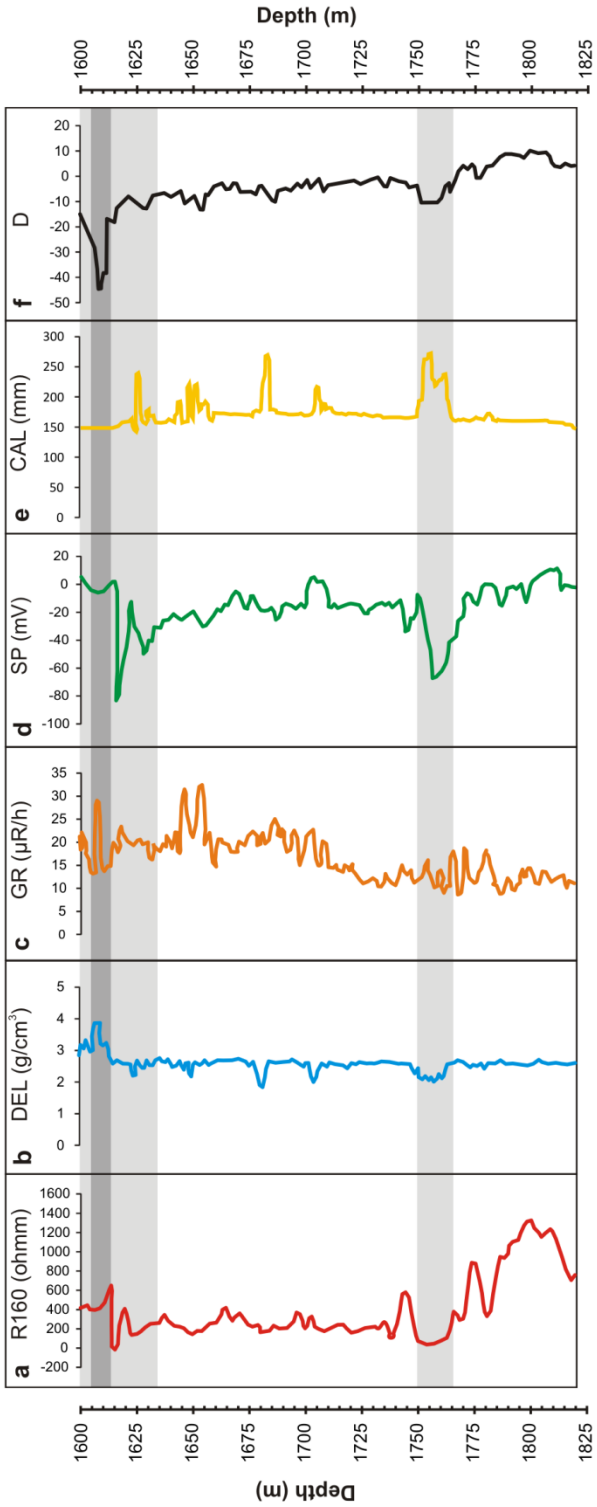
Depth (m)
1600
1625
1650
1675
1700
1725
1750
1775
1800
1825
f D
e CAL (mm)
d SP (mV)
c GR (µR/h)
b DEL (g/cm³)
a R160 (ohmm)
Depth (m)

<<
Figure III.5: Well-logs of the Sztl-1 well (1600–1820 m) using brittle shear zone localisation: (a) resistivity (R160), (b) density (DEL), (c) gamma ray (GR), (d) spontaneous potential (SP), (e) calliper log (CAL), (f) composite log (D) computed by discriminant function analysis. The grey bands display the potential brittle shear zones

The spontaneous potential log *(Fig. III.5/d)* displays a significant potential reduction between 1615–1640 and 1750–1770 m.

The calliper log *(Fig. III.5/e)* records an appreciable increase in the borehole diameter at 1680 m and between 1750–1765 m, while less significant borehole enlargement could be observed at approximately 1625, 1650 and 1705 m.

III.6. Discussion

III.6.1 Ductile deformation

The distribution of the strain inside a shear zone is not homogeneous in most cases; instead, it tends to be localised into planar horizons. Shear zones and faults develop along these shear localisation structures, and both involve displacement parallel to the walls (Passchier and Trouw, 2005; Fossen, 2010). The shear zones are tabular zones in which strain is notably higher than in the surrounding rock body (Fossen, 2010). The shear zones can be ductile, brittle (fault) or transitional brittle-ductile structures. In the case of ductile shear zones, the central zone with a higher deformation grade is enveloped by lower deformation grade belts. Thus, the intensity of deformation decreases from the middle of the shear zone outward (Wibberley et al., 2008).

Quartz is a stable mineral under wide *P-T* conditions; it nevertheless deforms in different ways at diverse *P*, *T* and strain rates following diverse deformation mechanisms, resulting in grains with various microstructures (Hirth and Tullis, 1992; Vernon, 2004; Passchier and Trouw, 2005). As a consequence, in quartz-bearing rocks, each quartz grain may provide valuable information about the deformation history of the rock body itself.

The proportion of recrystallized (R) and dominantly recrystallized (*R>S*) quartz grains displays two maxima inside of the studied well section between 1610–1635 m and 1750–1765 m *(Fig. III.6)*. Away from these depth intervals, the amount of recrystallized grains gradually decreases, while U and S type quartz grains and domains become dominant.

The three microstructural quartz classes (U, S, R) develop due to different deformation mechanisms (BLG, SGR I, SGR II) and thus represent a range of changing deformation conditions (Hirth and Tullis, 1992; Passchier and Trouw, 2005; Skultéti et al., 2014). During the deformation of minerals, temperature is an important factor. However, there are also other considerations such as strain rate, differential stress and the presence of water in the lattice and along grain boundaries, which also have relevant contributions to quartz deformation behaviour. In most cases, under high-temperature conditions, the recovery and recrystallization processes are promoted. At high strain rates, the role of crystal distortion increases, and due to the increased differential stress, more slip systems become active because of the reduction of the critical resolved shear stress of other slip systems (Hirth and Tullis, 1992; Passchier and Trouw, 2005). Thus, from U to R type, a continuous change of deformation conditions associated with increasing temperature (ΔT=250–500 °C) or with decreasing strain rate can be assumed.

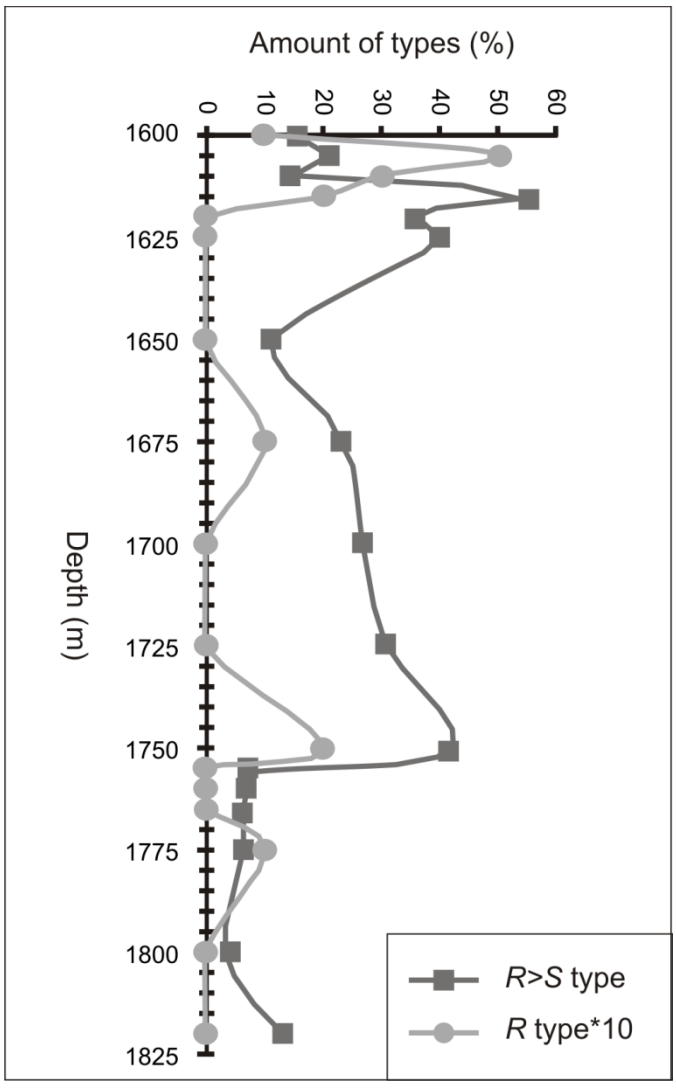

Figure III.6: Proportion of the R>S (microstructurally transitional quartz grain types in which R type grains are dominant) and R type (extreme quartz grain types with recrystallized grains) quartz grains along the well (1600–1820 m) in relation to depth. The proportion of the R type grains was represented in tenfold magnification because of the better visibility

There is no reason to presume a significant change in metamorphic temperature within a few tens of metres long section of the rock column. However, in shear zones with increasing strain, the quartz grains display a sequence of transient microstructures, indicating diverse deformation mechanisms. Thus, it can be assumed that toward the central region of a shear zone, simultaneously with increasing strain, the BLG, SGR I and SGR II dynamic recrystallization processes become dominantly active. Therefore, with increasing strain, the amount of recrystallized quartz grains (R type) should increase (Lloyd et al., 1992; Dell' Angelo and Tullis, 1996; Menegon et al., 2008). Thus it is probable that in the studied well, the R type quartz grains mark the most intensively deformed zones, while the U and S type grains denote the zones with weaker deformation. The intensively deformed core section of a ductile shear zone is usually dominated by R type grains, while further away the less deformed zones are denoted by increased frequency of U and S type quartz grains. Using this theoretical consideration, on the basis of our samples, ductile shear zones could be localised in two sections, one between 1610–1635 m and another at 1750–1765 m along the studied well section. An abrupt change in the mineralogical composition of the rock fragments (from muscovite and K-feldspar dominated to biotite and plagioclase dominated) also occurs at approximately 1750 m depth.

III.6.2 Brittle deformation

Brittle shear zones usually consist of a central slip surface or core, developed by intense shearing, and a surrounding volume of rock (damage zone) affected by less intense brittle deformation (Fossen, 2010; Wibberley et al., 2008). The fault core is frequently less permeable because of its high secondary clay mineral (fault gouge) content (Fossen, 2010). As the gamma ray value is related to the clay content of the formation (Asquith and Gibson, 1982; Schlumberger, 1989; Rider, 1996), it can be assumed that a fault gouge zone is situated between 1605–1615 m and surrounded on both sides (between 1580–1605 m and 1615–1635 m, respectively) by more permeable damage zones. In the studied well section between 1750–1765 m, a highly fractured and more permeable zone can be observed. Moreover, at approximately 1650, 1680 and 1705 m, local fractured rocks can also be identified.

To more precisely locate the most intensively fractured intervals along the well, discriminant function analysis was performed based on the digitised well-log data. For

this purpose, data representing the two most different sections 1754–1765 (fractured) and 1789–1800 m (fresh) were compared first. The calculations resulted in a discriminant function (*F*),

$$F = -5.52*DEL - 0.22*GR + 0.01*R160 + 0.06*SP + 11.75 \quad (1)$$

which describes the best linear combination of the geophysical parameters and separates the best the highly fractured and the fresh rock zones along the studied well. As a result, it could be established that the most important (large weights in the discriminant function) variable in separation is density, while gamma rays, resistivity and spontaneous potential have only minor roles. Based on the resulting *D* composite well-log *(Fig. III.5/f),* two major fractured zones become clear between 1580–1605 m and between 1750–1765 m, respectively.

On the basis of the available geophysical data, between 1580–1635 m, one can assume the presence of an intensively deformed brittle shear zone with a well-developed argillaceous core zone (between 1605–1615 m) enveloped by highly fractured damage zones on both sides. Moreover, at approximately 1650, 1680 and 1705, minor fractured zones could be assumed. During the seismic analysis of the study area in the environment of Sztl-1 well Tulinius et al. (2010) also identified a fault zone at the similar depth interval (1600–1700 m) of the crystalline basement.

The spontaneous potential log displays significant changes between 1615–1640 m and between 1750–1770 m. This phenomenon can be caused by the changing electrochemical behaviour of drilling mud that has been modified by the mixing of borehole fluid with formation water originated from an outward source. These peaks on the SP log mark water inflow zones along the well, confirming the positions of the highly fractured, permeable horizons.

III.6.3 Possible geodynamical interpretations

When comparing the depths and extensions of the deformed horizons of the Szentlőric-1 well, a notable coincidence of ductile and brittle (presumably cataclasite, breccia zones) shear zones becomes clear *(Fig. III.7).* This spatial appearance allows two different scenarios concerning structural evolution: they either formed due to the same tectonic episode or belong to different events.

In the continental lithosphere, the localisation of tectonic activity is influenced by many factors: beyond the temporal and spatial deviations in the thermal state of the lithosphere (Sonder and England, 1986; England, 1987), the presence of old faults and shear zones are also essential factors (Holdsworth, 2001). The formation of faults and shear zones is usually followed by a number of softening processes, which can cause substantial weakening both coincidentally with deformation and in the long-term. The generations of previous cohesionless fractures, grain refinement processes, general reaction softening, geometric and fabric softening and thermal perturbations in faults and shear zones lead to long-term weakening. Other processes, such as shear heating, increase in pore fluid pressure, transient fine-grained reaction products, transformational plasticity, variations in pore fluid chemistry and fluid-assisted diffusive mass transfer may cause transient weakening in faults and shear zones (Holdsworth, 1997).

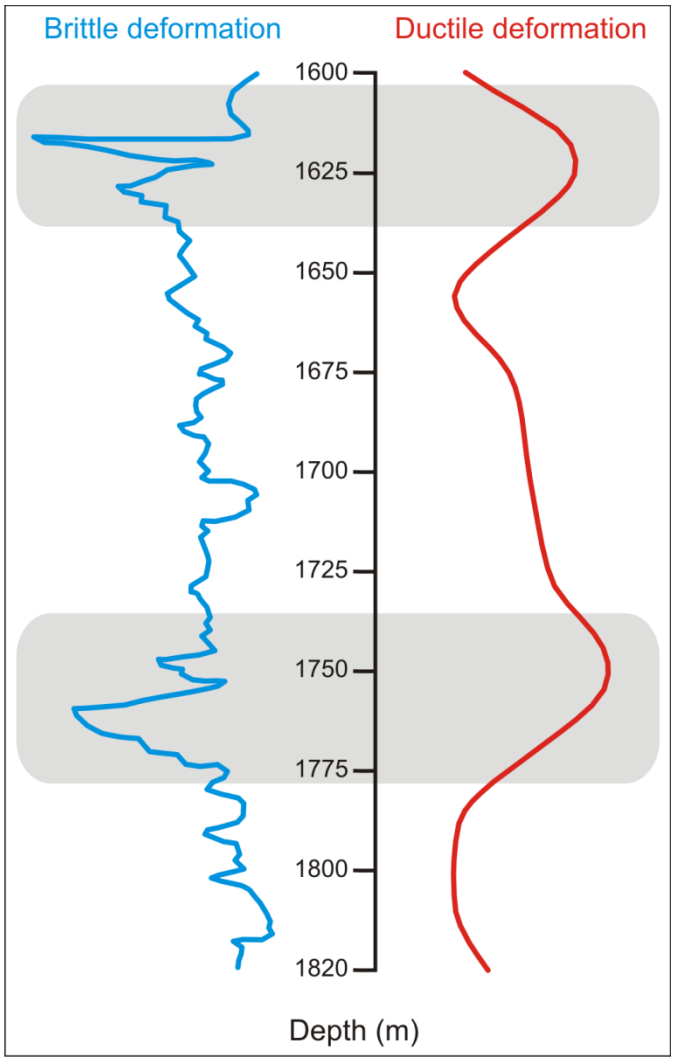

Figure III.7: Characterization of single quartz grain microstructures along the whole Sztl-1 well enables localization of the ductile shear zones inside the crystalline complex, these zones coincide very well with the brittle horizons defined by well-log evaluation

Thus, if the firstly evolved ductile shear zones caused softened regions inside the crystalline mass, it could reactivate later in a brittle way due to a tectonic event independent of the early one. The early faults and shear zones in the continental crust operate as softened planes, so when the crust is experienced new stress field, those areas perform as preferred regions for reactivation (White et al., 1986). Holdsworth (1997) defined the reactivation as the emplacement of geologically separable displacement episodes (intervals >1 Ma) along the primarily formed structures. In the continental crust, the structural reactivation is an essential procedure of the deformation. The long-lived weakening zones in the continental crust recurrently reactivate, and thus, the subsequent crustal strains may cause the formation of new regions of displacements (Hills, 1956; Prucha, 1992; Holdsworth, 1997). The stress in the continental crust is the particular cause of the reactivation, but it is also a function of the orientation of the fault-zone with respect to the imposed stress field, their capability to accommodate the resultant strains and the presence of rocks that form along faults (fault gouges, cataclasites, mylonites) (White et al., 1986). The repeated localisation of displacements along faults and shear zones over a very long time may lead to more intense weakening of these zones relative to the nearby crust (White et al., 1986; Holdsworth, 1997, 2001; Rutter et al., 2001).

The brittle reactivation of basement ductile shear zones during the early stages of continental rift evolution has been observed in many areas, such as the North Atlantic rift (Wilson, 1966), the Rio Grande rift (Olsen et al., 1987), the East African rift (Fairhead and Binks, 1991), and the West European rift (Michon et al., 2003) among many others. Provided that the ductile and brittle structures formed subsequently due to the same tectonic event, the deformed zones may represent a detachment fault. The detachment faults are long-term, low-angle normal faults with significant displacements and subregional-regional extent (Lister et al., 1986; Davis, 1988; Lister and Davis, 1989). These structures develop as the result of continental extension, when the middle and lower continental crust, deformed in a ductile way, is uplifted to the brittle upper crust. As a consequence, ductile and brittle deformations overlap along the same shear zones (Lister and Davis, 1989). As the lower crust rocks are raised from the deeper level to the surface, they carry over a series of various metamorphic and deformational conditions that include a continuously reducing metamorphic grade (usually amphibolite down to sub-greenschist facies) and different ways of deformation with the decreasing depth (Lister and Davis, 1989). Large-scale detachment faults usually divide

crystalline blocks of significantly different metamorphic evolutions in the footwall (lower plate) and the hanging wall (upper plate) (Lister et al., 1986; Lister and Davis, 1989). In the upper plate, the deformation processes occurred in a brittle way, but along the detachment fault, the shearing is primarily plastic. Detachment faults are often conjugate with lower plate mylonitic gneisses that form the metamorphic core complexes (Davis and Lister, 1988, Lister and Davis 1989). These core complexes are developed during continental extension and are characterised by a core of intensely deformed metamorphic rocks. The core complexes are usually restricted by low-angle detachment faults that are narrow in the upper plate; therefore, the metamorphic lower plate rocks eventually arrive at the surface (Lister and Davis, 1989).

The first mapping and defining of the metamorphic core complexes occurred in the Basin and Range region in Arizona and Nevada (Wernicke, 1985; Davis and Lister, 1988; Gans et al., 1989; Faulds and Geissman, 1992; Piper et al., 2010). Comparable structures have since been found in numerous places such as the Cordillera of Western North America (Kerrich, 1988; Lister and Davis, 1989; Foster and Raza, 2002), the Whipple Mountains, southeastern California (Davis, 1988; Lister and Davis, 1989; Stockli et al., 2006) and the Buckskin Mountains, western Arizona (Davis et al., 1979; Heidrick and Wilkins, 1980; Brady, 2002). Detachment faults and metamorphic core complexes are also well-known structures in the metamorphic basement of the Pannonian Basin, even close to the studied well (Tari et al., 1992; Posgay et al., 1996; Tari et al., 1999; M. Tóth et al., 2000; Schubert and M. Tóth, 2001; Zachar and M. Tóth, 2004).

The present area of the Pannonian Basin complex underwent extensional conditions several times during its evolution in the last 300 Ma. Following the totally unknown exhumation phase of the Variscan orogene, continental rifting occurred during the Jurassic, which was associated with the formation of the Magura-ocean (Haas and Péró, 2004). Finally, during the Neogene, complex basin subsidence occurred (Bergerat, 1989; Tari et al., 1992; Horváth and Cloetingh, 1996; Csontos and Nagymarosy, 1998), resulting in the formation of several kilometre deep sub-basins (Békés Basin, Makó Trough) and metamorphic basement highs among them. The explanation of reflection seismic profiles displays distinct mechanisms of upper crustal extension in the Pannonian basin (Tari et al., 1992). Underneath most parts of the basin, the amount of crustal extension is predicted to have been approximately 50–120% (Horváth et al., 1988). In the Pannonian Basin complex, there are subbasins with little extension (planar

rotational normal faults) and with large extension (detachment fault faults and formation of metamorphic core complexes) (Tari et al., 1992). Based on seismic sections from the Pannonian basin as interpreted by Tari et al. (1996), characteristic low-angle dipping fault planes and intensively tilted middle Miocene strata could be observed, indicating significant extension (Wernicke and Burchfiel, 1982).

Several boreholes reached the basement below Neogene sedimentary rocks at approximately 2 km depth. Petrological interpretation of the core material at numerous localities confirms the presence of low-angle faults, which separate blocks of different metamorphic evolutions inside the basement. In the Szeghalom Dome crystalline block, M. Tóth et al. (2000) described different zones with significantly distinct metamorphic and structural evolution. By detailed microstructural evaluation of a single borehole, the adjacent rock types with different *P-T* histories are separated by well-developed breccia zones of several tens of metres width (Molnár et al., 2015b). Molnár et al. (2015a) extended this detachment horizon using well-log data of numerous neighbouring wells, suggesting the presence of a low-angle fault zone. Based on the investigations of Nagy and M. Tóth (2012), there are four basic lithologies in the Kiskunhalas-NE basement area. In the lithological column between the uppermost graphitic carbonate phyllite and the lowermost orthogneiss formations, there is ~200 °C of peak metamorphic temperature deviation. It can be assumed that the two metamorphic blocks became juxtaposed along an extensional fault zone in the basement. Fiser-Nagy et al. (2014) described a series of south-dipping normal fault-bounded blocks in this area, with shallow dipping mylonite/gneiss boundaries. These low-angle (~5°) mylonitised zones refer to a detachment fault structure related to the formation of a metamorphic core complex. In the metamorphic block of the Görcsöny Ridge, the Baksa-2 borehole revealed two distinct realms with significantly different *P-T* histories of their metabasic rocks (M. Tóth, 2014). It can be assumed that the crystalline basement of the Görcsöny Ridge includes associated fragments of diverse origins. In the Pannonian Basin, detachment faults and metamorphic core complexes could be associated with the extension caused either by the Magura-ocean formation in the Jurassic (Csontos et al., 1992; Haas and Péró, 2004) or the opening of the basin during the middle Miocene (Tari et al., 1992). Detailed age data on the single detachment faults has not been published yet.

To decide which of the two scenarios may be valid in case of the studied Szentlőrinc-1 well, thermobarometric calculations below and above the shear horizons should be performed.

III.7 Summary and conclusions

The microstructure of available quartz grains may provide valuable information about the structural evolution of many different rock types. The microstructural analysis of the quartz grains enables the identification of various quartz grain types. The characterisation of single quartz grain microstructures using the above technique along the whole well enables localisation of the ductile shear zones inside of a crystalline complex even without available borecore information. In this study, the drill cutting samples of Szentlőrinc-1 geothermal well (SW Hungary) were investigated. The ductile deformation data were originated from the microstructural analysis was completed with well-log data, which provide information about the brittle deformation. Using these logs, brittle shear zones (presumably cataclasite, breccia zones) can also be localised along the well.

When comparing depths and extensions of the deformed horizons, a coincidence of the brittle and ductile zones becomes clear. This behaviour may suggest two different evolution schemes. If the first evolved ductile shear zones formed softened regions inside of the crystalline mass, it could reactivate later in a brittle way due to a tectonic event independent of the early event. However, if these structures formed due to the same tectonic event, these zones may represent a detachment fault. Thus, to know which of these schemes is true in the case of our study area, information about the metamorphic evolution of the footwall and hanging wall formations is essential. This information can be determined using the chemical compositions of the available quartz grains based on the "Ti-in-quartz" thermometer (Wark and Watson, 2006; Thomas et al., 2010; Huang and Audétat, 2012; Kidder et al., 2013; Haertel et al., 2013). If the metamorphic grades of the footwall and hanging wall formations are near-equivalent, then the coincidence of the brittle and ductile shear zones could be caused by primarily evolved softened regions. If their metamorphic grades are significantly different, we have successfully identified a detachment fault, using only single quartz grains of drill cuttings. These measurements and calculations are, nevertheless, outside the scope of this paper.

Chapter IV.: Metamorphic and deformation history of the Mecsekalja Zone around the Szentlőrinc-1 well using individual quartz fragments from drilling chips

Ágnes Skultéti

Department of Mineralogy Geochemistry and Petrology,
University of Szeged, Szeged, Hungary
skulteti.agi@gmail.com

Tivadar M. Tóth

Department of Mineralogy Geochemistry and Petrology,
University of Szeged, Szeged, Hungary
mtoth@geo.u-szeged.hu

István János Kovács

Magyar Földtani és Geofizikai Intézet,
kovacs.istvan.janos@mfgi.hu

Edit Király

Magyar Földtani és Geofizikai Intézet,
kiraly.edit@mfgi.hu

Judit K. Sándorné

Hungarian Institute for Forensic Sciences
sandornekj@nszkk.gov.hu

Central European Geology
(in press)

Metamorphic and deformation history of the Mecsekalja Zone around the Szentlőrinc-1 well using individual quartz fragments from drilling chips

Abstract

The Mecsekalja Zone is a strike-slip fault zone that plays an essential role in the structural framework of South Transdanubia. The metamorphic and deformation history of the crystalline basement of the Mecsekalja Zone has been determined thus far based exclusively on a few surface outcrops and near-surface samples. The Szentlőrinc-1 well penetrated the shear zone at a depth of approximately 2 km and brought drilling chips from a 220 m long section of the basement to the surface. The aim of this study is to reconstruct the metamorphic and deformation history of the Mecsekalja Zone along the Szentlőrinc-1 well using these tiny samples. These drilling chips consist of single mineral and rock pieces that are dominated by quartz fragments. This study concentrates on the detailed analysis of quartz grains utilizing the physical conditions of metamorphic evolution as well as ductile and brittle deformation to determine the chemical composition and rheology of quartz. The evolution of the studied area can be determined by evaluating analytical data measured by Raman spectroscopy, LA-ICP-MS and FTIR spectroscopy. These data suggest that the maximum temperature of the early regional metamorphism was 500–575 °C, the temperature of the subsequent ductile deformation was below 500 °C, and recrystallization occurred between 400 and 475 °C. During the structural evolution of the study area, two independent, single deformation events occurred. The earlier, ductile deformation event was followed by a brittle event through the reactivation of the former ductile shear zone. This conclusion is in accordance with previous results concerning the evolution of the Mecsekalja Zone. Thus, the shear zone, with an identical evolution, can be extended towards the southwest at least to the Szentlőrinc-1 well.

Keywords: Mecsekalja Zone; gneiss; quartz; metamorphism; deformation; TitaniQ thermometer

IV.1 Introduction

The Mecsekalja Zone is a ~1.5 km wide strike-slip fault zone *(Fig. IV.1)* that has been active since the Permian and that significantly controls the structural evolution of

the adjacent areas (Szederkényi 1977, 1979). In the dislocation zone, intensively mylonitized metamorphic rocks of various lithologies crop out. Gneiss, quartz phyllite, crystalline limestone, serpentinite and amphibolite compose the Mecsekalja Zone and lithostratigraphically belong to the Ófalu Group. Previously, the metamorphic and deformation history of these rock types was studied basically from surface outcrops (Szederkényi 1977, 1983; Árkai and Nagy 1994; Lelkes-Felvári et al. 2000; Király and Török 2003; M. Tóth et al. 2005, Balla et al. 2009 among others). Recently, the Szentlőrinc-1 well reached the basement SW of the well-known surface outcrops at a depth of approximately 2 km and brought drilling chips to the surface, thus making it possible to investigate the shear zone. These drilling chips consist of mm-sized debris and contain mineral and rock pieces in an 80:20 ratio; these pieces are dominated by single quartz fragments.

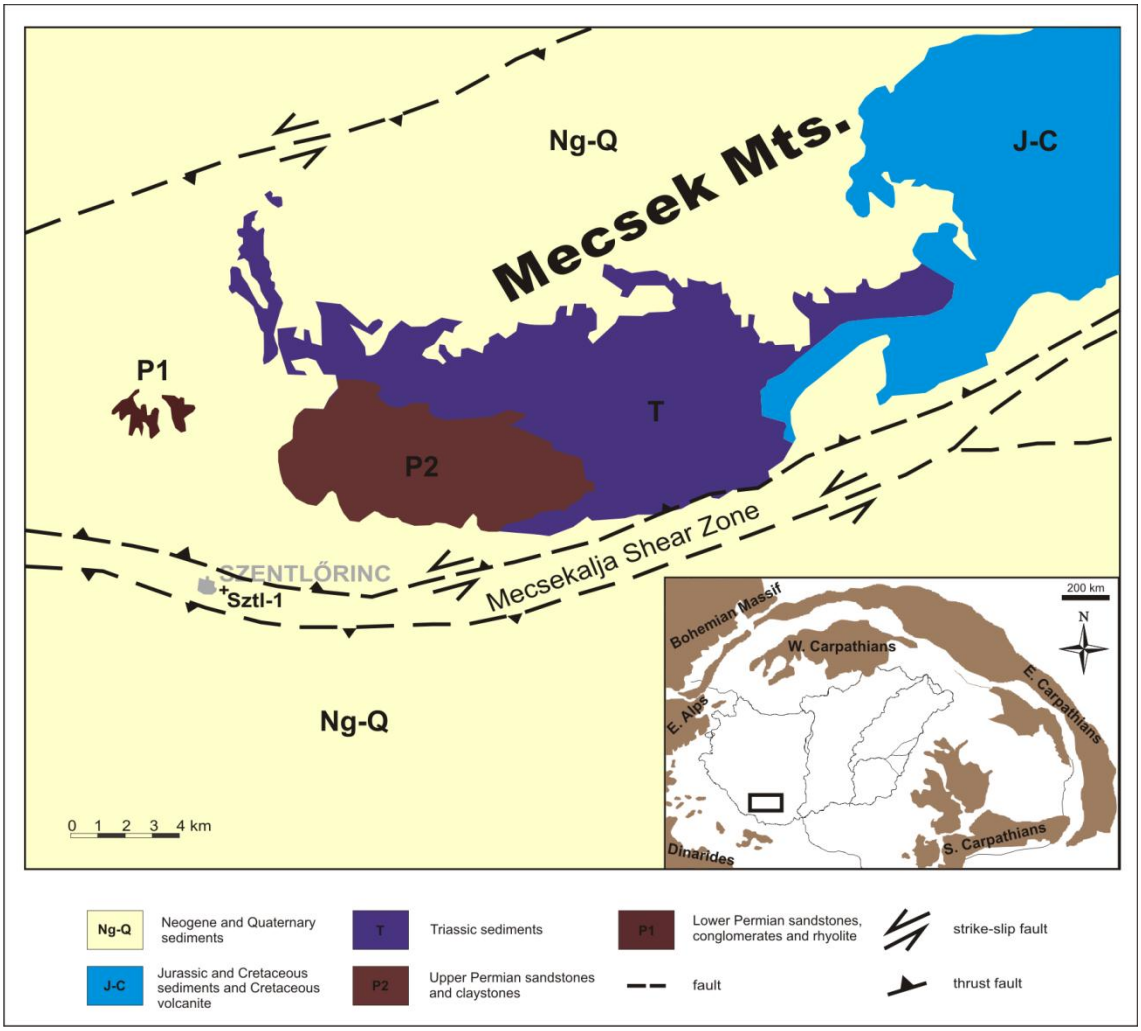

Figure IV.1: The Mecsekalja Zone with the studied Szentlőrinc-1 (Sztl-1) well (based on Konrád et al. 2010)

Quartz, which is one of the most frequently rock-forming minerals, is a common product of metamorphic reactions. In its crystal lattice, various trace elements (e.g., Al, Ti, Ge, Na, K, Li, B) (Götze et al. 2004) may appear connected to SiO_4 tetrahedrons under different physical conditions; thus, metamorphic evolution determines the chemical composition of quartz (Monecke et al. 2002; Sørensen and Larsen, 2009; Kempe et al. 2012). Although quartz is a "nominally anhydrous mineral" (NAM), in its crystal lattice, hydrogen ('water') may occur both in the form of hydroxyl defects (OH^-) and molecular water (H_2O) (Stenina 2004). Hydroxyl defects in the quartz lattice are mostly locked in crystal defects (point defects) and along grain boundaries, whereas molecular water appears freely in the form of fluid (nanoscale) inclusions (Stadler and Konzett 2012).

The amount of 'water' in the crystal lattice of quartz significantly influences its brittle and ductile behaviour, reduces its mechanical strength and resistivity and enhances its ductile deformation at low temperatures (200–300 °C; Griggs and Blacic, 1965; Blacic, 1975; Jones, 1975; Kekulawala et al., 1978, Kekulawala et al., 1981; Gleason and DeSisto, 2008). All these factors indicate that quartz is an excellent candidate for recording metamorphic evolution and structural changes in numerous rock types. Because quartz is a stable mineral over a rather wide range of *P-T* conditions, it can be deformed in different ways due to diverse deformation mechanisms to produce various microstructures (Hirth and Tullis, 1992; Passchier and Trouw, 2005). Consequently, each grain in a quartz-bearing rock may provide valuable information regarding the deformation history of the rock body itself (Stipp et al. 2002; Vernon 2004; Halfpenny et al. 2012).

The aims of this study are to reconstruct the metamorphic and deformation history of the Mecsekalja Zone around the Szentlőrinc-1 well using quartz fragments of drilling chips and to compare our data to previous evolutionary models of the study area.

IV.2 Geological setting

IV.2.1 Geology of the Mecsekalja Zone

The Mecsekalja Zone consists of rocks that originally belonged to distinct stratigraphic and tectonic units (Balla 2003a; Balla et al. 2009). The Palaeozoic rocks of the Ófalu Group were most likely juxtaposed along a regional ductile strike-slip zone (Mecsekalja Zone) during the main Early Carboniferous orogenic phase of the Variscan

cycle (Balla et al. 2009). Rock types of the Ófalu Group, including gneiss, amphibolite, crystalline limestone, quartz phyllite and serpentinite, represent the intensively deformed fragments of these stratigraphic and structural units (Balla 2003b).

The protolith of the highly mylonitic gneiss was presumably a granitoid rock, therefore classifying it as an orthogneiss (M. Tóth et al. 2005; Király 2005). Previous examinations by M. Tóth et al. (2005) indicated that the zircon grains of the Mórágy Granite differ from those typically found in the Ófalu gneiss mylonite. Thus, its protolith cannot be the Mórágy Granite but is instead another, currently unknown granitoid rock. The age of this protolith must be older than the Mórágy Granite (M. Tóth et al. 2005), and therefore older than Early Carboniferous. Szederkényi (1977, 1983) suggests that the protolith of amphibolite is partly volcanogenic and volcanogenic-sedimentary. The crystalline limestone has been identified as a metamorphic variety of a Devonian limestone based on the presence of conodonts as described by S. Kovács (personal communication).

The earliest detected event of the evolution of the crystalline basement is the magmatic crystallization of quartz grains in gneiss protolith granitoid rocks. This event occurred at ~710 °C based on quartz suture analysis performed by M. Tóth et al. (2005). Zoned garnet composition (specifically, increasing Mg and decreasing Fe contents from core to rim, Lelkes-Felvári et al. 2000) and quartz suture data of M. Tóth et al. (2005) suggest that the first regional metamorphic event occurred at upper greenschist/lower amphibolite facies (~550 °C) in both the gneissic rocks and amphibolite. Greenschist/amphibolite facies metamorphism in amphibolite was described by Szederkényi (1977, 1983) and has been confirmed by the cores of zoned amphibole porphyroclasts from Erdősmecske (~540 °C, 3.2 kbar, Árkai and Nagy 1994). As the crystalline limestone also metamorphosed at high-*T* greenschist facies, the age of this metamorphic event must be younger than the Devonian (Balla et al. 2009).

In the different rock types of the Ófalu Group, intensive ductile deformation is associated with this metamorphic event, leading to multiphase folding and intensive mylonitization. Based on the mineral composition of ultramylonite of the Mőcsény-I borehole, Lelkes-Felvári et al. (2000) estimated that high-*T* greenschist facies (~450 °C) mylonitization occurred under medium (Barrow type) pressure conditions. Király and Török (2003) estimated that the temperature of this mylonitization was approximately 450–500 °C based on garnets in deformed aplite. Szederkényi (1977, 1983) described intensive shearing at greenschist/amphibolite facies in amphibolite, whereas M. Tóth et

al. (2005) assumed the recrystallization temperature of mylonite to be approximately 350 °C. The $^{40}Ar/^{39}Ar$ muscovite age of the mylonite is 270–303 Ma (Lelkes-Felvári et al. 2000), although Tüske (2001) proposed an age of 294–307 Ma for ductile shearing based on $^{40}Ar/^{39}Ar$ dating of biotite and muscovite from a mylonitic biotite gneiss.

IV.2.2 Previous results from the Szentlőrinc-1 well

IV.2.2.1 Petrography

In the drilling chips of the Szentlőrinc-1 well, in addition to quartz, rock fragments, which consist of muscovite, biotite, K-feldspar and plagioclase, are also present. In the upper 100–150 m (1600–1750 m) of the studied well section, muscovite and K-feldspar are the prevailing phases, with mica dominating; further downward (1750–1820 m), the amount of plagioclase increases, and biotite also appears. Thus, the studied well section can be divided into two blocks of different gneiss types *(Fig. IV.2)*: the upper micaceous gneiss *(Fig. IV.2/a)* and the lower feldspathic gneiss *(Fig. IV.2/b)* (Skultéti and M. Tóth 2016).

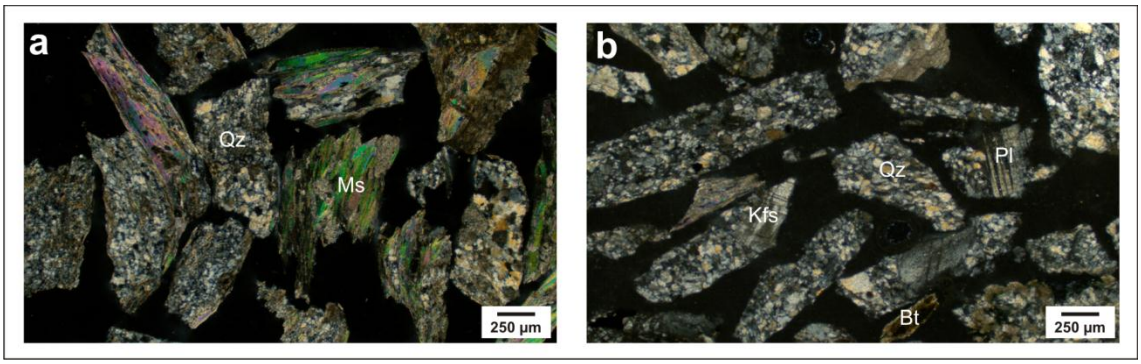

Figure IV.2: Different gneiss types along the studied well section (1600-1820 m) of the Sztl-1 well. a) Micaceous gneiss with dominant quartz (Qz) and muscovite (Ms) and b) feldspathic gneiss with dominant quartz (Qz), K-feldspar (Kfs), plagioclase (Pl) and biotite (Bt)

IV.2.2.2 Ductile and brittle deformation

Three microstructurally distinct quartz grain types *(Fig. IV.3)* in the subsurface shear zone were distinguished under a microscope: grains with undulose extinction *(Fig. IV.3/a)*, fragments with subgrains, and fragments of recrystallized grains *(Fig. IV.3/c)*, denoted as U (= undulatory), S (= subgrain) and R (= recrystallized), respectively. In addition to grains belonging to these groups, numerous grains with

heterogeneous microstructures *(Fig. IV.3/d)* were also observed. These transitional features exhibit the simultaneous presence of more extreme structure types within a single grain (Skultéti et al. 2014; Skultéti and M. Tóth 2016).

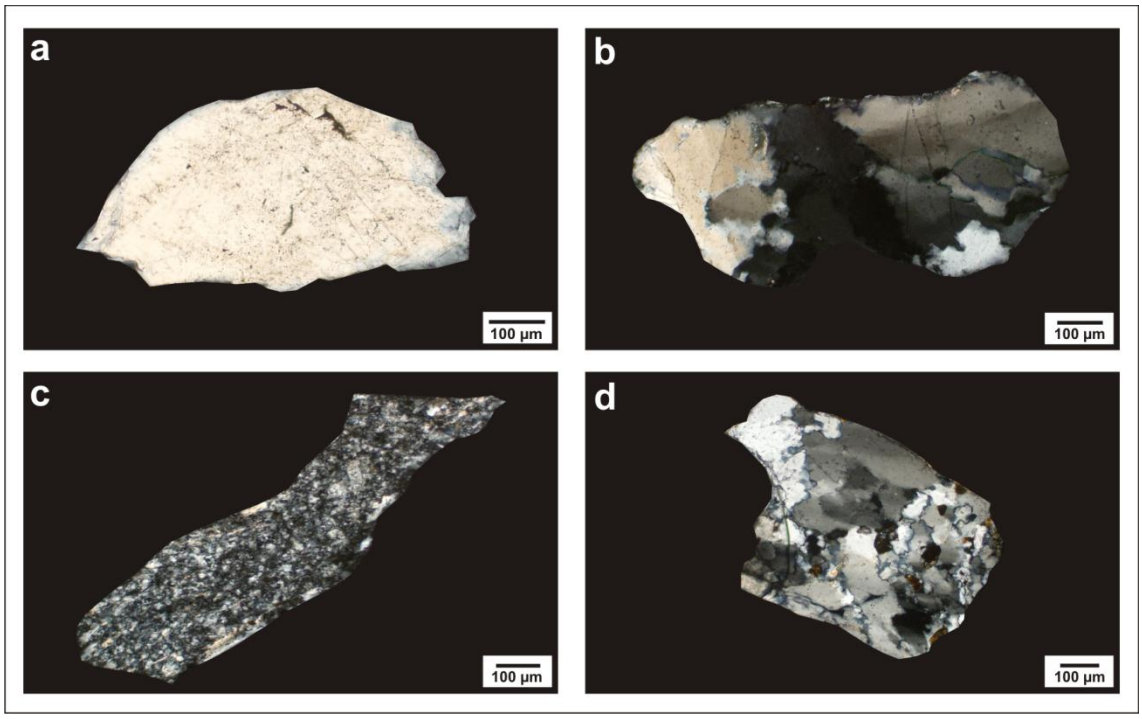

Figure IV.3: Microstructural groups of quartz fragments in the studied samples. a) Quartz grain with undulose extinction (U), b) quartz grain with subgrains (S), c) quartz grain with recrystallized grains (R), and d) transitional quartz grain with heterogeneous microstructures

Textural evidence indicates that the U type quartz grains were formed via bulging recrystallization (BLG) (Hirth and Tullis 1992). Bulging usually occurs at low temperatures (~400 °C) (Passchier and Trouw 2005) and high strain rates. In contrast, the S and R type quartz grains probably developed via subgrain rotation recrystallization (SGR) (Hirth and Tullis 1992) at different temperature ranges (SGR I ~450 °C, SGR II ~500 °C) (Skultéti et al. 2014). The latter process generally occurs at medium temperatures (~500 °C) and strain rates (Passchier and Trouw 2005). Thus, these three extreme microstructural types were formed by two different mechanisms (namely, BLG and SGR) representing distinct deformation conditions.

Using Raman microspectroscopy, monomineralic quartz domains characterized by different deformation conditions can be identified and separated. Statistical analysis indicates that the microscopically identified extreme grains (U, S, and R) possess significantly different spectral attributes; thus, they can be distinguished on the basis of

certain combinations of their respective Raman spectra (*F1*, *F2* discriminant functions in Skultéti et al. 2014) *(Fig. IV.4)*. The U-S-R spectral space (or the U-S-R "triangle") can therefore also be considered to represent a virtual deformational space.

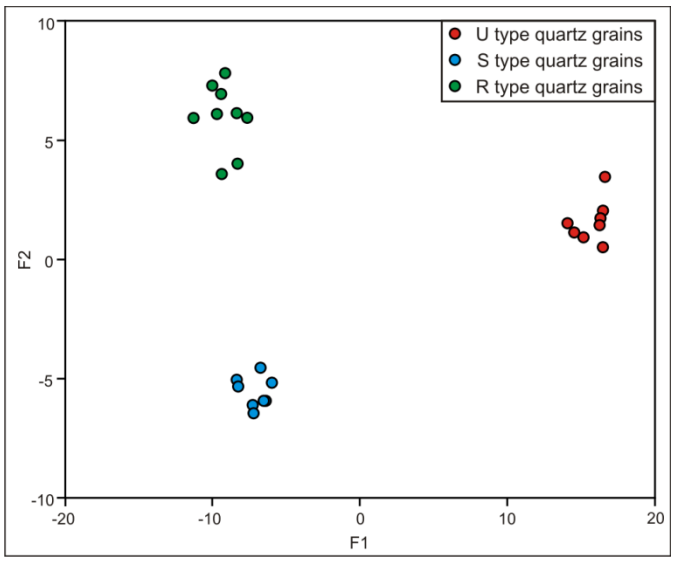

Figure IV.4: Separation of U-S-R extreme quartz grain types in the spectral space using Raman spectroscopy on the basis of F1, F2 discriminant functions

Based on the microstructures and recrystallized grain sizes (45 ± 20 μm) (Stipp et al. 2002) of quartz fragments, the maximum temperature of ductile deformation of the samples from the Szentlőrinc-1 well was below 500 °C (Skultéti et al. 2014). Throughout the well, the proportion of microstructurally distinct quartz grains changes with depth (Skultéti and M. Tóth 2016). Thus, based on these investigated samples, ductile shear zones can be localized at depths of approximately 1610–1635 m and 1750–1765 m *(Fig. IV.5)* (Skultéti and M. Tóth 2016). Additionally, two brittle shear zones can be identified by manual and statistical (discriminant analysis) interpretations of well logs (density, gamma, resistivity, spontaneous potential and calliper logs) at depth intervals of approximately 1580–1635 m and 1750–1765 m *(Fig. IV.5)*.

IV.2.2.3 Geodynamics

The positions of the ductile shear zones coincide very well with the brittle horizons defined by well-log evaluations (for details, see Skultéti and M. Tóth 2016). This behaviour may suggest two different evolution schemes (Skultéti and M. Tóth 2016). (1) If the first evolved ductile shear zones produced softened regions inside the crystalline mass, then they could reactivate later in a brittle manner due to a tectonic event independent of the early one (White et al. 1986; Holdsworth et al. 1997). (2) If

these structures formed due to the same tectonic event, then these zones may represent a detachment fault (Lister et al. 1986; Davis 1988). Detachment faults develop as the result of continental extension when the middle and lower continental crust, which was previously deformed in a ductile manner, is uplifted to the brittle upper crust (Lister and Davis 1989). Consequently, ductile and brittle deformation overlaps along the same shear zones that separate blocks of different metamorphic evolutions.

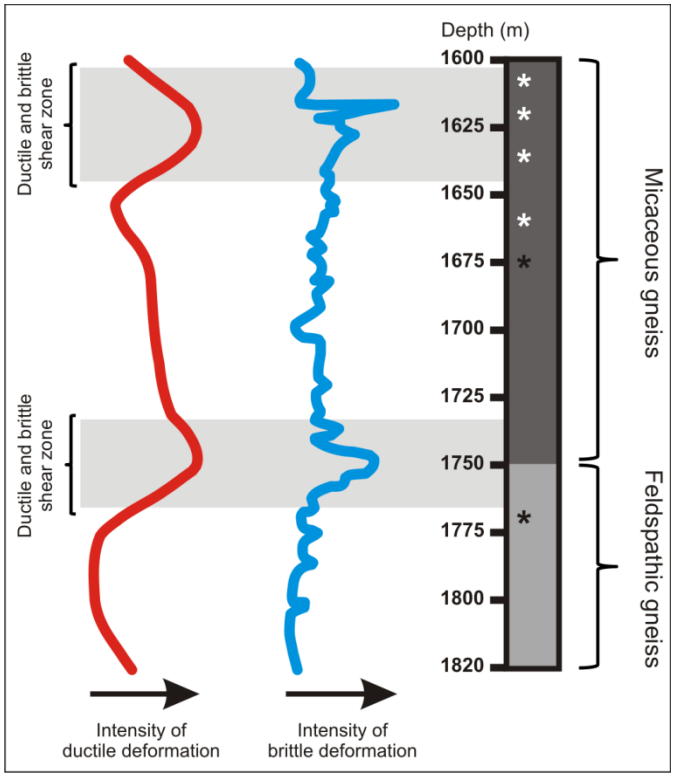

Figure IV.5: Position of ductile (red line) and brittle (blue line) shear zones in the studied section of the Sztl-1 well (Skultéti and M. Tóth, 2016). White stars represent the depths of micro-FTIR measurements, while black stars represent the depths of Raman spectroscopy and LA-ICP-MS measurements

IV.3 Samples

This study area is located in the South Transdanubian region of Hungary and is part of the Mecsekalja Zone at the forefront of the Mecsek Mountains. The investigated samples represent the Szentlőrinc-1 (Sztl-1) deep drilling well (Thorbergsdottir et al. 2010), the base of which reached a depth of 1820 m. Under Cenozoic and Mesozoic sedimentary formations, the well penetrated rocks of the Mecsekalja Shear Zone. Drilling chips were obtained at every 5 m in the 1600–1820 m interval (analysed samples are from depths of 1605, 1620, 1635, 1660, 1675, and 1770 m).

IV.4 Methods

IV.4.1 Raman spectroscopy

Measurements were performed on 100 μm thick sections so that these samples could be used for further analysis. This sample thickness hinders the optical analysis of quartz fragments; therefore, Raman spectroscopy was used for the detailed study of quartz microstructures. In the samples obtained from depths of 1675 and 1770 m *(Fig. IV.5)*, ten random points were measured in each selected extreme or transitional quartz fragment. Based on the resulting Raman spectral attributes, the analysed quartz grains were situated in the *F1-F2* spectral space and in the U, S and R "triangle".

Analyses were performed on a Thermo Scientific DXR Raman microscope equipped with a diode-pumped frequency-doubled Nd-YAG laser at a maximum laser power of 10 mW. Samples were irradiated by laser light at a wavelength of 532.2 nm, with the laser beam focused using a 100x objective lens, resulting in a spot size of ca. 0.7 μm. The backscattered light collected by the microscope objective was filtered via an edge filter, dispersed by a single grating (1800 grooves mm^{-1}) and gathered in a CCD detector cooled to -20 °C by the Peltier effect. This instrument has a spectral resolution better than 2 cm^{-1} and a spatial resolution of a few μm^3; a 50 μm pinhole confocal aperture was used for each measurement. In every case, 10 mW laser power was used to record the spectra. Sample exposures were obtained by operating the DXR Raman microscope in auto-exposure operating mode, in which the instrument attempts to reach a specified signal-to-noise ratio (S/N) during the measurement (in this case, S/N=100). In this measuring mode, a maximum exposure time must also be set (i.e., if the specified S/N value cannot be achieved); a value of 1 min was set for each spectrum selected in the present study. The applied Raman microscope was equipped with a laser source operating with a depolarized laser beam. Due to the depolarized nature of the applied laser beam, the directional dependence of the Raman scattering did not influence the quality of the recorded spectra. Seasolve PeakFit 4.12 software was used for Raman spectral analysis. A Gaussian deconvolution method using the Voight type curve fitting procedure was used to determine the centre, amplitude, full width at half-max (FWHM), full width at base (FWHM base) and integrated area of the bands of interest.

IV.4.2 LA-ICP-MS and Ti-in-quartz thermometry

Measurements were performed using a New WaveUP 213 laser ablation system coupled to a quadrupole ICP-MS, Perkin Elmer Elan DRCII, at the Geological and Geophysical Institute of Hungary. He carrier gas was mixed with Ar gas, which acted as a make-up gas. Operating parameters of the ICP-MS and laser ablation system were optimized using NIST612 as the unknown material and NIST610 as the control. Conditions of the mass spectrometer are characterized by a nebulizer gas of 0.9 l/min, auxiliary gas of 1.1 l/min, plasma gas of 15.8 l/min, lens voltage of 7.25 V and RF power of 1450 kW. The He gas flow was as high as 1.8 l/min. The laser operated at an energy density of 4.7 J/cm^2 and a repetition rate of 5 Hz. The spot size was 55–100 μm. The background acquisition time was 40 sec, and the sample signal was measured over 60 sec. The total integration time for each isotope was 13 sec. NIST610 was used as an external standard, and ^{29}Si was used as an internal standard. Absolute concentrations were calculated to 100% of SiO_2 measured at the same time on the same spot by LA-ICP-MS (Liu et al. 2008).

These measurements were made on 100-μm-thick polished sections. Measured quartz fragments were selected by detailed Raman spectroscopy analysis. The concentration of ^{49}Ti in quartz fragments in two samples from different depths (1675 and 1770 m, Fig. 5) was determined by LA-ICP-MS. In total, 14 quartz fragments were analysed, and 50 measurements were performed on two samples. In the sample collected from a depth of 1675 m, 33 points from 9 quartz fragments were measured; in the sample collected from a depth of 1770 m, 17 points from 5 quartz fragments were measured. The intensity versus time signal was also checked for spikes and inclusions. To ensure good representation and to avoid accidental contamination of anatase inclusions or any other mineral forming on the grain boundary, 3 points per grain were measured, and their average was used to calculate the temperature if their deviation was small enough.

Temperatures were calculated from the measured Ti concentrations using a Ti-in-quartz thermometer (TitaniQ) of Thomas et al. (2010):

$$\mathrm{T}\,(^{\circ}\mathrm{C}) = \frac{\mathrm{a} + \mathrm{cP}}{\mathrm{b} - \mathrm{R} * \ln \mathrm{X}_{\mathrm{TiO_2}}^{\mathrm{Qtz}} + \mathrm{R} * \ln \mathrm{a}_{\mathrm{TiO_2}}} - 273.15$$

where R is the gas constant 8.3145 J/K, $X_{TiO_2}^{Qtz}$ is the mole fraction of TiO_2 in quartz (ppm), a_{TiO_2} is the activity of TiO_2 in the system, and the adjustable parameters a, b and c are a = 60952 ± 3122, b = 1.520 ± 0.04, and c = 1741 ± 63 (Thomas et al. 2010).

It was impossible to perform an independent pressure estimation from the available drill cuttings. Thus, a pressure of 5 kbar was used based on previous pressure estimations from the formations of the study area (Árkai and Nagy 1994: *P* = 3.2–4.0 kbar; Lelkes-Felvári et al. 2000: *P* = 5.7–6.3 kbar, Barrow type pressure conditions). In our calculations, a TiO_2 activity of $a_{TiO_2} = 1.0$ was used because anatase (TiO_2) inclusions were detected by Raman spectroscopy in most of the analysed quartz fragments (see later).

Ti concentrations and the calculated temperatures are interpreted as functions of the deformation conditions of the quartz fragments. The quartz fragments measured by LA-ICP-MS were also analysed in the *F1-F2* spectral space. Isotherms in the *F1-F2* space were fitted by Golden Software Surfer using the linear kriging method.

IV.4.3 Micro-FTIR measurements

Quartz grains were analysed by Fourier transform infrared spectroscopy. Four samples were measured along the previously localized ductile shear zone (rim: 1605 m; core: 1620 and 1635 m; rim: 1660 m; Fig. 5). During the measurement, the hydroxyl defects and molecular water content of the quartz lattice were also determined.

Unpolarized micro-FTIR measurements on unoriented quartz fragments were undertaken at the Hungarian Institute for Forensic Sciences using a Bruker Vertex 70 spectrometer attached to a Bruker Hyperion 1000 infrared microscope. KBr beam splitters and MCT detectors were deployed with a Globar light source. Measurements were conducted by using unpolarized IR light. The rectangular spot size was set at 100*100 μm. A nominal spectral resolution of 4 cm^{-1} was chosen with at least 64 scans, usually ranging between 400 and 4000 cm^{-1} for each measurement.

The indicatrix theory (Kovács et al. 2008; Sambridge et al. 2008) of unpolarized infrared light makes it possible to determine the concentration of anisotropic structural hydroxyl defects from a number (n>5) of unoriented crystals with reasonable accuracy. This method can only be applied to strongly anisotropic minerals (e.g., olivine, calcite, quartz) if the maximum linear unpolarized absorbance is less than 0.15, a criterion that is satisfied by the spectra measured in this study. Absorbers such as molecular water in

inclusions or interstitial crystallographic positions are isotropic; therefore, a single measurement is enough for precise quantitative evaluation.

The total polarized absorbance (A_{tot}) for structural hydroxyl in quartz fragments is estimated as three times that of the average integrated unpolarized absorbance (Sambridge et al. 2008; Kovács et al. 2008). The estimation of the average integrated unpolarized absorbance A_{tot} is more accurate when the number of measurements on unoriented grains is larger. In this study, sometimes only one grain was available for such analysis; consequently, the uncertainty is worse and can reach up to 30%. In the integrated area, the integration was undertaken using OPUS software for structural hydroxyl between 3365 and 3395 cm^{-1}. The A_{tot} was then converted to the absolute concentration of hydroxyl defects using the calibration factors of Thomas et al. (2009) for natural quartz (HQV, ε=94 000 $l/mol \cdot cm^2$, k~0.072). The approximate amount of molecular water in (nanoscale)inclusions was estimated following the methodology of Gleason and DeSisto (2008) and applying the absorption coefficient of Kats (1962) based on the integrated absorbance of the broad molecular water band at ~3400 cm^{-1}. For this analysis, the limits of integration were set between 3000 and 3695 cm^{-1}. In this case, anisotropy is not a factor; therefore, the uncertainty originates solely from the heterogeneity in the concentration of molecular water.

Thicknesses of quartz wafers were determined based on the integrated area under the Si-O bands between 1440 and 2110 cm^{-1} as described by Bíró et al. (2016). The determined thickness of the sample, possible heterogeneities in hydroxyl defect concentrations and the calibration factors may be all the sources of possible uncertainties. However, based on previous experience (Kovács et al. 2008, 2012), the overall precision in the absolute concentration of hydroxyl defects here should be as high as ~40%, and that of molecular water should be as high as ~15%.

IV.5 Results

IV.5.1 Raman spectroscopy

The analysed quartz fragments can roughly be divided into two groups based on their microstructures and deformation conditions. These are grains with undulose extinction (close to U) and recrystallized grains (close to R). In addition, numerous grains with heterogeneous microstructures were also observed; they exhibit the

simultaneous presence of domains with U, S and R microstructures within a single grain *(Fig. IV.6)*.

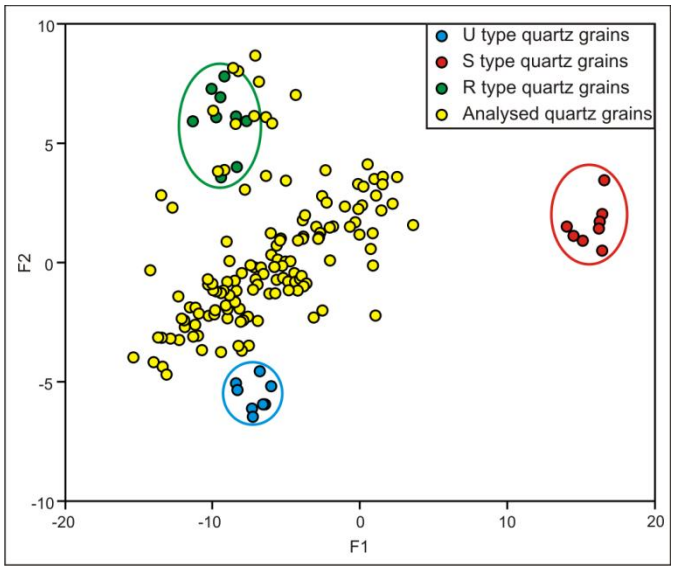

Figure IV.6: Position of analysed quartz grains in the U-S-R spectral space using Raman spectroscopy on the basis of F1, F2 discriminant functions

Numerous tiny (up to a few microns in diameter) anatase inclusions, formed by low-temperature modification of TiO_2 minerals, were detected by Raman spectroscopy in the analysed quartz fragments. In the studied quartz fragments, anatase appears as homogeneously distributed inclusions *(Fig. IV.7)*.

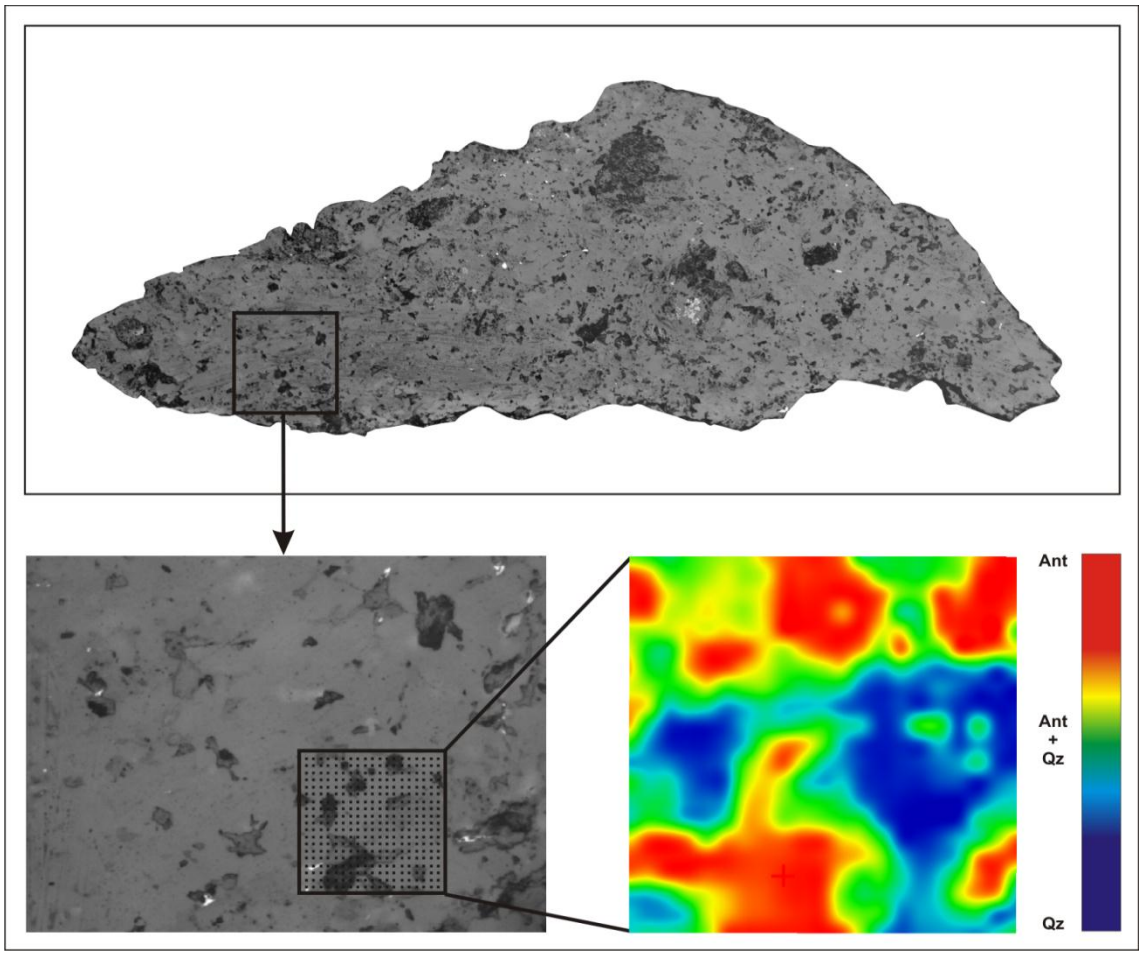

<<

Figure IV.7: Raman map of anatase inclusions in a representative quartz fragment

IV.5.2 LA-ICP-MS

IV.5.2.1 Ti concentration data

In the sample from 1675 m, Ti concentrations range between 4 and 70 ppm; in the sample from 1770 m, Ti concentrations vary between 5 and 42 ppm. Some concentration data are below the detection limit.

IV.5.2.2 TitaniQ thermometry

The temperature data calculated using a TitaniQ thermometer are presented as histograms *(Fig. IV.8)*. In the case of the sample obtained from a depth of 1675 m, temperatures vary between 390 and 590 °C *(Fig. IV.8/a)*; in the sample collected from a depth of 1770 m, *T*=410–547 °C *(Fig. IV.8/b)*. Both histograms appear to be bimodal: the 1675 m sample has one modus between 390 and 485 °C and another between 500 and 590 °C, and the 1770 m sample has one modus between 410 and 470 °C and another between 500 and 550 °C. The significant difference between the two temperature groups is also justified by two sample (independent) t-tests at the 95% significance level at both depths. The bimodality of these temperature distributions suggests that both high and low temperature events occurred in both studied samples.

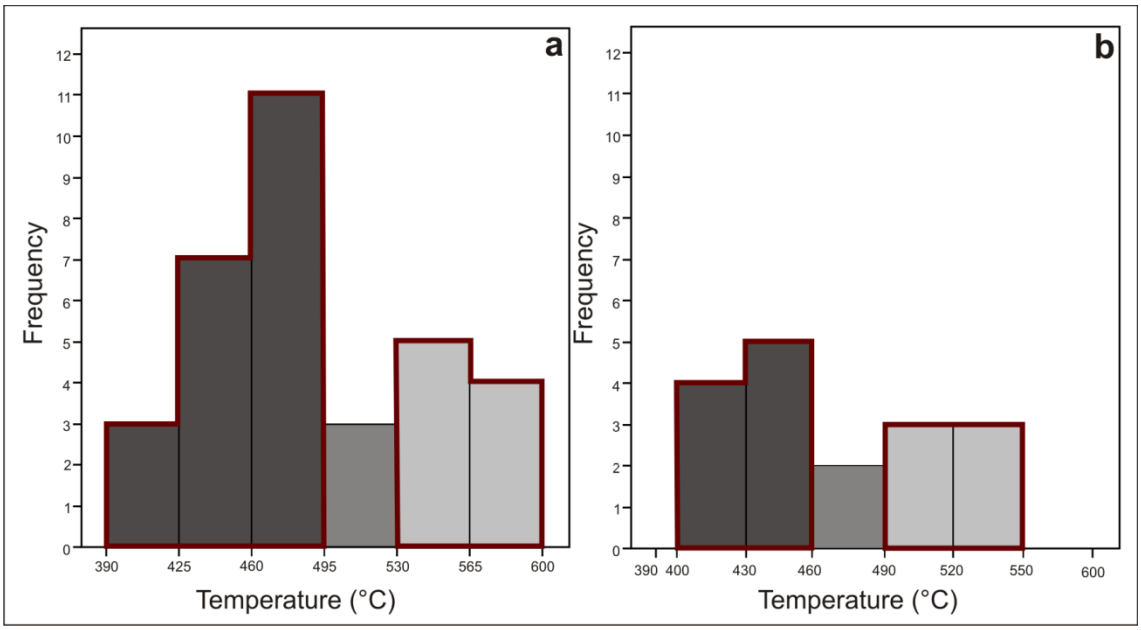

<<

Figure IV.8: Histograms of temperature data calculated by TitaniQ thermometer (Thomas et al., 2010). a) Histogram of temperature data from a 1675-m-deep sample and b) histogram of temperature data from a 1770-m-deep sample

IV.5.3 Combined Raman spectroscopy and LA-ICP-MS results

All temperature data were connected to the deformation state of the corresponding quartz grains based on their positions in the *F1-F2* spectral space *(Fig. IV.9)*. In this way, temperatures of the deformation mechanisms by which these structurally different grains were formed can be estimated *(Fig. IV.9/a)*. This figure shows clear covariation between deformation state and temperature; structurally different fragments contain different amounts of Ti. Grains that plot close to the U type field contain less Ti (4–19 ppm), while those close to R type grains are higher in Ti (23–70 ppm). Accordingly, temperatures related to the deformation conditions represented by U are between 400 and 475 °C, while for deformation conditions represented by R, *T*=500–575 °C. Moreover, interpolated and extrapolated isotherms fitted using each point with known temperatures in the U-S-R spectral space suggest a continuous temperature decrease from R to U *(Fig. IV.9/b)*.

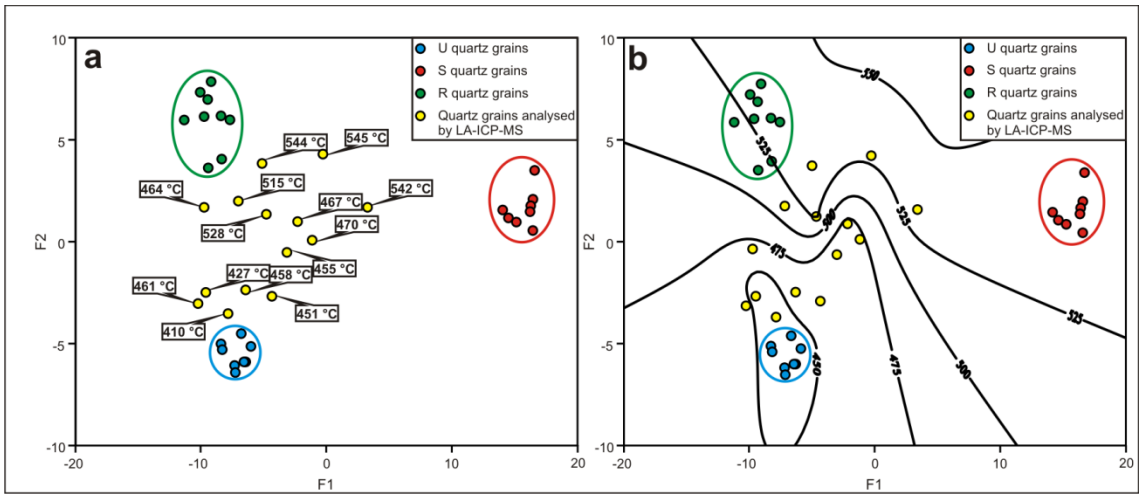

Figure IV.9: Combined Raman spectroscopy and LA-ICP-MS results. a) All temperature data (each temperature datum represents an average temperature of multiple points measured in the same quartz grain) are connected to the deformation state of the corresponding quartz grains based on their positions in the F1-F2 spectral space, and b) interpolated and extrapolated isotherms display a continuous temperature decrease from R to U

IV.5.4 Micro-FTIR results

The broad band at ~3400 cm^{-1} usually corresponds to molecular water in inclusions or interstitial positions in quartz (Kats 1962; Stenina 2004). The concentration of molecular water varies from 0.03 to ~0.1 wt% in the measured quartz grains *(Table IV.1)*. Samples collected from depths of 1605 and 1660 m have significantly more molecular water than the other two samples; this difference is well beyond analytical uncertainty *(Fig. IV.10)*. There is a narrower band superimposed on the 'water' band at ~3380 cm^{-1}, which is usually attributed to the coupled substitution of $Al^{3+} + H^{+}$ for Si^{4+}. The concentration of this substitution is rather low (0.8–2.8 ppm). The samples collected from depths of 1605 and 1660 m also display higher concentrations of structural hydroxyl *(Fig. IV.10, Table IV.1)*; however, due to their higher analytical uncertainty, this difference may be marginal. The bands at 2850 and 2920 cm^{-1} are related to alkyl groups ($-CH_3$) (representing organic contamination) and are therefore are not considered during quantitative evaluation.

Depth of sample (m)	Thomas et al. (2009) hydroxyl defect (ppm)	Kats (1962) molecular water (ppm)
1605	2.8	784
1620	0.8	384
1635	1.1	357
1660	2.0	1060

Table IV.1 'Water' content of quartz grains along the shear zone

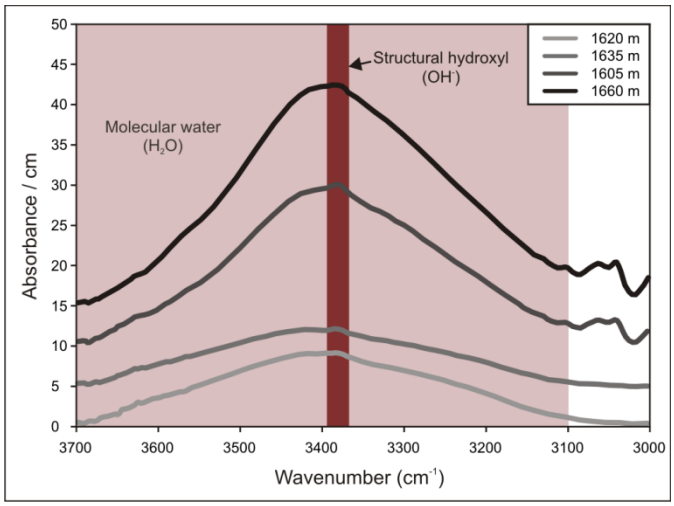

Figure IV.10: IR spectra (between 3700 and 3000 cm^{-1}) of analysed quartz samples from different depths along the localized ductile shear zone (rim: 1605 m; core: 1620 and 1635 m; rim: 1660 m). The wide light grey band (3100–3500 cm^{-1}) displays the band of molecular water (H_2O), while the narrow dark grey band (3380 cm^{-1}) displays the band of structural hydroxyl (OH^-)

IV.6 Discussion

IV.6.1 Evolution

The drill cuttings representing the gneissic rocks of the crystalline basement of the Mecsekalja Zone contain monomineralic quartz grains in addition to tiny rock fragments, the latter of which consist essentially of quartz, K-feldspar, plagioclase and mica (muscovite and biotite). In this quartzofeldspathic system, quartz may be a relict phase of the pre-metamorphic protolith or a product of metamorphic reactions. In the studied samples, quartz grains can be subdivided into two main groups based on their microstructures and deformation conditions. There are quartz grains with undulose extinction (U) that are formed by a bulging (BLG) recrystallization mechanism. The temperatures related to this deformation event are 390–485 °C in the upper gneiss type and 410–470 °C in the lower zone. The other dominant grain type (R) is formed during subgrain rotation recrystallization (SGR) at temperatures of 500–590 °C in the upper zone and 500–550 °C in the lower gneiss zone. Based on previous studies (Hirth and Tullis 1992; Passchier and Trouw 2005, among others), in quartz, the BLG dynamic recrystallization mechanism occurs at ~400 °C, while SGR II is active at ~500 °C. These data are in accordance with the above temperature estimates for U and R type grains and confirm that the two subsequent deformation events occurred at different conditions.

IV.6.2 Metamorphism and ductile deformation

In the quartz lattice, trace elements, hydroxyl defects and molecular water may be present in various amounts (Götze et al. 2004; Stenina 2004). The incorporation of Ti into quartz during metamorphism depends only on the *P-T* conditions, provided that Ti is present in excess. An obvious textural method for determining whether sufficient amounts of Ti were present is the occurrence of anatase inclusions in each studied grain. At a high *T*, the quartz lattice contains the highest amount of Ti, which precipitates as anatase (TiO_2) when the rock cools down. In this way, "quartz-anatase myrmekite" forms through subsolidus exsolution. The U type quartz grains contain the highest Ti concentrations (23–70 ppm). The Ti concentrations and corresponding temperatures (500–575 °C) of these grains imply that they experienced the highest-temperature metamorphic event in the study area. The newly recrystallized R type grains formed during coeval ductile deformation and recrystallization. In the quartz lattice, the

microtextural and chemical equilibrium states depend on the rates of dislocation migration and diffusion, respectively. The rates of both processes significantly depend on temperature and fluid content (Hirth and Tullis 1992; Fossen 2010). During BLG and SGR, dislocation migration and diffusion are usually too slow to obtain total equilibrium because of their low temperatures (<500 °C). Nevertheless, local equilibrium can be reached on the scale of some grains in terms of both microtexture and chemistry (Grujic et al. 2011; Haertel et al. 2013). In the quartz lattice, the appearance of 'water' (OH^-, H_2O) causes hydrolytic weakening (Griggs and Blacic 1965; Kronenberg and Wolf 1990). Moreover, water also promotes dislocation migration and diffusion and thus may cause ductile deformation to occur at relatively low temperatures (200–300 °C, Griggs and Blacic, 1965; Blacic, 1975; Jones, 1975; Kekulawala et al., 1978, Kekulawala et al., 1981; Gleason and DeSisto, 2008). Consequently, equilibrium can presumably be reached even at this physical condition. Among the studied quartz grains, the U type grains contain the lowest concentrations of Ti (4–19 ppm). The temperature represented by these grains (400–475 °C) represents the temperature of recrystallization along the retrograde pathway.

IV.6.3 Effect of 'water' on the brittle deformation of quartz

In the localized ductile shear zone (1610–1635 m), the water content (OH^-, H_2O) of quartz grains decreases from the rims to the central part of the shear zone. As a consequence of intensive shear deformation, these quartz grains became microstructurally very fine grained. As a result, intragranular structures, which contain hydroxyl defects and molecular water, were destabilized in these crystals, and water, which was present in the quartz lattice before deformation, was liberated from the crystal structure (Zhou et al. 2008). Thus, in regions where quartz suffered intensive ductile deformation (in the core part of the shear zone), the grains are partly dehydrated. In regions where quartz was not as intensively deformed (away from the shear zone), the water content (OH^-, H_2O) of the grains has been preserved.

Results of fracturing tests performed on quartz (Doukhan 1995; Kornev and Razvorotneva 1998) indicate that brittle deformation is most intensive if the quartz lattice is dry or contains only a small amount of water. Although the strength of wet quartz is an order of magnitude lower than the strength of dry quartz, the limiting deformation of wet quartz is larger than that of dry quartz (Kornev and Razvorotneva

1998). Limiting deformation is the maximum deformation that a material can carry without failing (Protosenya et al. 2016). Nevertheless, the presence of a small amount of water in the quartz lattice reduces the stress required for fracturing (Ball and Payne 1976). Thus, brittle shear zones were able to form in rock sections that previously suffered intensive ductile deformation and became partly dehydrated.

IV.6.4 Geodynamics

Theoretically, the coincidence of the border between different gneiss types with the depths of the ductile and brittle shear zones allows for two different interpretations regarding the structural evolution of this region. First, if the evolved ductile shear zone created softened regions inside the crystalline mass, then it could reactivate later in a brittle manner due to a tectonic event independent of the early one. On the other hand, if these structures were formed by the same tectonic event, causing ductile and brittle deformation to overlap along the same shear zones, then these zones may represent a detachment fault.

Based on the TitaniQ thermometer results, the formations above and below the shear zone display the same maximum metamorphic temperature (T_{max}=500–575 °C) and retrograde overprint. Thus, the analysed structural zone features the border of two rock bodies with the same metamorphic history. By definition, a detachment fault divides crystalline blocks of significantly different metamorphic evolutions; consequently, the studied shear zone is likely not a detachment fault. The coincidence of the ductile and brittle zones along the Szentlőrinc-1 well can be explained instead by the behaviour of quartz. These grains were dehydrated in the central part of the shear zone due to intensive ductile deformation relative to that of nearby rocks. Therefore, gneisses inside the shear zone became more rigid and ready to deform in a brittle style. These data indicate that in the studied section of the Mecsekalja Zone, there were most likely at least two independent, single, consecutive deformation events in which the ductile shear zone was reactivated in a brittle way.

IV.6.5 Connections with previous results from the study area

Based on our results, during the metamorphic and structural evolution of the Mecsekalja Zone, the maximum temperature of early regional metamorphism was between 500 and 575 °C. The temperature of the subsequent ductile deformation was

below 500 °C, and recrystallization occurred at a temperature between 400 and 475 °C. During the structural evolution of the study area, there were at least two independent, single deformation events. The earlier ductile deformation event was followed by a brittle one through the reactivation of the former ductile shear zone *(Fig. IV.11)*.

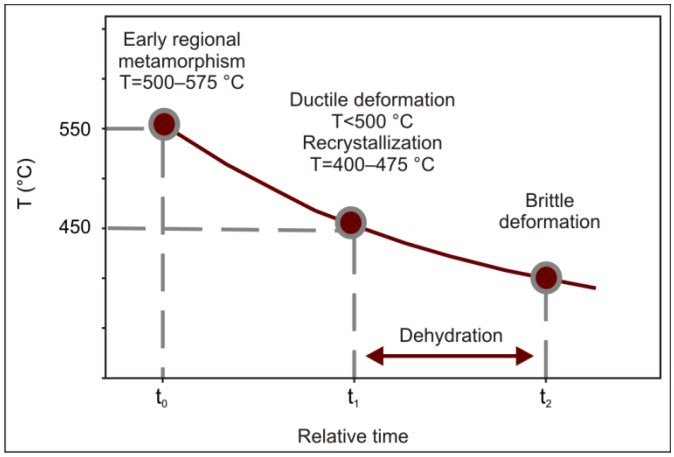

Figure IV.11: Metamorphic and structural evolution of the Mecsekalja Zone around the Sztl-1 well

The estimated temperatures of regional metamorphism (500–575 °C) display good coincidence with the previous results of Szederkényi (1977, 1983), Árkai and Nagy (1994), Lelkes-Felvári et al. (2000), and M. Tóth et al. (2005), who also estimated that greenschist/amphibolite facies metamorphism occurred at a temperature of 540–550 °C. The temperature of ductile deformation and mylonitization, <500 °C (400–475 °C), is also in good agreement with the previous results of Lelkes-Felvári et al. (2000), Király and Török (2003), and M. Tóth et al. (2005). These researchers estimated a temperature of ~500 °C for metamorphism under greenschist facies conditions and a recrystallization temperature of 350–400 °C.

Based on the detailed analysis of quartz chips from the Szentlőrinc-1 well, our schematic model is in accordance with previous results concerning the evolution of the Mecsekalja Zone (Szederkényi 1977, 1983; Árkai and Nagy, 1994; Lelkes-Felvári et al. 2000; Király and Török, 2003; M. Tóth et al. 2005) *(Fig. IV.12)*. Thus, previous evolution models of the Mecsekalja Zone can be extended towards the southwest, at least to the Szentlőrinc-1 well.

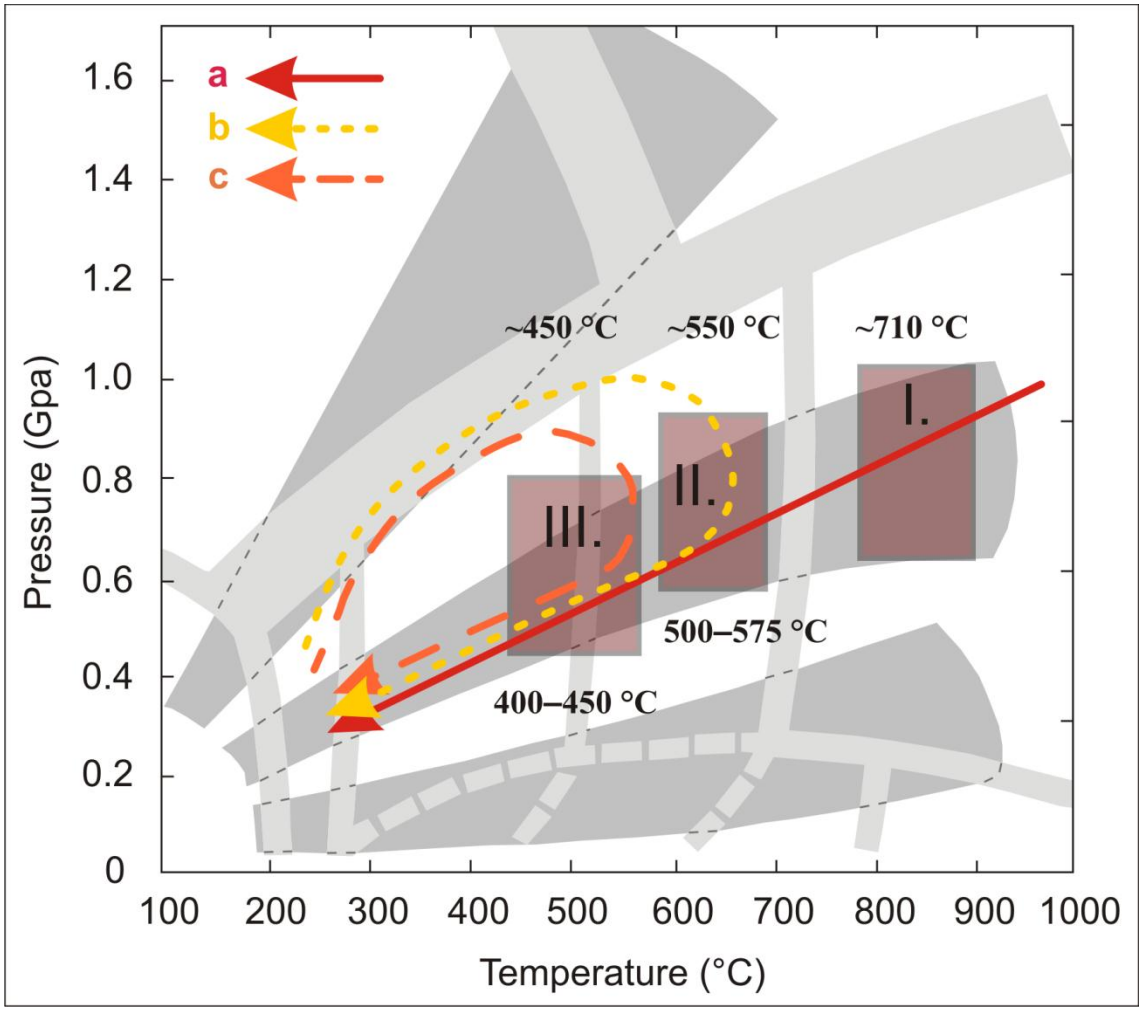

Figure IV.12: Comparison of Sztl-1 well with previous results concerning the evolution of the Mecsekalja Zone. Grey fields show the main metamorphic facies series of Miyashiro (1973, 1994) and Winter (2014). a, b, and c are the development models of different rock types of the Ófalu Group: a: gneiss; b: amphibolite; c: crystalline limestone, quartz phyllite, and metasandstone. I., II., and III. are the previously defined events during the evolution of Mecsekalja Zone: I. magmatic crystallization of quartz grains of gneiss protolith granitoid rocks (~710 °C, M. Tóth et al. 2005), II. regional metamorphic event at upper greenschist/lower amphibolite facies (~550 °C, Szederkényi 1977, 1983; Árkai and Nagy 1994; Lelkes-Felvári et al. 2000; M. Tóth et al. 2005) in both gneissic rocks and amphibolites, and III. all rock types of the Ófalu Group uniformly suffered high-temperature greenschist facies regional metamorphism, mylonitization and recrystallization (~450 °C, Szederkényi 1977, 1983; Lelkes-Felvári et al. 2000; Király and Török 2003; M. Tóth et al. 2005). Based on the current results, the early regional metamorphism (II.) occurred between 500 and 575 °C, while recrystallization (III.) occurred between 400 and 475 °C

Chapter V.: Conclusions

V.1 Summary of the results

In the introductory section of the dissertation *(Chapter I.)* first the complex characterization of shear zones and the importance of these structures were written in detail. Afterwards the special importance of the metamorphic and structural reconstruction of the basement along Mecsekalja Zone was presented. Finally, I deal with those physical and chemical features of quartz which can be used for recognition of metamorphic and structural evolution of a rock body.

Chapter II. revealed a new method based on Raman microspectroscopy analysis enables single quartz grains and its monomineralic domains, which are characterized by different deformation conditions, to be identified and classified. Three microstructurally extreme quartz grain types were discriminated in the subsurface shear zone: U type grains with undulose extinction, S type grains with subgrains, and R type grains consisting of small, undeformed recrystallized grains. The above extremes exhibit significantly different spectral attributes, and thus the quartz grains can accordingly be divided on the basis of certain Raman spectral variables. The three extreme quartz grain types were formed by different deformation mechanisms (BLG, SGR I, SGR II), and thus represent a range of deformation conditions associated with increasing temperature from U-R ($\Delta T \approx 250–500$ °C). The U-S-R spectral space can therefore also be considered a virtual deformational space. Although each complex quartz grain analyzed appears elsewhere in the deformation process defined by the U-S-R extreme conditions, they together represent a deformation development pathway. This combined pathway can be assumed characteristic for the whole rock volume under study.

Determination of the virtual deformational space enabled the reconstruction of the deformation history of the examined shear zone based on the available detrital quartz grains. The computed discriminant functions can be used only in case of the study area, but the method can be used independently for the study of other areas.

In *Chapter III.,* based on the characterisation of single quartz grain microstructures and analysis of the available well-log data ductile and brittle shear zones were localised along the Sztl-1 well. During the microscopic analysis of quartz fragments microstructurally different types were separated. The analysis of the proportion of these microstructurally different quartz grain types with depth enables the

localisation of ductile shear zones (1610–1635 m and 1750–1765 m) along the well. The ductile deformation data were completed with well-log data, which provide information about the brittle deformation. Using these logs, brittle shear zones (1580–1635 m and 1750–1765 m) can also be localised along the well. When comparing depths and extensions of the deformed horizons, a coincidence of the brittle and ductile zones becomes clear. This behaviour may suggest two different evolution schemes. If the first evolved ductile shear zones formed softened regions inside of the crystalline mass, it could reactivate later in a brittle way due to a tectonic event independent of the early event. However, if these structures formed due to the same tectonic event, these zones may represent a detachment fault.

Chapter IV. introduces the metamorphic and structural reconstruction of the Mecsekalja Zone based on chemical composition, microstructure and water content (OH^-, H_2O) of the quartz fragments from the Sztl-1 well. Afterwards the novel evolution model is compared with the previous surface-subsurface ones from the study area. Based on the Ti concentration (LA-ICP-MS) of the analysed quartz grains the maximum temperature of the early regional metamorphism during the evolution of Mecsekalja Zone was between 500–575 °C. The temperature of the subsequent ductile deformation, based on microstructure of quartz fragments, was below 500 °C, while based on TitaniQ thermometer recrystallization went on between 400–475 °C. In the rock sections, suffered intensive ductile deformation, the water content (OH^-, H_2O) of quartz grains decreased (FTIR), so they became mainly dehydrated. Thus these rock sections could favour to form of brittle shear zones. During the structural evolution of the study area most probably there were at least two independent, single, consecutive deformation events, and the ductile shear zones reactivated in a brittle way. These data are conform to the previous surface-subsurface results concerning the evolution of the Mecsekalja Zone, thus the previous evolution models of the Mecsekalja Zone can be extended toward SW at least to the Szentlőrinc-1 well.

Overall, the complex analysis (detailed microstructural analysis, Raman Spectroscopic evaluation, water (OH^-, H_2O) and Ti content determination, analysis of well-logs can be used for direct-indirect definition of fracture zones. Understanding behaviour of quartz fragments from the drill cuttings of the Sztl-1 well enabled localization of the ductile and brittle shear zones along the well and the recognition of the mechanical and rheological features of the rock body. Based on these data

reconstruction of the metamorphic, structural and thermal histories of the Mecsekalja Zone became possible *(Fig. V.1)*.

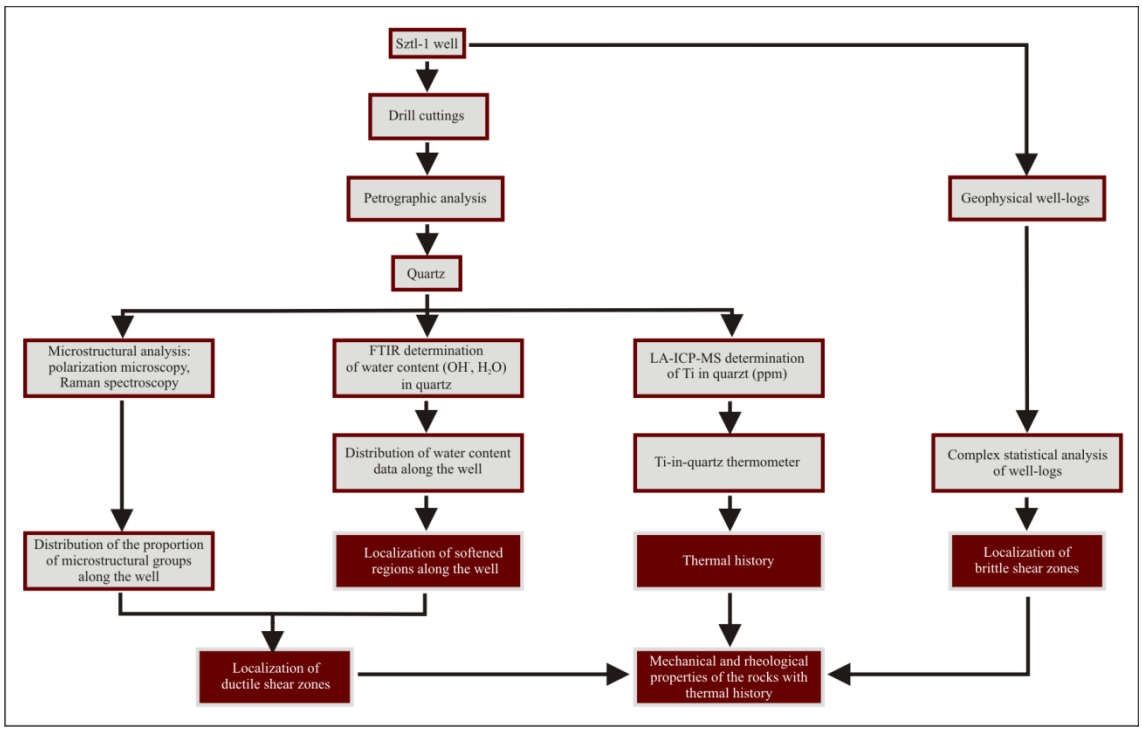

Figure V.1: Flow chart of the methods, used during the complex analysis of drill cuttings from the Sztl-1 well, and results

V.2 Outlook

Reservoirs are storage spaces for fluids such as water or hydrocarbons. Understanding of the different geological parameters of fluid reservoirs is essential to their development, production, and management. Generally, geophysical data (seismic and well-logs) and cores are utilized to map and characterize fluid reservoirs.

Drill cuttings are small pieces of rocks and minerals that are chipped away by the bit while a well is being drilled. Cuttings are typically the first piece of data available from the subsurface during drilling and often the only physical lithological data that are recovered from a well. These samples are continuous source of physical rock data. Drill cuttings collection is inexpensive, and can allow for high density sampling even in heterogeneous reservoirs.

However geologists usually prefer core data over data from cuttings. There is a general distrust of drill cuttings in today's geoscience world because they may not be representative of the reservoir because of poor sample collection techniques and the imprecise data they provide. The sample sizes obtained from cuttings are typically too

small for quantitative analysis using conventional techniques. Therefore, new, high-precision methods are required to analyse the smaller cuttings samples.

Recently there has been renewed interest in the data available from drill cuttings and the application of advanced approaches. Experimental procedures and modelling techniques are developed for extracting reservoir properties from small sizes of drill cutting samples (Sliwinski et al., 2009; Khojasteh et al., 2015; Clarkson and Haghshenas, 2016; Haghshenas et al., 2016).

Since generally the amount of available drill cuttings is much larger than that of core samples, cuttings enable to study whole boreholes. The continuous analysis of the drill cuttings along a well allows getting information about the analysed formation both in small and large scale. The simplest and the most obvious method to analyse drill cuttings because of their small sample size is microscopy and polarization microscopy to petrographic analysis (Richards, 1930). However, the method of digital image analysis enables to get much more information about the small sized samples than using of the conventional optical analysis (Sliwinski et al., 2009; Khojasteh et al., 2015). The recognition of the reservoir properties from drill cutting samples can be fulfilled by different analytical methods such as X-Ray Diffraction (XRD), X-Ray Fluorescence (XRF), Scanning Electron Microscopy (SEM) and Pyrolysis. As a result of these methods one can get mineralogical (mineral composition, texture/microstructure), geochemical (major and trace element concentration, TOC), petrographic (lithology, rock structure) and petrophysical (porosity, pore size) information about the drilled formation using exclusively the drill cuttings. This information enables the lithological identification (Bradbury et al., 2007; Khojasteh et al., 2015) as well as the change in rock quality in heterogenic reservoirs and also geological correlation. The numerous data revealed during the analysis of drill cutting samples can be integrated into various petrophysical and reservoir geological models. As a result of these modelling processes special reservoir properties (e.g.: permeability, diffusivity and fluid storage capacity) (Clarkson and Haghshenas, 2016; Haghshenas et al., 2016) become determinable and help during development of suitable production strategies. Thus cutting samples are a cut out for recognition the reservoir properties, evolution and the producibility of petroleum and geothermal reservoirs. So the drill cuttings can provide valuable information about the reservoir formations, especially in the presence of sparse core and log data, and also shows some limitations (Hartel, 2010).

The Pannonian Basin has special geological characteristics: small crust thickness: 20–25 km, high heat flow: 80–100 mW/m^2, more than average geothermic gradient: 6–7 °C/100 m (Dövényi et al., 2002; Lorberer, 2004). During the Neogene basin subsidence (Bergerat, 1989; Tari et al., 1992; Horváth and Cloetingh, 1996; Csontos and Nagymarosy, 1998) numerous geological structures, more km deep sub-basins and basement highs (e.g.: Békés Basin, Jászság Basin, Makó Trough, Derecske Trough, Jánoshalma High, Endrőd High, Szeghalom High, Mezősas-Furta High, Sarkadkeresztúr High Tari et al., 1992; Tari et al., 1999; Schubert and M. Tóth, 2001; M. Tóth et al., 2000; M. Tóth and Zachar, 2006) formed. There are several formations: Pannonian sandstones, Paleogene clastic sedimentary rocks, Mesosoic fractured carbonates, Paleozoic crystalline rocks (Teleki et al., 1994; Horváth and Tari, 1999). These geological structures and formations together can function as good petroleum or geothermal reservoirs. The wider recognition of these complex reservoir formations is very important because of their efficient operation.

The methodology introduced in this dissertation, based on the detailed analysis of drill cutting samples, enables the reambulation of the fluid reservoir formations in the Pannonian Basin even in those cases, when drilling cores do not exist, but historical drill cuttings are still available.

Summary

I. Introduction, objectives

In the Earth's crust the shear zones are deformation localisation structures, in which strain is notably higher than in the surrounding rock body (Ramsay, 1980; Ramsay and Huber, 1987; van der Plujim and Marshak, 2004; Passchier and Trouw, 2005; Fossen, 2010). In several places, because of their intensive deformation, shear zones behave as excellent fractured fluid reservoirs. Therefore, the petrographic and structural characterisation of these formations is extremely important. The metamorphic rocks in the crystalline basement of the Pannonian Basin contain numerous faults and shear zones. In the Pre-Neogene basement of the Tisza Mega-unit these formations are mostly known from a few surface outcrops and drill core specimens, which provide only rather diffuse information and their bring up is costly. However the drill cuttings are mainly continuously available from the wells that penetrated the basement and their collection is inexpensive.

The drill cutting samples usually include μm-mm size rock and mineral fragments, dominantly quartz grains. Quartz (SiO_2) is the second most frequent rock-forming mineral in the Earth's crust. It is stable and resistant within a wide range of temperature and pressure conditions. Quartz is a common product of metamorphic reactions and its metamorphic evolution determines the chemical composition of quartz grains. In the crystal lattice of quartz various trace elements (Al, Ti, Ge, Na, K, Li, B) (Götze et al., 2004) may also appear connected to the SiO_4 tetrahedrons. Although quartz is a "nominally anhydrous mineral" (NAM), in its crystal lattice hydrogen ('water') may occur both in the form of hydroxyl defects (OH^-) and molecular water (H_2O) (Stenina, 2004). The amount of 'water' in the crystal lattice of quartz significantly influences its ductile and brittle behaviour and decreases its mechanical strength and rigidity (Jones, 1975). Under different pressure and temperature conditions quartz deforms in different ways following diverse deformation mechanisms. Thus, each quartz grain of the available drill cutting samples in its microstructure may provide valuable information regarding its deformation history (Hirth and Tullis, 1992; Stipp et al., 2002; Vernon, 2004; Passchier and Trouw, 2005; Halfpenny et al., 2012).

The aim of the project is to work out a reproducible method for metamorphic and deformation history reconstruction using single quartz grains of drill cuttings. Based on

the developed method and using the drill cuttings of the Szentlőrinc-1(Sztl-1) well from almost 2 km depth, the project aims the metamorphic and structural reconstruction of the Mecsekalja Zone in SW Hungary. Moreover the project aims spatial correlation of the borehole data with previous models concerning the evolution of the Mecsekalja Zone.

II. Methods applied

During this research because of the tiny grainsize of the drill cutting samples development and application of special methods was required. Primarily the microstructural analysis of the quartz grains was made optically by polarization microscopy. The microstructurally different quartz grains was identified using Raman spectroscopy based on certain spectral attributes of Raman spectra measured on quartz grains. The linear combination of the spectral attributes, which in the best way describe the difference between the microstructurally different quartz grains, was computed using discriminant function analysis.

Ductile shear zones along the studied well were localized by counting the proportion of the microstructurally different quartz grains with depth. During the analysis, 100 pieces of randomly selected (JMicroVision: point counting method) quartz grains were microstructurally examined in every 25 m, and analysis was performed every 5 m in the possible fractured zones defined by well-log interpretation.

The brittle shear zones got localized along the studied well by statistical evaluation (discriminant function analysis) of the available direct-indirect well-logs (density, gamma ray, resistivity, spontaneous potential and calliper log), which are able to follow fractured state of the rock body.

Temperature data that are preserved in microstructurally different quartz grains was determined on the basis of the Ti content of quartz grains. The Ti content was measured by LA-ICP-MS. From the resulted Ti concentrations (ppm) temperatures were calculated with using the Ti-in-quartz (TitaniQ) thermometer of Thomas et al. (2010). The ‘water’ content (OH^-, H_2O) of quartz grains was measured by micro-FTIR.

III. New scientific results

The following new scientific results have been got in the course of these investigations:

1) The quartz grains of the drill cuttings from the Sztl-1well can be classified into three groups microstructurally (grains with undulose extinction (U), grains with subgrains (S), and grains with recrystallized grains (R)). These different quartz grain types presumably formed due to diverse dynamic recrystallization mechanisms; bulging (BLG) and subgrain rotation (SGR).

2) Raman spectroscopy enables discrimination of quartz grain types using certain spectral attributes of the Raman spectra. In the resulting *F1-F2* spectral space the U, S, R extreme grain types define closed clouds, while the microstructurally transitional grains are situated between them.

3) Along the studied interval of Szentlőrinc-1 well two gneiss types can be defined with different mineral compositions. Rocks of the upper 100–150 m (1600–1750 m) of the analysed well section beside quartz contain large amount of mica, mainly muscovite. In the lower part (1750–1820 m) the amount of mica decreases, while the amount of feldspars increase. Thus the studied well section can be divided into the upper micaceous and the lower feldspathic gneiss.

4) Along the analysed section of Sztl-1well two ductile (1610–1635 and 1750–1765 m) and two brittle (1580–1635 and 1750–1765 m) shear zones can be localised. Based on the proportion of the microstructurally different quartz grains (U, S, R) two ductile shear zones can be localised along the studied well section. The complex statistical analysis of the available direct-indirect well-logs, which follow fracturing (DEL, GR, R, SP, CAL) allow the localization of brittle shear zones.

5) Based on the Ti content of the analysed quartz grains the same two metamorphic events can be identified in both gneiss types. The temperature of the early regional metamorphic event was between 500–575 °C, while the following recrystallization went on between 400–475 °C. Thus the two different gneiss types presumably went through the same metamorphic and deformation history.

6) Quartz grains with different microstructures and deformation conditions formed at different temperatures. Previous studies (Hirth and Tullis, 1992; Passchier and Trouw, 2005, among others) suggest that bulging (BLG) dynamic

recrystallization mechanism acts at ~ 400 °C, while the subgrain rotation (SGR II) is active at ~ 500 °C in quartz. This statement is confirmed by Ti in quartz thermometry proving that quartz grains with different deformation conditions display different temperatures (BLG ~ 400–475 °C, SGR II ~ 500–575 °C).

7) In the Sztl-1 well, along the ductile shear zones the 'water' content of the quartz grains decreases towards the central zone.

8) Along the Sztl-1 well the coincidence of the ductile and brittle shear zones can be explained through formation of softened zones. Due to the intensive ductile deformation in the central part of the shear zone the quartz grains got dehydrated relative to the nearby rocks. Therefore, the rocks inside the shear zone became more rigid than the surrounding rock bodies with higher water content and were ready to deform in a brittle way.

9) During the deformational history of the Mecsekalja Zone two single, successive deformation events can divided: the ductile shear zones, because of the partial dehydration of quartz grains, reactivated in a brittle way.

10) The evolution scheme, based on the detailed analysis of quartz chips from the 2 km depth section of the Sztl-1 well, is conform with the previous surface models concerning to the metamorphic and deformation history of the Mecsekalja Zone. (Szederkényi, 1977, 1983; Árkai and Nagy, 1994; Lelkes-Felvári et al., 2000; Király and Török, 2003; M. Tóth et al., 2005). Thus the previous evolution models of the Mecsekalja Zone can be extended toward SW at least until the Sztl-1 well.

Összefoglalás

I. Bevezetés és célok

A földkéregben a nyírási zónák olyan deformációt lokalizáló szerkezetek, amelyekben a deformáció jelentősen nagyobb, mint a környező kőzetekben (Ramsay, 1980; Ramsay and Huber, 1987; van der Plujim and Marshak, 2004; Passchier and Trouw, 2005; Fossen, 2010). Számos helyen az intenzív deformáció következtében a nyírási zónák kőzetei kiváló repedezett fluidum rezervoárként működnek. Ezért ezen képződmények kőzettani- és szerkezetfejlődésének megismerése kiemelkedő fontosságú. A Pannon-medence kristályos aljzatát felépítő metamorf kőzetek számos vető és nyírási zóna által tagoltak. Ezek a képződmények a Tiszai Egység pre-neogén aljzatában többnyire csupán néhány felszíni kibúvásból, illetve fúrómag minták alapján ismertek, melyek nem szolgáltatnak folytonos információt a nyírási zónák kőzeteiről, és felszínre hozataluk is igen költséges. Ezzel szemben furadékanyag közel folytonosan rendelkezésre áll az aljzatból és jóval költségkímélőbb.

A furadékanyag minták általában μm-es, mm-es nagyságrendű ásvány és kőzetszemcséket, főként kvarcszemcséket tartalmaznak. A kvarc (SiO_2) a földkéreg második leggyakoribb kőzetalkotó ásványaként széleskörű nyomás és hőmérséklet viszonyok között stabil, ellenálló ásvány. A kvarc metamorf reakciók gyakori terméke, metamorf fejlődése meghatározza a kvarcszemcsék kémiai összetételét. A kvarc kristályszerkezetében az SiO_4 tetraéderekhez kapcsolódóan eltérő mennyiségben különböző nyomelemek (Al, Ti, Ge, Na, K, Li, B) (Götze et al., 2004) szintén megjelennek. Habár a kvarc „névlegesen vízmentes ásvány" (NAM) kristályrácsában a hidrogén („víz") mind szerkezeti hidroxil (OH^-), mind molekuláris víz (H_2O) formájában megtalálható (Stenina, 2004). A kvarc kristályrácsában jelenlévő „víz" mennyisége jelentősen befolyásolja annak töréses és képlékeny viselkedését, csökkenti mechanikai erősségét, ellenálló képességét (Jones, 1975). A kvarc kristályszerkezetét eltérő nyomás és hőmérséklet viszonyok között különböző deformációs mechanizmusok alakítják. Így a rendelkezésünkre álló furadékanyag kvarcszemcséi mikroszerkezetükben információt hordoznak az őket ért deformációs folyamatokról (Hirth and Tullis, 1992; Stipp et al., 2002; Vernon, 2004; Passchier and Trouw, 2005; Halfpenny et al., 2012).

A kutatás célja egy reprodukálható módszertan kidolgozása arra, hogy hogyan rekonstruálhatjuk a metamorf- és deformációtörténetet furadékanyag egyedülálló kvarcszemcséiből. Majd a kidolgozott módszer alkalmazásával és a Szentlőrinc-1 (Sztl-1) fúrásból, közel 2 km-es mélységből rendelkezésre álló furadékanyag kvarcszemcséinek felhasználásával a Mecsekalja-zóna metamorf- és szerkezeti rekonstrukciója. Ezt követően pedig az így kapott eredmények földtani kiterjesztése és összevetése a Mecsekalja-zóna fejlődésével kapcsolatos korábbi felszíni modellekkel.

II. Alkalmazott módszerek

A rendelkezésre álló furadékanyag minták kis szemcsemérete speciális vizsgálati módszerek kidolgozását és alkalmazását tette szükségessé a kutatás során.

A furadékanyag kvarcszemcséinek mikroszerkezeti elemzése elsődlegesen optikailag, polarizációs mikroszkópia alkalmazásával történt. Az eltérő mikroszerkezeti megjelenésű kvarcszemcsék elkülönítése a Raman spektroszkópia alkalmazásával, az egyes szemcsékből felvett Raman spektrumok bizonyos spektrális tulajdonságai alapján történt. Az eltérő mikroszerkezeti megjelenésű kvarcszemcsék közti különbséget leginkább leíró spektrális tulajdonságok lineáris kombinációját statisztikai vizsgálatok eredményeként, diszkriminancia analízis végrehajtása során kaptuk meg.

A vizsgált fúrás mentén a képlékeny nyírási zónák kijelölése az eltérő mikroszerkezeti megjelenésű kvarcszemcsék mennyiségi arányának elemzése alapján történt a mélység függvényében. Az elemzés során a vizsgált fúrás mentén a rendelkezésre álló furadékanyag mintákat 25 méterenként vizsgáltuk, míg a geofizikai szelvények alapján feltételezett töréses zónákban a mintákat 5 méterenként elemeztük. Az egyes mintákban 100 db véletlenszerűen kiválasztott (JMicroVision: point counting módszerrel) kvarcszemcse mikroszerkezetét elemeztük.

A töréses nyírási zónák mélységi pozíciójának kijelölése a vizsgált fúrás mentén a rendelkezésre álló direkt-indirekt töréslokalizálásra alkalmas geofizikai szelvények (sűrűség, természetes gamma, ellenállás, természetes potenciál és lyukbőség szelvény) optikai és statisztikai (diszkriminancia analízis) elemzése alapján történt.

Az egyes eltérő mikroszerkezeti megjelenésű kvarcszemcsék által megőrzött, vagyis az azokat létrehozó hőmérséklet meghatározása a kvarcszemcsék Ti-tartalma alapján történt, melyet lézerablációs induktív csatolású plazma tömegspektrometria (LA-ICP-MS) alkalmazásával határoztunk meg. Az így kapott Ti koncentrációkból

(ppm) Thomas et al., (2010) Ti a kvarcban termométere (TitaniQ) alapján számoltunk hőmérsékletet. A kvarcszemcsék víz tartalmának (OH^-, H_2O) meghatározása mikro-Fourier transzformációs infravörös spektrometria (mikro-FTIR) alkalmazásával történt.

III. Új tudományos eredmények

A dolgozatban bemutatott kutatás során az alábbi új tudományos eredmények születtek:

1) A Sztl-1 fúrásból rendelkezésre álló furadékanyag kvarcszemcséi mikroszerkezetileg három csoportra oszthatók (unduláló kioltású (U), alszemcsés (S), rekrisztallizált (R)), melyek vélhetően különböző dinamikus rekrisztallizációs mechanizmusoknak megfelelő körülmények között jöttek létre („bulging" (BLG), alszemcse rotáció (SGR I-II)).

2) A Raman spektroszkópia segítségével, a Raman spektrumok bizonyos spektrális tulajdonságai alapján, elkülöníthetők az eltérő mikroszerkezeti megjelenésű és deformációs állapotú (U, S, R) kvarcszemcsék. Az U, S, R szélső tagok az *F1-F2* spektrális térben egy-egy tartományt definiálnak, együtt azonban meghatároznak egy spektrális teret. A vegyes mikroszerkezeti megjelenésű kvarcszemcsék a spektrális térben a három szélső tagot képviselő U, S, R típus által kijelölt spektrális térben helyezkednek el.

3) A Sztl-1 fúrás vizsgált szakasza mentén két eltérő ásványos összetételű gneisz típus különíthető el. A vizsgált fúrásszakaszon belül kb. a felső 100–150 méteren a furadékanyag a kvarc mellett nagy mennyiségű csillámot, főként muszkovitot tartalmaz. A vizsgált fúrás szakasz alsóbb részében a csillámok mennyisége némileg csökken és nő a földpátok mennyisége. Ez alapján a vizsgált fúrásszakaszon belül egy felső csillámos és egy alsó földpátos gneiszként azonosítható kőzetblokkot különíthetünk el.

4) A Sztl-1 fúrás vizsgált szakasza mentén két képlékeny (1610–1635 és 1750–1765 m) és két töréses (1580–1635 és 1750–1765 m) nyírási zóna lokalizálható, melyek mélysége egybeesik. Az eltérő mikroszerkezeti megjelenésű (U, S, R) kvarcszemcsék mennyiségi aránya alapján a mélység függvényében a vizsgált fúrás szakasz mentén képlékeny nyírási zónák lokalizálhatók. A rendelkezésre

álló direkt-indirekt, repedés követő geofizikai szelvények (DEL, GR, R, SP, CAL) komplex statisztikai elemzése töréses nyírási zónák kijelölését teszik lehetővé.

5) A vizsgált kvarcszemcsék Ti-tartalma alapján a Mecsekalja-zóna metamorf és deformációtörténeti fejlődése során mindkét gneisz típusban ugyanaz a két eltérő hőmérsékletű esemény különíthető el. A korai metamorfózis hőmérséklete 500–575 °C-nak tekinthető, míg az ezt követő rekrisztallizáció hőmérséklete feltételezhetően 400–475 °C körüli volt. Így a két eltérő gneisz típus vélhetően azonos metamorf- és deformációtörténeti fejlődésen ment keresztül.

6) Az eltérő mikroszerkezeti megjelenésű és deformációs állapotú kvarcszemcsékhez különböző hőmérsékletek kapcsolódnak. Hirth and Tullis (1992) és Passchier and Trouw (2005) alapján, a kvarc esetén a „bulging" (BLG) dinamikus rekrisztallizációs mechanizmus hőmérséklete ~ 400 °C, míg az alszemcse rotáció (SGR II) hőmérséklete ~ 500 °C. A Ti a kvarcban mérések ezt igazolták, az elemzett eltérő deformációs állapotú kvarcszemcsék eltérő hőmérsékleten keletkeztek (BLG ~ 400–475 °C, SGR II ~ 500–575 °C).

7) A Sztl-1 fúrásban a kvarcszemcsék víztartalma (OH^-, H_2O) a képlékeny nyírási zónák mentén, annak közepe felé, csökken az intenzív képlékeny deformáció következtében.

8) A Sztl-1 fúrás mentén lokalizált képlékeny és töréses nyírási zónák mélységi helyzetének egybeesése gyengeségi zónák kialakulásával magyarázható. A képlékeny és a töréses nyírási zónák pozíciója a vizsgált fúrás mentén vélhetően azért esik egybe, mert az intenzív képlékeny deformáció hatására a nyírási öv centrumában a kvarcszemcsék részben dehidratálódtak a szomszédos kőzetrészekhez képest. Így a nyírási zónákban a gneisz ridegebbé vált, mint a környező, magasabb víztartalmú kőzetek és egy adódó töréses felújulásra kevésbé ellenállóan reagáltak, könnyebben eltörtek.

9) A Mecsekalja-zóna deformációtörténeti fejlődése során két független, egymást követő deformációs esemény különíthető el: a képlékeny nyírási zónák a kvarcszemcsék részleges dehidratációja miatt töréses módon reaktiválódtak.

10) A Sztl-1 fúrásból, közel 2 km-es mélységből származó furadékanyag komplex elemzése során kapott eredmények jó egyezést mutatnak a Mecsekalja-zóna fejlődésével kapcsolatos korábbi felszíni modellekkel (Szederkényi, 1977, 1983; Árkai and Nagy, 1994; Lelkes-Felvári et al., 2000; Király and Török, 2003; M. Tóth et al., 2005). A Mecsekalja-zóna fejlődésével kapcsolatos felszíni modellek DNY felé – legalább a Sztl-1 fúrásig – térben kiterjeszthetők.

Acknowledgements

First of all, I would like to express my sincere gratitude to my supervisor *Dr. Tivadar M. Tóth* for his valuable and continual assistance, thoughtful guidance, understanding, knowledge and also his critical comments.

I would like to say thanks to my colleagues in the *Department of Mineralogy, Geochemistry and Petrology in the University of Szeged* because of their assistance provided in numerous ways. I acknowledge the *Institute of Geography and Geology, University of Szeged* for their financial support granted through a pre-doctoral fellowship. This work was supported with a fellowship of TÁMOP-4.2.2.A-11/1/KONV-2012-0047 („Biological and environmental answers induced by new, functional materials").

I thank to *Mannvit Ltd.* and *Dr. László Ádám* for providing the samples and the *Geo-Log Ltd.* and the *PannErgy Plc.* for geophysical data.

I would like to thank *Dr. István János Kovács (Hungarian Geological and Geophysical Institute)* and *Sándorné K. Judit (Hungarian Institute for Forensic Sciences, Department of Physics & Chemistry)* for the micro-FTIR measurements and I also thank to his gainful advices. Thanks to *Dr. Edit Király (Hungarian Geological and Geophysical Institute)* for the LA-ICP-MS measurements and helpful comments. I thank to *Dr. Krisztián Fintor* for guidance with the Raman spectroscopy. I also thank to *Attila Bencsik* for sample preparation.

Last, but not least, I am extremely grateful to *my family* for their continuous support and patience, which was essential for this work.

References

Asell, J. F., Nicol, M. (1968): Raman Spectrum of α Quartz at High Preassures. The Journal of Chemical Physics, Vol. 49, No. 12.

Asquith, G.B., Gibson, C.R. (1982): Basic Well Log Analysis for Geologists. The American Association of Petroleum Geologists, Tulsa, Oklahoma, USA

Árkai, P., Nagy, G., Dobosi, G. (1985): Polymetamorpic evolution of the South-Hungarian crystalline basement, Pannonian Basin: geothermometric and geobarometric data. Acta Geol. Hung., 28, 165–190.

Árkai, P., Nagy, G. (1994): Tectonic and magmatic effects on amphibole chemistry in mylonitized amphibolites and amphibole-bearing enclaves associated with granitoid rocks, Mecsek Mountains, Hungary. Acta Geol. Hung., 37, 235-268.

Árpási, M., Lorberer, Á., Pap. S. (2000): High pressure and temperature (geopressured) geothermal reservoirs in Hungary: World Geothermal Congress

Ball, A., Payne, B.W. (1976): The tensile fracture of quartz crystals. Journal of Material Science, 11, 731–740.

Balla, Z. (2003a): Ófalui Formáció, paleozoikum. In: Balla et al., 2003, 3.1.1., 103–105.

Balla, Z. (2003b): Magmás képződmények In: Balla et al., 2003 3.1.2.1. 109–112.

Balla, Z., Császár, G., Gulácsi, Z., Gyalog, L., Kaiser, M., Király, E., Koloszár, L., Koroknai, B., Magyari, Á., Maros, Gy., Marsi, I., Molnár, P., Rotárné Szalkai, Á., Tóth, Gy. (2009): A Mórágyi-rög északkeleti részének földtana. Magyarország tájegységi térképsorozata. MÁFI, Budapest

Barber, D.J., Wenk, H.R. (1991): Dauphiné twinning in deformed quartzites: implications of an in-situ TEM study of the α-β-phase transformation. Phys. Chem. Miner., 17, 492–502.

Bergerat, F. (1989): From pull-apart to the rifting process: the formation of the Pannonian Basin. Tectonophysics, 157, 271–280.

Blacic, J. D. (1975): Plastic-deformation mechanisms in quartz: the effect of water. Tectonophysics, 27, 271–294.

Bíró, T., Kovács, I.J., Király, E., Falus, Gy., Karátson, D., Bendő, Zs., Fancsik, T., Sándorné, J. K. (2016): Concentration of hydroxyl defects in quartz from various rhyolitic ignimbrite horizons: results from unpolarized micro-FTIR analyses on unoriented phenocryst fragments. Eur. J. Mineral., 28, 313–327.

Bradbury, K. K., Barton, D. C., Solum, J. G., Draper, S. D., Evans, J. P. (2007): Mineralogic and textural analyses of drill cuttings from the San Andreas Fault Observatory at Depth

(SAFOD) boreholes: Initial interpretations of fault zone composition and constraints on geologic models. Geosphere, Vol. 3, No. 5, 299–318.

Brady, R.J. (2002): Very high slip rates on continental extensional faults: new evidence from (U-Th)/He thermocronometry of the Buckskin Mountains, Arizona. Earth Planet. Sci. Lett., 197, 95–104.

Chalmers, B. (1959): Physical Metallurgy. New York: Wiley

Clarkson, C.R., Haghshenas, B. (2016): Characterization of multi-fractured horizontal shale wells using drill cuttings: 1. Fluid-in-place estimation. Journal of Natural Gas Science and Engineering, 32, 574–585.

Csontos, L., Nagymarosy, A. (1998): The Mid-Hungarian line: the zone of repeated tectonic inversion. Tectonophysics, 297, 51–71.

Csontos, L., Nagymarosy, A., Horváth, F., Kovac, M. (1992): Tertiary evolution of the Intra-Carpathian area: a model. Tectonophysics, 208, 221–241.

Davis, G.A. (1988): Rapid upward transport of mid-crustal mylonitic gneisses in the footwall of a Miocene detachment fault, Whipple Mountains, southeastern California. Geol Rundsch, 77/1, 191–209.

Davis, G.A., Anderson, J.L., Frost, E.G., Shackleford. T.J. (1979): Regional Miocene detachment faulting and early Tertiary (?) mylonitization, Whipple-Buckskin-Rawhide Mountains, southeastern California and western Arizona. In: Abott, P.L. (eds.) Geological Excursions in the Southern California Area. Dept Geol Sci., San Diego State University Publications, San Diego, California 74–108.

Davis, G.A., Lister, G.S. (1988): Detachment faulting in continental extension: perspectives from the southwestern U.S. Cordillera, John Rodgers symposium volume. Spec. Pap. Geol. Soc. Am. 218, 133–159.

de Boer, K., Jansen, A.P.J., van Santen, R.A., Watson, G.W., Parker S.C. (1996): Free-energy calculations of thermodynamic, vibrational, elastic, and structural properties of α-quartz at variable pressures and temperatures. Physical Review B, Vol. 54, No. 2.

Dell'Angelo, L.N., Tullis, J. (1996): Textural and mechanical evolution with progressive strain in experimentally deformed aplite. Tectonophysics, 256, 57–82.

Dionot, J., Brändlein, M. (2011) Nanomat Master Program – Group 2, Université Pierre et Marie Curie, Paris.

Doukhan, J. (1995): Lattice Defects and Mechanical Behaviour of Quartz SiO2. Journal de Physique III, EDP Sciences, 5/11, 1809–1832.

Dövényi, P., Horváth, F,. Drahos, D. (2002): Geothermal thematic map. In: Hurter S., Haenel, R. (eds.) Atlas of Geothermal resources in Europe. Publ. No.17811 of the EC.

England, P.C. (1987): Diffuse continental deformation; length scales, rates and metamorphic evolution. Phil. Trans. R. Soc. Lond., 321, 2–22.

Etchepare, J., Merian, M., Smetankine, L. (1974): Vibrational normal modes of SiO_2. I. α and β quartz. Journal of Chemical Physics, Vol. 60, No. 5.

Fairhead, J.D., Binks, R.M. (1991): Differential opening of the Central and South Atlantic Oceans and the opening of the West African Rift System. Tectonophysics, 187, 191–203.

Faulds, J.E., Geissman, J.W. (1992): Implications of palaeomagnetic data on Miocene extension near a major accomodation zone in the Basin and Range Province. Tectonics, 11, 204–227.

Fiser-Nagy, Á., Varga-Tóth, I., M. Tóth, T. (2014): Lithology identification using open-hole well-log data in the metamorphic Kiskunhalas-NE hydrocarbon reservoir, South Hungary. Acta Geod. Geophys., 49, 57–78.

Fossen, H. (2010): Structural geology. Cambridge University Press, New York, 481.

Foster, D.A., Raza, A. (2002): Low temperature thermocronological record of exhumation of the Bitterrot metamorphic core complex, northern Cordilleran Orogen. Tectonophysics, 349, 23–36.

Gans, P., Mahood, G.A., Schermer, E. (1989): Synextensional magmatism in the Basin and Range Province: a case study from the eastern Great Basin. Geol. Soc. Am. Spec. Pap., 233, 53.

Gifkins, R.C. (1976): Grain boundary sliding and its accommodation during creep and superplasticity. Metall. Trans. A 7A:1225–1232.

Gleason, G., S. DeSisto 2008: A natural example of crystal-plastic deformation enhancing the incorporation of water into quartz. – Tectonophysics, 446, 16–30.

Götze, J., Plötze, M., Graupner, T., Hallbauer, D.K., Bray, C.J. (2004): Trace element incorporation into quartz: A combined study by ICP-MS, electron spin resonance, cathodoluminescence, capillary ion analysis, and gas chromatography. Geochimica et Cosmochimica Acta, Vol. 68, No. 18, 3741–3759.

Griggs, D.T., Blacic, J.D. (1965): Quartz: anomalous weakness of synthetic crystals. Science, 147, 292–295.

Grujic, D., Stipp, M., Wooden, J.L. (2011): Thermometry of quartz mylonites: Importance of dynamic recrystallization on Ti-in-quartz reequilibration. Geochem. Geophys. Geosyst., 12, Q06012.

Haas, J., Péró, Cs. (2004): Mesozoic evolution of the Tisza Mega-unit. Int. J. Earth Sci. 93/2, 297–313.

Haas, J., Budai, T., Csontos, L., Fodor, L., Konrád, Gy. (2010): Pre-Cenozoic geological map of Hungary, 1:500 000. Geological Institute of Hungary

Haertel, M., Herwegh, M., Pettke, T. (2013): Titanium-in-quartz thermometry on synkinematic quartz veins in a retrograde crustal-scale normal fault zone. Tectonophysics, 608, 468–481.

Haghshenas, B., Clarkson, C.R., Aquino, S.D., Chen, S. (2016): Characterization of multi-fractured horizontal shale wells using drill cuttings: 2. Permeability/diffusivity estimation. Journal of Natural Gas Science and Engineering, 32, 586–596.

Halfpenny, A., Prior, D.J., Wheeler, J. (2012): Electron backscatter diffraction analysis to determine the mechanisms that operated during dinamic recrystalisation of quartz-rich rocks. Journal of Structural Geology, 36, 2–15.

Hartel, T.H.J. (2010): Reservoir Characterization by Means of Drill Cuttings; An Example of Hydrothermal Dolomite in Cuttings from the West Sukunka River Area of British Columbia. GeoCanada – Working with the Earth.

Heidelbach, F., Kunze, K., Wenk, H.R. (2000): Texture analysis of a recrystallised quartzite using electron diffraction in the scanning electron microscope. Journal of Structural Geology, 22, 91–104.

Heidrick, T.L., Wilkins, J.W. (1980): Field guide to the geology and ore deposits of the Buckskin Mountains, Arizona. Ariz. geol. Soc. Spring Field Trip Guide, 31045.

Hills, E.S. (1956): A contribution to the morphotectonics of Australia. Journal of Geological Society of Australia, 3, 1–15.

Hirth, G,. Tullis, J. (1992): Dislocation creep regimes in quartz aggregates. Journal of Structural Geology, 14, 145–159.

Hobbs, B.E., Means, W.D., Williams, P.F. (1976): An Outline of Structural Geology. New York: Wiley

Holdsworth, R.E., Butler, C.A., Roberts A.M. (1997): The recognition of reactivation during continental deformation. J. Geol. Soc. Lond., 154, 73–78.

Holdsworth, R.E., Hand, M., Miller, J.A., Buick, I.S. (2001): Continental reactivation and revorking: an introduction In: Miller, J.A., Holdsworth, R.E., Buick, I.S., Hand, M. (eds) Continental Reactivation and Reworking. Geological Society, London, Special Publications 184, 1–12.

Horváth, F., Tari, G. (1999): IBS Pannonian Basin project: A review of the main results and their bearings on hydrocarbon exploration. In: Durand, B., Jolivet, L., Horváth, F., Seranne, M. (eds.): The Mediterranean basins: Tertiary extension within the Alpine orogen. Geological Society, London, Special Publications, 156, 195–213.

Horváth, F., Dövényi, P., Szalay, Á., Royden, L.H. (1988): Subsidence, thermal, and maturation history of the Great Hungarian Plain. Am. Assoc. Pet. Geol. Mem. 45, 355–372.

Horváth, H., Cloetingh, S. (1996): Stress-induced late-stage subsidence anomalies in the Pannonian Basin. Tectonophysics, 266, 287–300.

Huang, R., Audétat, A. (2012): The titanium-in-quartz (TitaniQ) thermobarometer: a critical examination and re-calibration. Geochim. Cosmochim. Acta, 84, 75–89.

Jones, M.E. (1975): Water weakening of quartz, and its application to natural rock deformation. Jlgeol. Soc. Lond., 131, 429–432.

Kassai, M. (1977): Data for paleogeographic reconstruction of Transdanubia, Hungary, at the end of Paleozoic time. Acta Miner. Petr., 23(1), 41–48.

Kats, A. (1962): Hydrogen in alpha-quartz. Phillips Res. Rep., 17/1-31, 133–279.

Kempe, U., Götze, J., Dombon, E., Monecke, T., Poutivtsev, M. (2012): Quartz regeneration and its use as a repository of genetic information. In: Götze, J., Möckel, R. (eds.), Quartz: Deposits, Mineralogy and Analytics, Springer, 313–355.

Kekulawala, K.R.S.S., Paterson, M.S., Boland, J.N. (1978): Hydrolytic weakening in quartz. Tectonophysics, 46, T1–T6.

Kekulawala, K.R.S.S., Paterson, M.S., Boland, J.N. (1981): An experimental study of the role of water in quartz deformation. Geophysical Monograph Series, 24, 49–60.

Kerrich, R. (1988): Detachment zones of Cordilleran metamorphic core complexes: thermal, fluid and metasomatic regimes. Geol. Rundsch., 77/1, 157–182.

Khojasteh, P., Ahmadyfard, A., Tokhmechi, B., Mirmahdavi, S. A. (2015): Automatic detection of formations using images of oil well drilling cuttings. Journal of Petroleum Science and Engineering, 125, 67–74.

Kidder, S., Avouac, J-P., Chand, Y-C. (2013): Application of titanium-in-quartz thermobarometry to greenschistfacies veins and recrystallized quartzites in the Hsüehshan range, Taiwan. Solid Earth, 4, 1–21.

Király, E., Török, K. (2003): Magmatic garnet in deformed aplite dykes from the Mórágy granitoid, SE-Transdanubia. Acta. Geol. Hung., 46/3, 239–254.

Király. E. (2005): Microscopic description of the field samples. Manuscript, MÁFI, Bp., Tekt. 1242.

Konrád, Gy., Sebe, K., Halász, A., Babinszki, E. (2010): Sedimentology of Permian playa lake: the Boda Claystone Formation, Hungary. Geologos, 16/1, 27–41.

Kornev, V.M., Razvorotneva, L.I. (1998): Comparative estimates of the strength of dry and wet quartz in griding. Journal of Applied Mechanics and Technical Physics, 39/1, 121–125.

Kovács, I., Hermann, J., O'Neill, H.St.C., FitzGerald , J.D., Sambridge, M., Horváth, G. (2008): Quantitative absorbance spectroscopy with unpolarized light, Part II: Experimental evaluation and development of a protocol for quantitative analysis of mineral IR spectra. American Mineralogist, 93, 765–778.

Kovács, I., Green, D., Rosenthal, A., Hermann, J., O'Neill, H.St.C., Hibberson, W.O., Udvardi, B. (2012): An experimental study of water in nominally anhydrous minerals in the upper mantle near the water saturated solidus. J. Petrol., 53, 2067–2093.

Kovács, S., Szederkényi, T., Haas, J., Buda, Gy., Császár, G., Nagymarosy, A. (2000): Tectonostratigraphic terranes in the pre-Neogene basement of the Hungarian part of the Pannonian area. Acta Geol. Hung., 43/3, 225–328.

Kronenberg, A.K., Wolf, G.H. (1990): Fourier transform infrared spectroscopy determinations of intragranular water content in quartz-bearing rocks: implications for hydrolytic weakening in the laboratory and within the earth. Tectonophysics, 172, 255–271.

Krishnamurti, D. (1958): The Raman spectrum of quartz and its interpretation. Memoir No. 108 from Raman Research Institute, Bangalore-6.

Lelkes-Felvári, Gy., Árkai, P., Frank, W., Nagy, G. (2000): Late Variscan ultramylonite from the Mórágy Hills, SE Mecsek Mts., Hungary. Acta Geol. Hung., 43/1, 65–84.

Lelkes-Felvári, Gy., Frank, W. (2006): Geochronology of the metamorphic basement, Transdanubian part of the Tisza Mega-Unit. Acta Geol. Hung. 49/3, 189–206.

Levien, L., Prewitt, C.T., Weidner, D.J. (1980): Structure and elastic properties of quartz at pressure. American Mineralogist, Vol. 65, 920–930.

Lin, S-Y. (1997): Vibrational local modes of a-SiO^2: H and variation of local modes in different local environments. J. Appl. Phys., 82 (12).

Lister, G.S., Davis, G.A. (1989): The origin of metamorphic core complexes and detachment faults formed during Tertiary continental extension in the northern Colorado River region. USA J. Struct. Geol, 11(1/2), 65–94.

Lister, G.S., Etheridge, M.A., Symonds, P.A. (1986): Application of the detachment fault model to the formation of passive continental margins. Geology, 14, 246–250.

Liu, Y., Hu, Z., Gao, S., Günther, D., Xu, J., Gao, C., Chen, H. (2008): In situ analysis of major and trace elements of anhydrous minerals by LA-ICP-MS without applying an internal standard. Chem. Geol., 257, 34–43.

Lloyd, G.E., Law, R.D., Mainprice, D., Wheeler, J. (1992): Microstructural and crystal fabric evolution during shear zone formation. J. Struct. Geol. 14, 1079–1100.

Lloyd, G.E. (2000): Grain boundary contact effects during faulting of quartzite: an SEM/EBSD analysis. J. Struct. Geol. 22, 1675–1693.

Lorberer, Á. (2004): A geotermális energiahasznosítás hazai fejlesztési Koncepciója 2010-ig. Jelentés a Környezetvédelmi és Vízügyi Minisztérium részére. VITUKI, Budapest, 19–27.

M. Tóth, T., Schubert, F., Zachar, J. (2000): Neogene exhumation of the Variscan Szeghalom Dome, Pannonian Basin, E. Hungary. Geol. J., 35, 265–284.

M. Tóth, T., Kovács, G., Schubert, F., Dályay, V. (2005): Az ófalui „migmatit" eredete és deformációtörténete. Földtani Közlöny 135/3, 331–352.

M. Tóth, T., Zachar, J. (2006): Petrology and deformation history of the metamorphic basement in the Mezősas-Furta crystalline high (SE Hungary). Acta Geol. Hung. 49/2, 165–188.

M. Tóth, T. (2014): Geochemistry of the Görcsöny Ridge amphibolites (Tisza Unit, SW Hungary) and its geodynamic consequences. Geologica Croatica 67/1, 17–32.

Menegon, L., Pennacchioni, G., Heilbronner, R., Pittarello, L. (2008): Evolution of quartz microstructure and c-axis crystallographic preferred orientation within ductilely deformed granitoids (Arolla unit, Western Alps). J. Struct. Geol., 30, 1332–1347.

Michon, L., Van Balen, R.T., Merle, O., Pagnier, H. (2003): The Cenozoic evolution of the Roer Valley rift system integrated at a European scale. Tectonophysics, 367, 101–126.

Miyashiro, A. (1973): Metamorphism and Metamorphic Belts. Allen & Unwin, London, 492.

Miyashiro, A. (1994): Metamorphic Petrology. UCL Press, London, 404.

Molnar, L., M. Tóth, T., Schubert, F. (2015a): Structural controls on the petroleum migration and entrapment within faulted basement blocks of Szeghalom Dome (Pannonian Basin, SE Hungary). Geologia Croatica, 68/3, 247-259.

Molnar, L., Vásárhelyi, B., M. Tóth, T., Schubert, F. (2015b): Integrated petrographic – rock mechanic borecore study from the metamorphic basement of the Pannonian Basin, Hungary. Open. Geosci., 7/1, 53–64.

Monecke, T., Kempe, U., Götze, J. (2002): Genetic significance of the trace element content in metamorphic and hydrothermal quartz: a reconnaissance study. Earth Planet. Sci. Lett., 202, 709–724.

Nagy, Á., M. Tóth, T. (2012): Petrology and tectonic evolution of the Kiskunhalas-NE fractured hydrocarbon reservoir, South Hungary. Central European Geology 55/1, 1–22.

Nishikawa, O., Takeshita, T. (1999): Dynamic analysis and two types of kink bands in quartz veins deformed under subgreenschist conditions. Tectonophysics, 301, 21-34.

Olsen, K.H., Baldridge, W.S., Callender, J.F. (1987): Rio Grande rift: an overview. Tectonophysics, 143, 119–139.

Ostroumov, M., Faulques, E., Lounejeva, E. (2002): Raman spectroscopy of natural silica in Chicxulub impactite, Mexico. C. R. Geoscience 334, 21-26.

Passchier, C.W., Trouw, R.A.J. (2005): Microtectonics. Springer-Verlag, 371.

Piper, J.D.A., Dagley, P., Carpenter, A.H. (2010): Detachment and rotation of a metamorph core complex during extensional deformation: Palaeomagnetic study of the Catalina-Rincon Core Complex, Basin and Range Province, Arizona. Tectonophysics, 488, 191–209.

Posgay, K., Takács, E., Szalay, I., Bodoky, T., Hegedűs, E., Kántor, J.I., Timár, Z., Varga, G., Bérczi, I., Szalay, Á., Nagy, Z., Pápa, A., Hajnal, Z., Reilkoff, B., Mueller, S., Ansorge, J., De Iaco, R., Asudeh, I. (1996): International deep reflection survey along the Hungarian Geotraverse. Geophysical Transactions, 40/1-2, 1–44.

Protostenya, A.G., Karasev, M.A., Petrov, D.N. (2016): Investigating mechanical properties of argillaceous grounds in order to improve safety of development of megalopolis underground space. International Journal of Applied Engineering Research, 11/16, 8949–8956.

Prucha, J.J. (1992): Zone of weakness concept: A review and evaluation. In: Bartholomew, M.J., Hyndman, D.W., Mogk, D.W., Mason, R. (eds) Basement tectonics 8: Characterization and comparison of ancient and Mesozoic continental margins. Proceedings of the Eighth International Conference on Basement Tectonics held in Butte, Montana, USA, August 1988. Kluwer Academic Publishers, Netherlands, 83–92.

Ramsay, J.G. (1980): Shear zone geometry: a review. Journal of Structural Geology, Vol. 2, No. 1/2, 83–99.

Ramsay, J.G., Huber, M.I. (1987): The technics of modern structural geology. Volume 2: Folds and fractures. Academic Press, 462.

Richards, J.T. (1930): The collection and interpretation of drill cuttings. Oklahoma Academy of Science Proceedings, Vol. 10, 97–99.

Rieder, M. (1996): The Geological Interpretation of Well Logs. 2nd edition, Whittles, Caithness

Rutter, E.H., Holdsworth, R.E., Knipe, R.J. (2001): The nature and tectonic significance of fault-zone weakening: an introduction. In: Holdsworth, R.E., Strachan, R.A., Magloughlin, J.F., Knipe, R.J. (eds) The Nature and Tectonic Significance of Fault Zone Weakening. Geol. Soc. Lond. Spec. Publ., 186,1–11.

Sambridge, M., Fitz Gerald, J.D., Kovács, I., O'Neill, H.St.C., Hermann, J. (2008): Quantitative IR spectroscopy with unpolarized light, Part I: Physical and mathematical development. American Mineralogist, 93, 751–764.

Schlumberger (1989): Log interpretation principles/applications. Schlumberger Wireline & Testing, Texas

Scholz, C.H. (2002): The Mechanics of Earthquakes and Faulting. Cambridge University Press, 471.

Schubert, F., M. Tóth, T. (2001): Structural evolution of mylonitized gneiss zone from the Norther flank of the Szeghalom dome (Pannonian Basin, SE, Hungary). Acta Min. Pet. Szeged, 42, 59–64.

Shigematsu, N. (1999): Dynamic recrystallization in deformed plagioclase during progressive shear deformation. Tectonophysics, 305, 437–452.

Skultéti, Á., M. Tóth, T., Fintor, K., Schubert, F. (2014): Deformation history reconstruction using single quartz grain Raman microspectroscopy data. Journal of Raman Spectroscopy, 45/4, 314–321.

Skultéti, Á., M. Tóth, T. (2016): Localisation of ductile and brittle shear zones along the Szentlőrinc-1 well in the Mecsekalja Zone using quartz microstructural and well-log data. Acta Geod. Geophys., 51/2, 295–314.

Sliwinski, J., Le Strat, M., Dublonko, M. (2009): A New Quantitative Method for Analysis of Drill Cuttings and Core for Geologic, Diagenetic and Reservoir Evaluation. Frontiers + Innovation – CSPG CSEG CWLS Convention, 185–188.

Sonder, L., England, P.C. (1986): Vertical averages of rheology of the continental lithospheric; relation to thin sheet parameters. Earth Planet. Sci. Lett., 7, 81–90.

Sørensen, B.E., Larsen, R.B. (2009): Coupled trace element mobilisation and strain softening in quartz during retrograde fluid infiltration in dry granulite protoliths. Contrib. Mineral. Petrol., 157, 147–161.

Stadler, R., Konzett, J. (2012): OH defects in quartz in the system quartz–albite–water and granite–water between 5 and 25 kbar. Phys. Chem. Minerals, 39, 817–827.

Stenina, N.G. (2004): Water related defects in quartz. B. Geosci., 79, 251–268.

Stipp, M., Stünitz, H., Heilbronner, R., Schmid, S.M. (2002): The eastern Tonale fault zone: a 'natural laboratory' for crystal plastic deformation of quartz over a temperature range from 250 to 700 °C. Journal of Structural Geology 24, 1861–1884.

Stockli, D.F., Brichau, S., Dewane, T.J., Hager, C., Schroeder, J. (2006): Dynamics of large-magnitude extension in the Whipple Mountains metamorphic core complex. Goldschmidt Conference Abstracts A616.

Szederkényi, T. (1974): Paleozoic magmatism and tectogenesis in southeast Transdanubia. Acta Geol. Hung., 18/3-4, 305–313.

Szederkényi, T. (1977): Geological evolution of South Transdanubia (Hungary) in Paleozoic time. Acta Min. Pet. Szeged, 23/1, 3–14.

Szederkényi, T. (1979): Origin of amphibolites and metavolcanics of crystalline complexes of south Transdanubia, Hungary. Acta Geol. Hung., 26/1-2, 103–136.

Szederkényi, T. (1983): Origin of amphibolites and metavolcanics of crystalline complexes of South Transdanubia, Hungary. Acta Geol. Ac. Sci. Hung., 26, l03–136.

Szederkényi, T. (1984): Az Alföld kristályos aljzata és földtani kapcsolatai. DSc thesis

Szederkényi, T. (1996): Metamorphic formations and their correlation in the Hungarian part of the Tisza Megaunit (Tisza Composite Terrane). Acta Min. Petr. Szeged, 37, 143–160.

Szederkényi, T., Haas, J., Nagymarosy, A., Hámor, G. (2012): Geology and history of the evolution of the Tisza Mega-unit. In: Haas, J. (ed.) Geology of Hungary, Regional geology reviews. Springer-Verlag, 103–148.

Tari, G., Horváth, F., Rumpler, J. (1992): Styles of extension in the Pannonian basin. Tectonophysics, 208, 203–219.

Tari, G., Dövényi, P., Dunkl, I., Horváth, F., Lenkey, L., Stefanescu, M., Szafián, P., Tóth, T. (1999): Lithospheric structure of the Pannonian basin derived from seismic, gravity and geothermal data. Geol. Soc. Lond. Spec. Publ., 156, 215–250.

Teleki, P.G., Mattick, R.E., Kókai, J. (eds.) (1994): Basin Analysis in Petroleum Exploration. A Case Study from the Békés Basin, Hungary. Kluwer Academic Publishers

Thomas, J.B., Watson, E.B., Spear, F.S., Shemella, P.T., Nayak, S.K., Lanzirozzi, A. (2010): TitaniQ under pressure: the effect of pressure and temperature on the solubility of Ti in quartz. Contrib. Mineral. Petrol., 160, 743–759.

Thomas, S-M., Koch-Müller, M., Reichart, P., Rhede, D., Thomas, R., Wirth, R., Matsyuk, S. (2009): IR calibrations for water determination in olivine, r-GeO2, and SiO2 polymorphs. Phys. Chem. Minerals., 36, 489–509.

Thorbergsdottir, I.M., Tulinius, H., Ádám, L., Gudmundsson, G., Halldórsdottir, H.B., Traustason, S., Hu, Z., Yu, G. (2010): Geothermal Drilling for Space Heating in the Town of Szentlőrinc in SW Hungary. Proceedings World Geothermal Congress, Bali, 1–5.

Tittman, J., Wahl, J.S. (1965): The physical foundations of formation density logging (gamma-gamma). Geophysics, 31/2, 284–294.

Tóth, J., Almási, I. (2001): Interpretation of observed fluid potential patterns in a deep sedimentary basin under tectonic compression: Hungarian Great Plain, Pannonian Basin. Geofluids, 1, 11–36.

Tulinius, H., Thorbergsdottir, I.M., Ádám, L., Hu, Z., Yu, G. (2010): Geothermal Evaluation in Hungary using integrated interpretation of well, seismic and MT Data. Proceedings World Geothermal Congress, Bali, 1–7.

Tullis, J., Stünitz, H., Teysser, C., Heilbronner, R. (2000): Deformation microstructures in quartzo-feldspathic rocks. In: Jessel, M.W., Urai, J.L. (eds.): Stress, Strain and Structure. A Volume in Honour of W D Means. Journal of the Virtual Explorer, 2.

Tüske, T. (2001): A Mórágyi-rög metamorfitjainak szerkezeti értékelése (szakdolgozat). Kézirat. ELTE Természettudományi Kar, Általános és Történeti Földtan Tanszék, Budapest.

Twiss, R. J., Moores, E. M. (2006): Structural Geology. W.H. Freeman and Company, 736.

van der Plujim, B.A., Marshak, S. (2004): Earth Structure – An introduction to structural geology and tectonics. W. W. Norton & Company, 656.

Vernon, R.H. (2004): A practical guide to Rock Microstructure. Cambridge University Press, 650.

Vitale, S., Mazzoli, S. (2016): From finite to incremental strain: Insights into heterogeneous shear zone evolution. In: Mukherjee, S., Mulchrone, K.F. (eds.) Ductile Shear Zones: From Micro- to Macro-scales. John Wiley & Sons, 51–70.

Wark, D.A., Watson, E.B. (2006): TitaniQ: a titanium-in-quartz geothermometer. Contrib. Mineral. Petrol., 152, 743–754.

Wernicke, B. (1985): Uniform-sense normal simple shear of the continental lithosphere. Can. J. Earth Sci., 22, 108–125.

Wernicke, B., Burchfiel, B.C. (1982): Modes of extensional tectonics. J. Struct. Geol., 4, 105–115.

Wernicke, B., Axen, G.A. (1988): On the role of isostasy in the evolution of normal fault systems. Geology, 16, 848–851.

White, S.H. (1976): The role of dislocation processes during tectonic deformation with special reference to quartz. In: Strens, R.J. (ed.) The physics and chemistry of minerals and rocks. Wiley, London, 75–91.

White, S.H., Burrows, S.E., Carreras, J., Shaw, N.D., Humphreys, F.J. (1980): On mylonites in ductile shear zones. Journal of Structural Geology, Vol. 2, No. 1/2, 175–187.

White, S.H., Bretan, P.G., Rutter, E.H. (1986): Fault-zone reactivation: kinematics and mechanisms. Philos. Trans. R. Soc. Lond., A317, 81–97.

White, S.M. (1977): Geological significance of recovery and recrystallisation processes in quartz. Tectonophysics, 39, 143–70.

Wibberley, C.A.J., Yielding, G., Di Toro, G. (2008): Recent advances in the understanding of fault zone internal structure: a review. In: Wibberley, C.A.J., Kurz, W., Imber, J., Holdsworth, R.E., Collettini, C. (eds.) The Internal Structure of Fault Zones: Implications for Mechanical and Fluid-Flow Properties. Special Publication 299, London: Geological Society, 5–33

Winter, J.D. (2014): Principles of Igneous and Metamorphic Petrology. Pearson, 745.

Wintsch, R.P., Yi, K. (2002): Dissolution and replacement creep: a significant deformation mechanism in mid-crustal rocks. Journal of Structural Geology, 24, 1179–93.

Wilson, J.T. (1966): Did the Atlantic close and then reopen? Nature, 211, 676–681.

Zachar, J., M. Tóth, T. (2004): Petrology of metamorphic basement of the Tisza Block at the Jánoshalma High, S Hungary. Acta Geol. Hung., 47/4, 349–371.

Zhou, Y., He, C., Yang, X. (2008): Water contents and deformation mechanism in ductile shear zone of middle crust along Red River fault in southwestern China. Science in China Series D: Earth Sciences, 51/10, 1141–1425.